Complexes of thiophene derivatives as potential metallomesogens

by

Mary Solly Thomas

A thesis submitted in partial fulfillment of the requirements for

the degree of

Doctor of Philosophy

in

Chemistry

in the Faculty of Natural & Agricultural Science

University of Pretoria

Pretoria

April 2006

Supervisor: Prof. Simon Lotz

Co-Supervisor: Dr. Marilé Landman

Declaration

I declare that the thesis that I submit for the degree of Doctor of Philosophy in Chemistry at the University of Pretoria has not previously been submitted by me for degree purposes at any other university, and all the sources that were used or quoted have been indicated and acknowledged.

Signature…….. Date……..

Mary Solly Thomas

Contributions of the following collaborators and institutes are acknowledged:

(i) Mr David Liles for data collection, structure determination and discussions regarding the single crystal X-ray diffraction studies

(ii) The Department of Chemistry, Katholieke Universiteit Leuven, Belgium for Polarizing Optical Microscopy (POM) measurements and much needed discussions

(iii) Dr Liezel van der Merwe, University of South Africa (UNISA) for DSC and TGA measurements

(iv) Dr Tommie van der Merwe, University of the Witwatersrand for recording the mass spectra

Summary

Complexes of thiophene derivatives as potential metallomesogens

Candidate:	Mary Solly Thomas
Supervisor:	Prof Simon Lotz
Co-Supervisor:	Dr. Marilé Landman
Department:	Chemistry
Degree:	Doctor of Philosophy

This study involves the synthesis and structural characterization of new metal complexes of thiophene derivatives that have (potential) liquid crystalline properties. Thiophene has been selected because of its stability and versatility in lending itself to synthetic modification and hence forms links in chain structures for rod-like metallomesogens. Thiophene, when compared with 1,4-disubstituted benzene units, can change considerably the polarity, polarizability and also the geometry of the compounds, altering the types of mesophases, phase transition temperatures, dielectric constants and other properties of mesogens.

The reactions of a series of 5-alkyl-2-thiophenedithiocarboxylates with nickel(II) chloride formed two types of complexes, blue mononuclear nickel(II) complexes with two terminal dithiocarboxylate ligands, $[Ni(S_2CTR)_2]$ (T = 2,5-disubstituted thiophene) and violet mononuclear nickel(II) complexes with perthio- and dithiocarboxylate ligands, $[Ni(S_3CTR)(S_2CTR)]$ (R = alkyl groups). The blue monomers are preferred for the shorter alkyl chains (C_4 and C_6), and the violet compounds for the longer chain lengths (C_8, C_{12} and C_{16}) in the alkylthiophene complexes. In addition to the above series, $[Ni(S_2CTCH_3)_2]$, was prepared in a one-pot reaction and it was possible to isolate both the blue and violet products. The

thermal properties of the complexes were studied by using differential scanning calorimetry (DSC) and polarizing optical microscopy (POM). Nickel complexes of the violet type with longer alkyl chains showed liquid crystalline properties.

Zinc(II) complexes analogous to nickel(II) complexes prepared similarly. A crystal structure determination of one of those complexes revealed the fusion of two monomers to give a dimeric structure with bridging sulfur atoms, $[Zn_2(\mu\text{-}S_2CTR)_2(S_2CTR)_2]$. Although an irregular melting pattern was observed, the complexes did not show any liquid crystalline properties.

In an attempt to extend the study towards organometallic compounds, complexes of the type $[Re(CO)_4(S_2CTR)]$ or $[Re(CO)_4(S_2CTTR)]$ (T = 2,5-disubstituted thiophene, TT = 2,5-disubstituted bithiophene; R = H, CH_3, $C_{14}H_{29}$) were synthesized and characterized by IR and NMR spectroscopy. Further characterization of $[Re(CO)_4(S_2CTTH)]$ by single crystal X-ray diffraction confirmed the molecular structure of the complexes. These compounds showed sharp single melting points.

Fischer-type carbene complexes of manganese(I) with octahedral coordination of the type $[MnMeCp(CO)_2\{C(OEtTR)\}]$ or $[MnMeCp(CO)_2\{C(OEtTTR)\}]$ (R = H, C_6H_{13}, $C_{12}H_{25}$, $C_{16}H_{33}$) were synthesized and characterized by IR, NMR and mass spectrometry. Thermal properties of the complexes were studied by using thermogravimetric analysis (TGA). All the organometallic rhenium(I) and Fischer-type carbene complexes of manganese(I) showed weight loss upon heating due to decomposition. Therefore it can be assumed that these complexes are not suitable as liquid crystals.

Acknowledgements

I would like to express my sincere gratitude and appreciation to:

Professor Simon Lotz, my supervisor and Dr. Marilé Landman, co-supervisor for suggesting the problem and for their continuous guidance and support throughout the study.

Professor Koen Binnemans, Katholieke Universiteit Leuven, Belgium, for the opportunity to visit his lab, and for the measurements of the samples by polarizing optical microscope.

Katleen Lodewyckx and Rik Van Deun, Katholieke Universiteit Leuven, Belgium for providing me with the much needed insight into liquid crystals.

My colleagues at the Chemistry Department and at the Foundation Year program (UNIFY) of the University of Limpopo for their support and encouragement.

My fellow student, Andrew Olivier for support and encouragement.

NRF, National research foundation for financial assistance to attend conferences.

Finally my husband Solly and children for continuous support and encouragement, especially Cynthia, my youngest daughter for helping mummy with some of the drawings and other computer applications.

Table of contents

List of Complexes

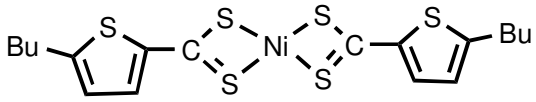

1a

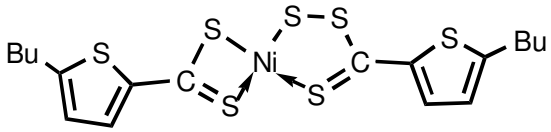

1b

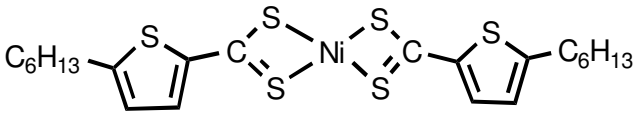

2a

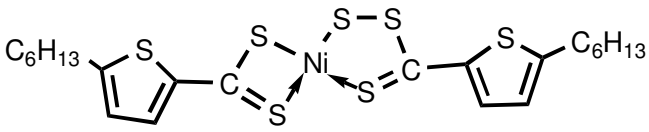

2b

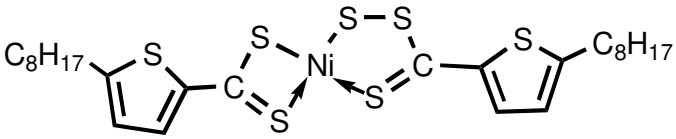

3b

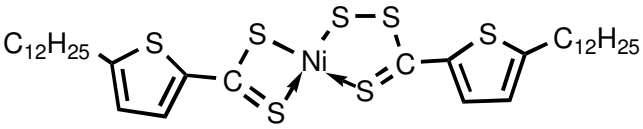

4b

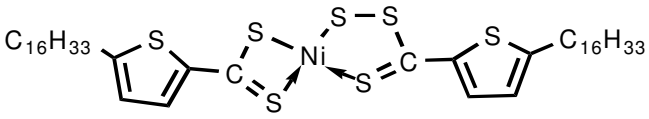

5b

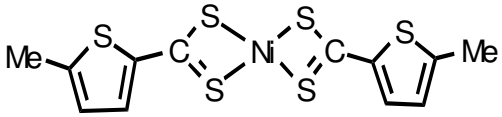

6a

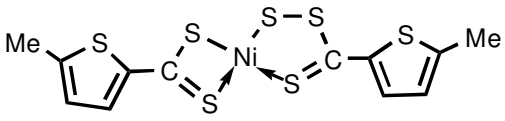

6b

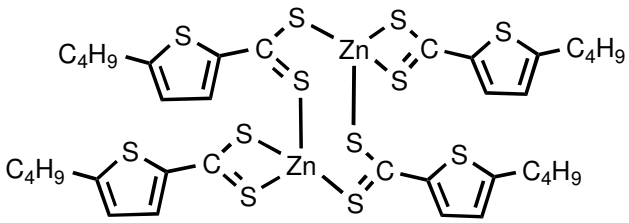

7

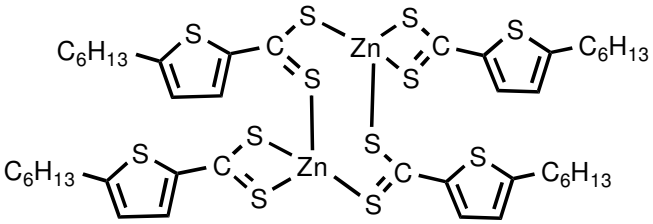

8

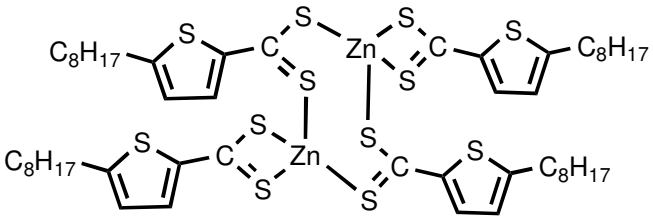

9

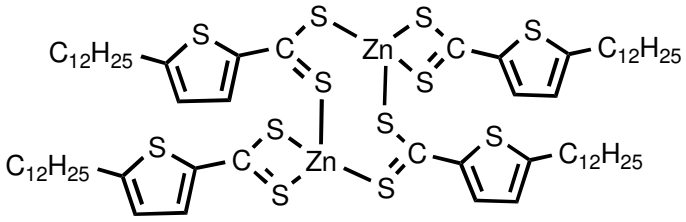

10

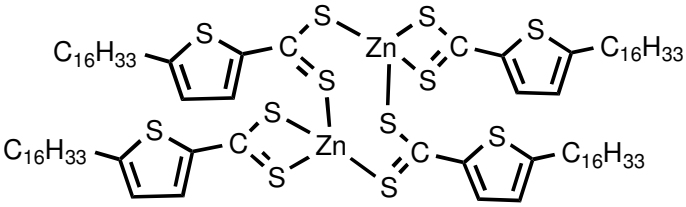

11

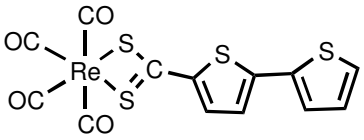

12

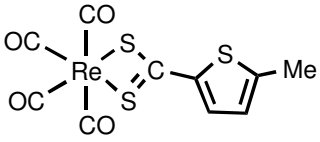

13

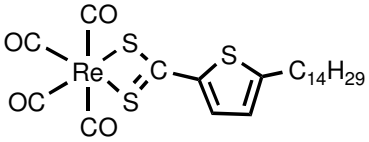

14a

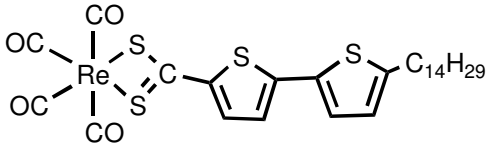

14b

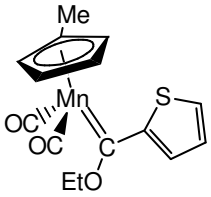

15a

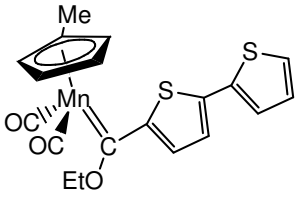

15b

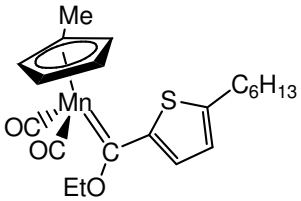

16a

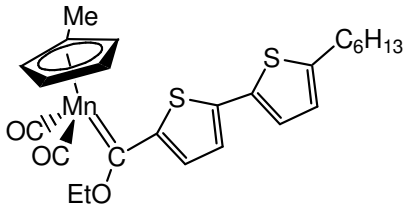

16b

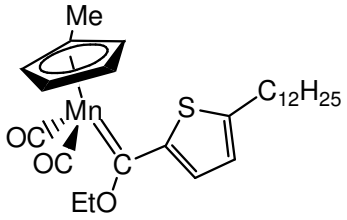

17a

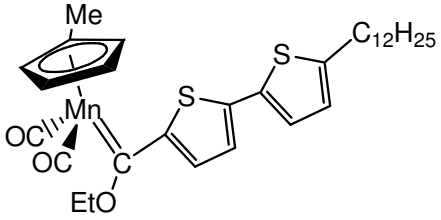

17b

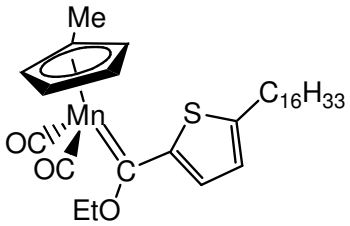

18a

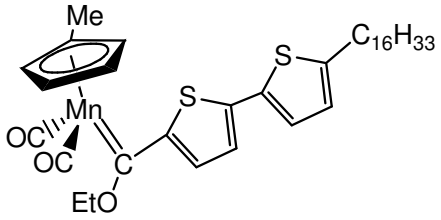

18b

List of Abbreviations

B	Benzene
Bu	butyl
CRT	cathode-ray tube
CAD	computer-aided drawing
Cr	crystal
Cp	cyclopentadienyl
DSC	differential scanning calorimetry
d	doublet
Et	ethyl
FAB	fast atom bombardment
I	isotropic liquid
IR	infrared spectroscopy
vs	very strong
s	strong
m	medium
w	weak
LCD	liquid crystal display
LMM	low molar mass
MS	mass spectrometry
Me	methyl
m	multiplet
N	nematic mesophase
N_D	discotic nematic mesophase
NMR	nuclear magnetic resonance
NLO	non-linear optical
n	director
POM	polarizing optical microscopy
ppm	parts per million

R	alkyl
RF	radio frequency
SmA	smectic A mesophase
SmC	smectic C mesophase
T	thiophene
TT	bithiophene
TGA	thermogravimetric analysis
THF	tetrahydrofuran
TN	twisted nematic display
t	triplet
UV	ultraviolet
XRD	X-ray diffraction

List of Figures

List of Tables

Chapter 1

General Introduction

1.1 Liquid Crystals

Liquid crystals represent a state of matter intermediate between the solid and liquid phase. They have been defined as "orientationally ordered" liquids or "positionally disordered" crystals with combined properties of both the crystalline and the liquid states[1]. Most solids when heated directly change into liquid state, however certain solids do not change directly into liquid state on heating, but pass through phases which have properties intermediate between solids and liquids. Compounds that exhibit these phases are called liquid crystals. Schematic melting behaviour of a liquid crystal[2] is given in Figure 1.1.

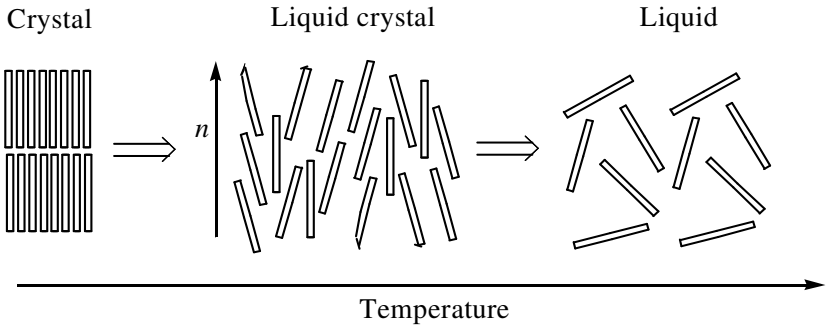

Figure 1.1 Schematic melting behaviour of a liquid crystal

A liquid crystal molecule is called a mesogen and the different phases it forms are mesophases. Liquid crystal mesophases are fluids, which due to partial orientational ordering of the constituent molecules, have material properties such as permittivity, refractive index, elasticity and viscosity which are anisotropic (i.e., their magnitude will differ from one direction to another).

1.2 Classification

Liquid crystalline (mesogenic) compounds can be differentiated into thermotropic, and lyotropic[3]. Thermotropic liquid crystals change phase with temperature. The transition from the crystalline solid to the mesophase is often termed as the melting point, while that from the highest mesophase to the isotropic liquid is called the clearing point. The mesophases often appear turbid while the isotropic liquid is clear. Thermotropic liquid crystals change phase upon heating or cooling. When the mesophase is obtained by heating the crystalline solid as well as by cooling the isotropic liquid, the mesophase is said to be enantiotropic. Sometimes however, it is only possible to obtain a mesophase by cooling the isotropic liquid. Such a mesophase is said to be monotropic. Lyotropic phases are formed by molecules in a solvent (generally water), and the concentration as well as the temperature control the appearance of the mesophase. Soap is an everyday example of a lyotropic liquid crystal.

Thermotropics can be further subdivided into two main groups, depending on their structural features. Liquid-crystal mesophases may be classified on the basis of the shape of the molecules, which give rise to the properties of the phase. The rod-like molecules are calamitic and the disc-like molecules are discotic[4]. Calamitic compounds have a structure in which the axial part is larger than the radial part (Figure 1.2).

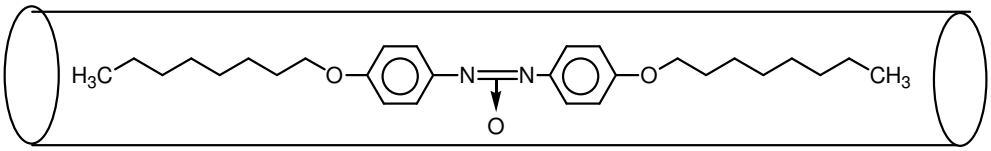

Figure 1.2 Example of a calamitic (rod-like) liquid crystal

Discotic compounds are disc-like as the name implies. The radial parts are larger than the axial part (Figure 1.3).

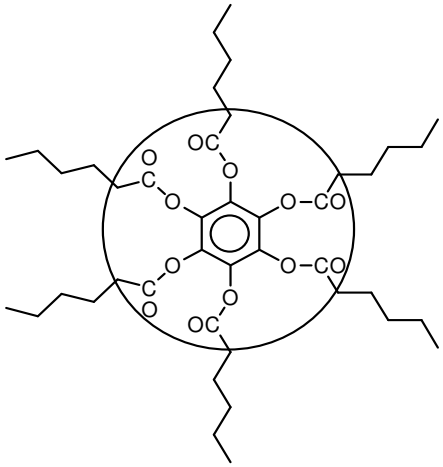

Figure 1.3 Example of a discotic liquid crystal

1.2.1 Calamitic phases

Rod-like molecules can form calamitic mesophases. There are two types of calamitic mesophases; nematic mesophase and smectic mesophase[5,6]. The less ordered mesophase is the nematic mesophase (N). In this, the molecules align with their long molecular axis more or less parallel to a preferred direction indicated by the director, *n* (Figure 1.4). The molecules can move freely within the nematic phase and are able to rotate around the long molecular axis.

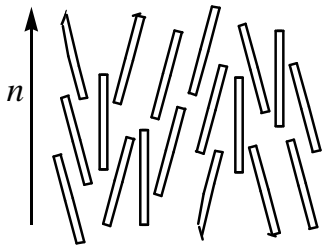

Figure 1.4 Schematic representation of a nematic phase

The nematic liquid-crystalline phase is technologically the most important among the many different mesophases. It is virtually used in all commercially available liquid crystal displays (LCD).

Smectic mesophases (Sm) show a higher degree of order than the nematic phase. There is orientational order as well as some positional order. The molecules are not only oriented in one direction, but also positioned to one another in layers. A number of smectic phases exist which differ in the degree of order present both within and between the layers.

The simplest smectic phase is the smectic A (SmA) phase, in which the molecules are aligned parallel to the normal without having positional order within the layer. In smectic C (SmC) phase, the normal to the layers is tilted by an angle other than 90^{o} (Figure 1.5).

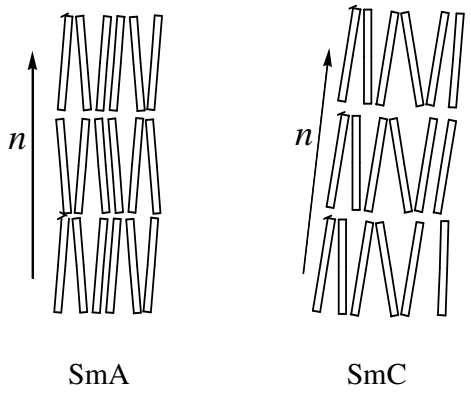

Figure 1.5 Schematic representation of smectic A and smectic C phases

1.2.2 Discotic mesophases

Materials that generate discotic mesophases have a disc-like molecular structure[8]. There are two different classes of discotic mesophases, nematic and columnar. The simplest one is the discotic nematic phase, which has orientational order but no positional order. The discotic nematic phase is denoted by N_D where the subscript D is used to avoid confusion with the normal nematic phase. The discotic nematic phase, like its analogue, is the least ordered liquid crystalline phase. Most of the molecules in the columnar discotic phase tend to position themselves in columns, the different columns constituting a two-dimensional lattice. There are several types of columnar mesophases because of the different symmetry classes of the two-dimensional lattice of columns and the order or the disorder of the molecules stacking within the columns. Examples of nematic columnar phase (N_C) and hexagonal columnar phase (Col_h) are shown in Figure 1.6.

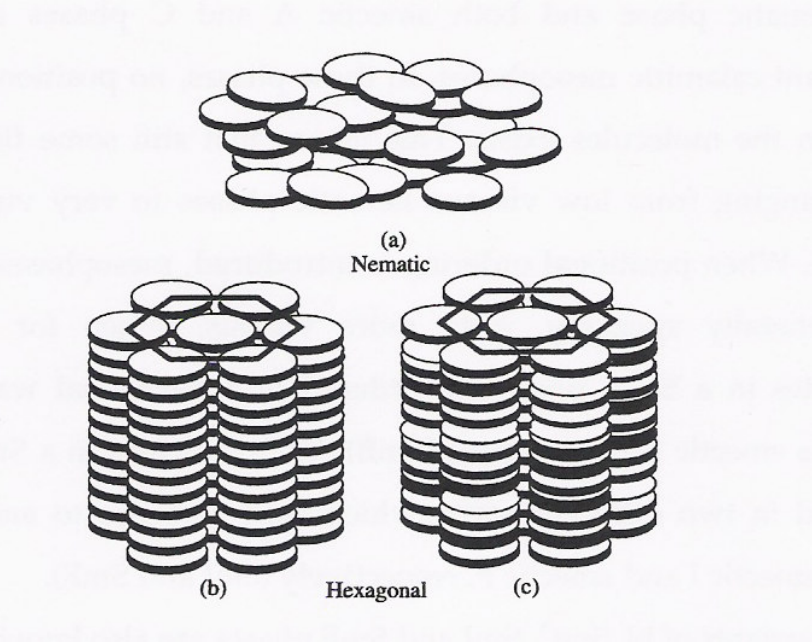

Figure 1.6 Discotic nematic and hexagonal columnar phases[10]

1.3 Mesophase characterization

There are three main techniques to identify the liquid-crystalline properties of a compound[8,9]. The first technique is based on the birefringence of the mesophase and is called Hot-stage Polarizing Optical Microscopy (POM). It is used to look at the optical textures that are typical for a given mesophase. The second technique that is used complimentary to POM is Differential Scanning Calorimetry (DSC). DSC reveals the phase transition temperatures as well as transition enthalpies. A third way to study mesogenic behaviour is by using X-ray Powder Diffraction (XRD). When an X-ray beam interacts with the typical structure of the mesophase, a characteristic diffraction pattern is observed, which allows identification of the mesophase.

1.3.1 Hot-stage Polarizing Optical Microscopy (POM)

This technique is based on the fact that the mesophase is anisotropic and birefringent. This means that the mesophase has two different refractive indices, parallel and perpendicular to the liquid crystal's director. When the sample, in its liquid-crystalline state, is struck by a polarized beam of light two refracted rays are formed, which interact with each other to give a typical pattern under the microscope. This pattern is called texture and is different for each mesophase. A schematic representation of polarizing optical microscopy is depicted in Figure 1.7.

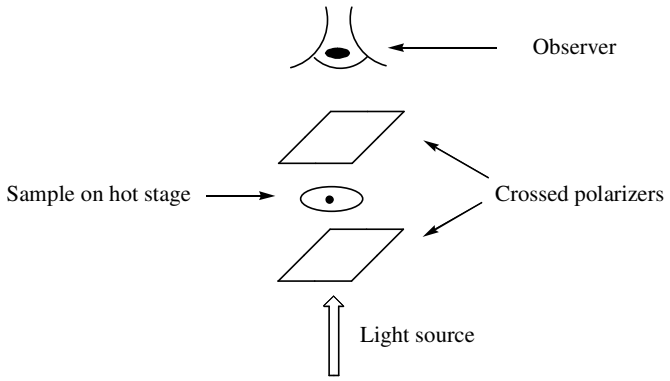

Figure 1.7 Schematic representation of Polarizing Optical Microscopy (POM)

A small amount, approximately 1-2 mg of the sample, is placed between two microscope cover slips and is positioned on the hot stage. This hot stage is made of silver, because of its high thermal conductivity, and can be heated or cooled by means of a computer-driven temperature controller. The microscope is equipped with two polarizers; one is placed between the light source and the hot stage and the other is localized between the hot stage and the observer. The polarizers can be rotated, but are typically placed in a crossed configuration. This means their

polarization directions are perpendicular. In this way, only birefringent materials, like most mesophases, can cause an image to appear. Isotropic materials, like the isotropic molten phase, are not birefringent and therefore cannot cause an image to occur.

The best textures are obtained when the sample is cooled from the isotropic liquid. These are called natural textures. The sequence in which the different textures are observed upon heating or cooling can also be diagnostic for the mesophase transitions. The natural texture of a nematic phase (N) occurred when 4-nonyloxybenzoic acid is cooled from the isotropic phase (Figure 1.8)[10].

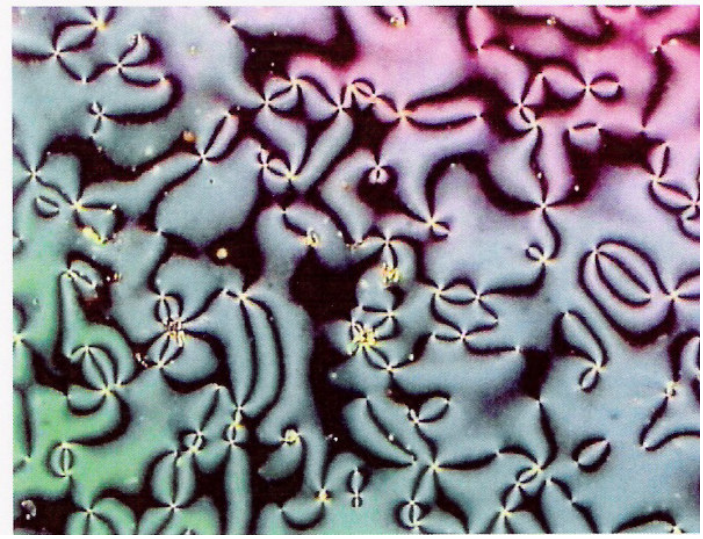

Figure 1.8 Schlieren texture of a nematic phase[10]

Typical characteristics for a nematic phase is the presence of dark brushes called Schlieren, which seem to emerge from bright spots in the texture. These 'spots'

are called singularities and are formed when areas of differently oriented molecules collide. A typical picture of smectic A is given (Figure 1.9).

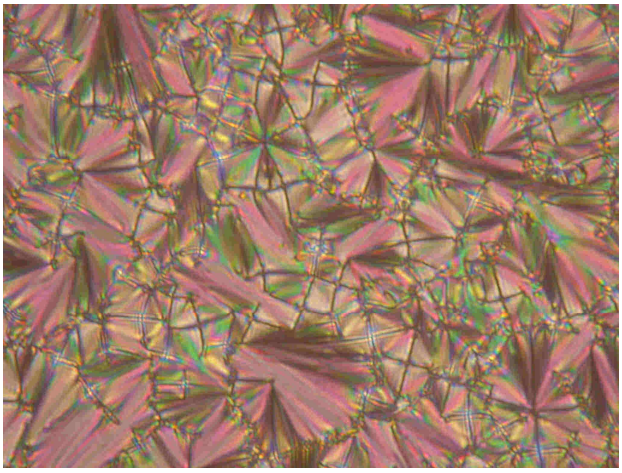

Figure 1.9 Texture of a smectic A phase[11]

The fan-shaped texture occurs when cooling from the isotropic liquid. During the cooling, rod-like features appear first and these are called batonnets. Gradually these batonnets coalesce to form the fan-shaped texture. A typical texture of a hexagonal phase is shown in Figure 1.10.

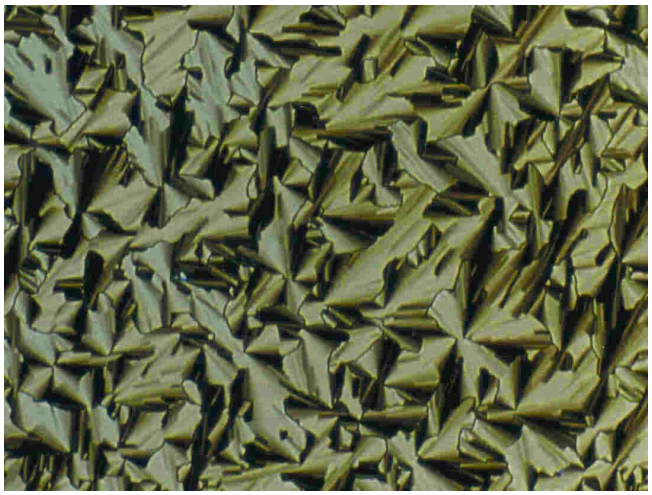

Figure 1.10 Texture of a hexagonal phase[11]

Hexagonal columnar phase is different from the textures of nematic phase and smectic phase.

1.3.2 Differential Scanning Calorimetry (DSC)

Many physical or chemical transformations are associated with heat absorption (endothermic) or heat evolution (exothermic). These events are easily detected by a difference in temperature and heat flow between a sample and an inert reference material. Since liquid crystals show physical and/or chemical transformations by increasing the temperature, which involve a change in enthalpy or heat capacity, DSC is a widely used technique in the investigation of the thermal behavior of these compounds. A DSC thermogram of 4-nonyloxybenzoic acid[2] is given in Figure 1.11.

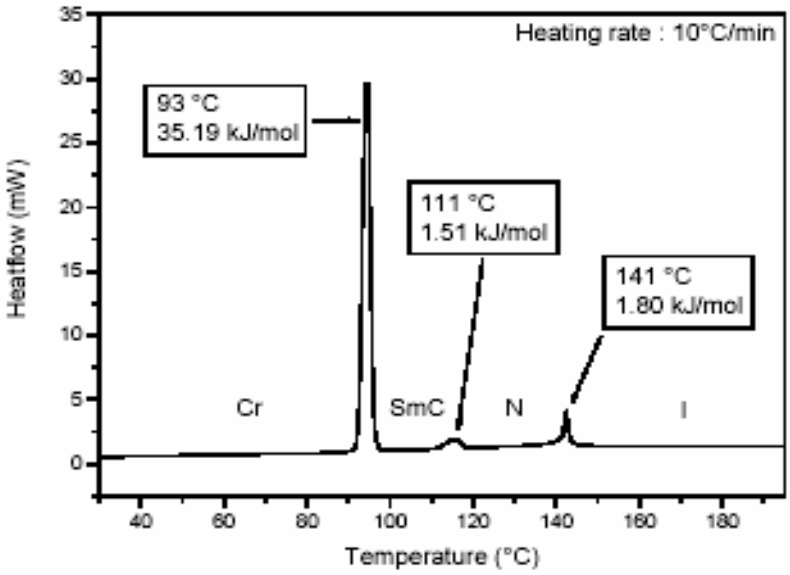

Figure 1.11 DSC thermogram of 4-nonyloxybenzoic acid[2]

Typically enthalpy changes between successive liquid-crystalline phases or between a liquid-crystalline phase and an isotropic liquid (clearing enthalpy) are small and at around 1-10 kJ/mol, while transitions between a crystal and a liquid-crystalline phase (melting enthalpy) are strongly first order and often in the range 20-50 kJ/mol. Typically heating rates are 10^{o}C/min. DSC provides information on enthalpy of phase transitions which cannot be obtained from POM. DSC cannot be used to identify mesophases as POM is used. Thus the two methods, DSC and POM are complimentary to each other for the characterization of liquid-crystalline materials.

1.3.3 X-Ray Diffraction (XRD)

X-ray diffraction is a very useful method of identifying liquid crystal phases and determining how the molecules pack together. X-rays interact with the electrons in a material and pick out any periodically repeating features of a structure. The X-ray technique is based on Bragg's law, which relates the angle of incidence of the X-ray beam θ with the X-ray wavelength λ and the distance d between two planes.

$$n\lambda = 2d\sin\theta \qquad (1.1)$$

The diffraction pattern of all the phases (mesophases) gives a very small number of independent Bragg reflections plus considerable structured diffuse scattering due to the large amount of disorder always present in these phases. For a true crystal the diffraction pattern consists of infinitely sharp peaks. For an isotropic phase only a diffuse peak is observed. For a liquid-crystalline phase the diffraction pattern shows generally one peak that is broadened at the base. Thus the liquid

crystalline phase shows X-ray characteristics that are intermediate between those of a true crystal and of a true isotropic fluid.

1.4 Applications of Liquid Crystals

Liquid crystal technology has had a major effect in many areas of science and engineering, as well as device technology. Applications for this special kind of materials are still being discovered and continue to provide effective solutions to many different problems.

1.4.1 Liquid crystal displays

By far the most important application of liquid crystals is in display devices. Liquid crystal display devices (LCDs) are now used in a wide range of equipment and apparatus such as watches, calculators, portable colour televisions, lap-top computer screens, car, and ship and aircraft instrumentation.

Liquid crystal display devices offer excellent features that are not provided by other types of display. LCDs are of a flat-panel design and are of low power consumption (mW). They are small and compact and hence used in portable displays. Another important feature of LCDs is the fast switching speed (ms-ms). The most common LCD that is used for everyday items like watches and calculators is called the twisted nematic (TN) display. A liquid crystal cell consists of a layer of nematic mesophase liquid crystal material between two glass plates with grooves. The glass plates have to be covered by a conductive layer. The direction of the grooves of the two glass plates are at 90^{o} to one another.

When the liquid crystal material comes into contact with the grooved surface of the glass plate, the molecules line up parallel along the grooves as shown in Figure 1.12a.

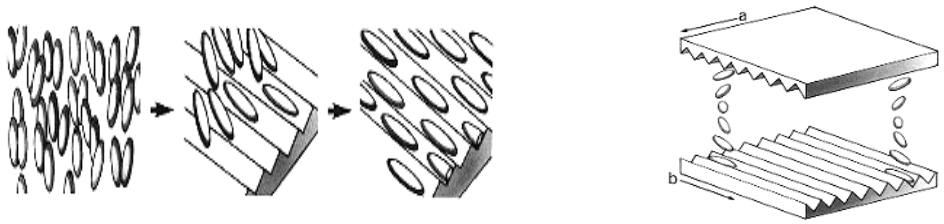

(a) (b)

Figure 1.12 Molecules line up in (a) the grooved surface of the glass and (b) shows liquid crystal molecules in a twisted structural arrangement[12]

When liquid crystal material is sandwiched between the two glass plates, the molecules line-up with grooves pointing in directions 'a' and 'b' into a twisted structural arrangement as shown in Figure 1.12b. When light passes through the liquid crystal cells it follows the direction in which the molecules are arranged. When the molecule arrangement is twisted 90^{o}, the light also twists 90^{o} as it passes through the liquid crystals.

The molecules in liquid crystals are easily rearranged by applying voltage or another external force. When voltage is applied, molecules rearrange themselves vertically and light passes straight through along the arrangement of molecules. When voltage is applied to a combination of two polarizing filters and twisted liquid crystal, it becomes a liquid crystal display (LCD). The principle of twisted nematic liquid crystal display is shown in Figure 1.13.

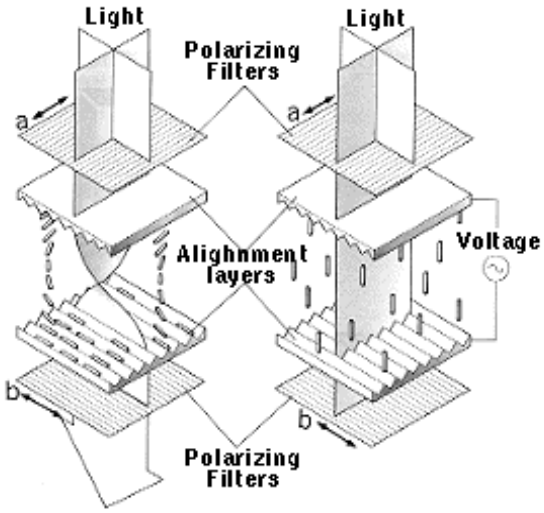

Figure 1.13 Principle of twisted nematic Liquid crystal displays (LCDs)[12]

When two polarizing filters are arranged along perpendicular polarizing axes, light entering from above is redirected 90^{o} along the helix arrangement of liquid crystal molecules so that it passes through the lower filter. When voltage is applied, the liquid crystal molecules straighten out of their helix pattern and stop redirecting the angle of the light, thereby preventing light from passing through the lower filter and the entire device appears dark. In this way, applying voltage can be used to make a pixel switch between clear or dark on command. Colour LCD systems use the same technique, with coloured filters used to generate red, green, and blue pixels.

One of the advantages of liquid crystal displays is its ease of viewing. Flat panel TV displays like LCDs and Plasmas are significantly brighter and feature higher contrasts than traditional cathode-ray tube (CRT) sets. An LCD television will perform exceedingly well under ambient light conditions. TV can be watched

almost anywhere in a room since flat-screen LCD television displays can have up to a 160^{o} viewing angle.

1.4.2 Liquid crystal thermometers

Certain liquid crystals reflect light with a wavelength equal to the pitch (the spacing between layers of similar orientation) and the reflected light will appear coloured. As the temperature of the liquid crystal changes, the spacing between layers also changes. The change in spacing changes the wavelength of the reflected light and its observed colour. Thus liquid crystals make it possible to accurately gauge temperature just by looking at the colour of the thermometer. By mixing different compounds, a device for practically any temperature range can be built. Special liquid crystal devices can be attached to the skin to show a "map" of temperatures. This is useful in finding tumors, because it has a different temperature than the surrounding tissue. Liquid crystal temperature sensors can be used to find bad connections on a circuit board by detecting the characteristic higher temperature.

1.4.3 Optical imaging

In this technology, a liquid crystal cell is placed between two layers of a photoconductor. Light is applied to the photoconductor, which increases the material's conductivity. This causes an electric field to develop in the liquid crystal corresponding to the intensity of the light. The electric pattern can be transmitted by an electrode, which enables the image to be recorded. This

technology is still being developed and is one of the most promising areas of liquid crystal research.

1.4.4 Other Liquid crystal applications

Liquid crystals have a multitude of other uses[13]. They are used for nondestructive mechanical testing of materials under stress. This technique is also used for the visualization of RF (radio frequency) waves in waveguides. They are used in medical applications where, for example, transient pressure transmitted by a walking foot on the ground is measured. Low molar mass (LMM) liquid crystals have applications including erasable optical disks, full colour "electronic slides" for computer-aided drawing (CAD), and light modulators for colour electronic imaging.

1.5 Metallomesogens

Metallomesogens are transition metal complexes with ligands that exhibit liquid-crystalline character[14]. Metal containing compounds that exhibit mesomorphism can be either organometallic or classical inorganic coordination complexes[15]. Currently there is much interest in the synthesis and characterization of liquid-crystalline materials containing metal atoms because of the potential to modify many physical properties *via* the inclusion of a metal centre[17]. The introduction of an electron-dense metal centre should influence properties such as birefringence and dielectric anisotropy. The scope for these metallomesogens is great, since metals show a remarkable variety of geometries in addition to the linear, trigonal or tetrahedral arrangements exhibited by carbon. Since every metal atom features

large and polarizable electron density and many have unpaired electrons and are deeply coloured, the inclusion of metals opens up possibilities of new physical properties for the liquid crystals. Liquid-crystalline materials containing transition metals are attracting special attention because of the ability of the transition metal centre to impart unique optical, magnetic and electrical properties[17].

1.5.1 Early Work on Metallomesogens

Vorlander reported the first thermotropic metal-containing liquid crystal in 1910[18]. He discovered that the alkali-metal carboxylates, $R(CH_2)_nC(O)ONa$, formed classical lamellar phases characteristic of soaps. Later, in 1923, he also found that the diarylmercury Schiff bases $(RC_6H_4CH=NC_6H_4)_2Hg$ form smectic phases[19]. Other alkali and alkaline earth salts of carboxylic acids with organized mesophases were characterized by Skoulios and his collaborators[20], while the smectic ferrocenyl Schiff bases were synthesized by Malthete and Billard in 1976[21]. Giroud and Muller-Westerhoff reported the mesogenic nickel and platinum dithiolenes[22] in 1977 and were the first to seek advanced materials (novel substances for electronic, optoelectronic and related applications) among such compounds.

This work laid the foundations for the study of mesogens containing d-block elements and marked the practical beginning of interest in the subject. Since then many new types of metallomesogens have been synthesized by using different varieties of ligands; monodentate (4-substituted pyridines[21-25], isonitriles[26], cyanobiphenyl derivatives[27]), bidentate (salicylaldimine derivatives, β-diketonates, dialdehydes, aminoketones, dithiobenzoates, glioxymates, alkanoates

etc.) [28-37], or polydentate (phthalocyanines[38-44], porphyrins[45-47], triazine[48,49], triphenylene[50-53]).

Since mesophase formation depends on the intermolecular forces and the space around the metal occupied by the ligand, the properties of metallomesogens are dominated by the ligands and their arrangement, in other words by the overall shape of the molecule. Thus, for example, long monodentate ligands or bidentate ones with small bite angles will tend to give rod-like nematics and smectics, while flat space-filling polydentate ligands (for example macrocycles) will give discotic materials.

Another type of metallomesogens is metal-containing ionic liquid crystals. Ionic liquid crystals are ionic compounds, having liquid crystalline properties with low melting points (below 100°C). The groups of Bruce[54] and Seddon[55] reported results of metal-containing liquid crystals based on imidazolium salts which can also be classified as organometallic liquid crystals because of the metal-carbon bonds. A typical example of this type is given below.

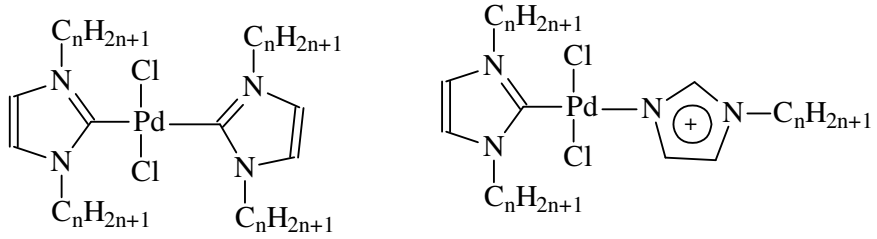

Figure 1.14 Metal containing liquid crystals based on imidazolium salts

The thermal stability of these compounds depends on the chain length; the longer the chain, the more stable the compound. The ordered environment and the unique structural properties possessed by metal-containing ionic liquid crystals can benefit the formation of nanomaterials with specific structure.

Recently Bruce and co-workers[56,57] reported that the mesomorphism can change from the typical calamitic materials to discotic mesogens, simply by varying the chain length. Tetracatenar mesogens of the type shown below were used.

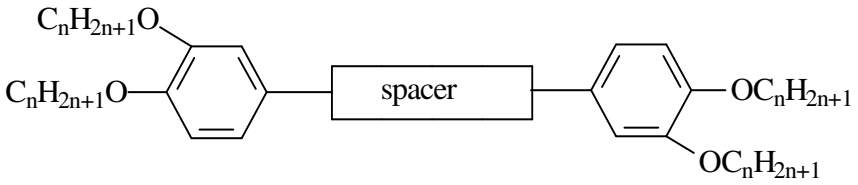

Figure 1.15 Tetracatenar mesogens

The compounds were constructed from long, rod-like cores that possessed four terminal chains arranged symmetrically. For short chain lengths the compounds displayed nematic and/or smectic C phases, while for longer chain lengths, they showed columnar phases.

1.5.2 Structural design of calamitic metallomesogens

The rod-shaped calamitic metallomesogens contain rigid central cores, with metal and the ligating atoms consist of ring structure phenyl or heterocycles, while flexible *n*-alkyl or –alkyloxy tails extend out along the molecular axes. The resulting rod-like polarizable core, together with the flexible end chains increase the molecular anisotropy and facilitate liquid crystal features[17].

The magnitudes of the weak dipole-dipole and disperson forces, which hold thermotropics together are critical: when they are too weak or when they are too strong, the liquid crystalline character is lost. Hence the molecular features, which optimize thermotropic behaviour, are very important.

1.6 Thiophene as building block

Thiophenes are aromatic compounds that display properties close to those of arenes. The thiophene molecule, C_4H_4S (Figure 1.16), is a five-membered, electron excessive heterocycle with excellent charge transfer properties. Thiophene has occupied an important position, firstly, because of its stability and secondly because of the versatility of the thiophene moiety in lending itself to synthetic modification.

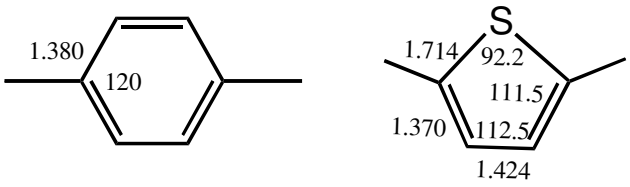

Figure 1.16 Structural properties of phenylene[58] vs thiophene[59] units

When comparing 1,4-disubstituted benzene units in chain structures, thiophene can change the polarity, polarizability and also the geometry of the compounds. This will alter the types of mesophases, phase transition temperatures, dielectric constants and other properties of mesogens. Thiophene systems generally have lower melting points because of poorer efficient packing in the solid state. The molecules have strong lateral dipoles with negative dielectric anisotropy and do

not require additional substituents such as F, CN, etc. to enhance these features. Additional substituents increase the breadth of the rod and can alter the viscosity of the system. Whereas 1,4-phenylene units promote linear structures, thiophene causes kinks or small bends in the chain. Because of these features thiophene-containing organic liquid crystals have been investigated extensively,[60-64] but as part of metallomesogens have greatly been neglected and we are not aware of any examples. In addition, five-membered heterocycles such as thiophene and pyrrole have widely been used as building blocks for the design of well-defined linear π-conjugated oligomers and polymers[65]. Conducting polymers based on thiophene and/or pyrrole have been reported to be soluble, and exhibit ordered crystalline or side chain liquid crystal phases [66]. Crystallinity or liquid crystallinity in these materials can provide not only an insight into the electronic conductivity, but is also expected to lead to new applications that exploit anisotropic behaviour associated with the discrete, orthogonal conductivity mechanisms along the conjugated strands of the polymer material and between adjacent strands. In addition to this, the anisotropic properties associated with the liquid crystal phases might be manipulated or switched through some external stimulus. Although significant progress has been made in the synthesis of soluble/processible polymer systems, very few examples of conducting polymer systems that exhibit liquid crystal phases have been reported[60].

1.7 Dithiocarboxylate ligands

The dithiocarboxylate ligand, RCS_2, is a strong bidentate chelating ligand with donor sulfur atoms. RCS_2 is considerably stable in complexes (all melt without

decomposition) contrary to the low chemical stability of the free ligands[67]. Reactions of dithiocarboxylates and derivatives were extensively studied in the period 1967-1975 resulting in some fascinating chemistry and new structurally interesting complexes[68-70]. Many structural types with different modes of coordination of dithiocarboxylate ligands with metals have been documented. These include four-membered chelate rings, bridging dithiocarboxylate ligands and sulfur inserted perthiocarboxylate ligands. Complexes with dithiocarboxylate ligands displaying liquid crystalline properties have been reported for Ni, Zn, Pd and Pt transition metals[33,71].

1.8 Aim of study

The main objective of this study was to synthesize metal complexes with ligands containing alkyl thiophene units in rod-like structures. The focus of the study was to find out the effect of the structural features of the new complexes and also to investigate their thermal properties. Dithiocarboxylate complexes of nickel(II) and zinc(II) with alkyl or alkyloxy substituted phenyl ring are reported to be mesomorphic[22,33,72-77] whereas there are no known dithiocarboxylate complexes of nickel(II) or zinc(II) with alkyl or alkyloxy substituted thiophene. Figure 1.17 shows the alkylthiophene dithiocarboxylate complexes of Ni(II) and Zn(II). Another feature of interest is the electronic properties of thiophene adjacent to the coordinating CS_2 and the length of the alkyl chain.

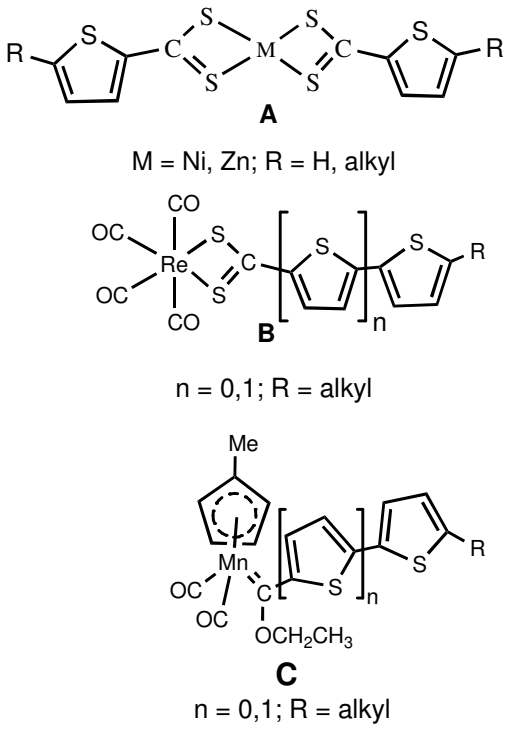

Figure 1.17 Target complexes with thiophene-containing ligands

The first chapter gives an overview of liquid crystals, their applications, early work on metallomesogens and structural design of calamitic metallomesogens. In the first part of the study, the synthesis, characterization, structural features and the liquid crystalline properties of the new complexes of nickel(II) with 5-alkyl-2-thiophenedithiocarboxylate ligands are investigated. The synthesis of the alkyl thiophene dithiocarboxylate ligands make use of known procedures adapted from dithiobenzoate[71] synthesis and is modified to accommodate thiophene chemistry. Due to the diversity of the coordination modes recorded for dithiocarboxylate ligands with nickel(II), a careful assessment of the molecular structures was required. It is anticipated that the thiophene could play a major role in determining coordination modes as it is in direct π-contact via the coordinating CS_2 moiety

with the metal. The same ligands used for nickel were also used for zinc(II) complexes (Figure 1.17**A**). The nickel(II) complexes are d^8 systems whereas the zinc(II) complexes are d^{10} and both could give tetrahedral complexes. A comparison of coordination properties, the structural features and melting point behaviour of the new complexes were studied. In the second part of the study potential rod-like liquid crystalline properties of organometallic compounds were investigated. Two different types of complexes of group VII transition metals were selected, both containing carbonyl ligands. Firstly, the same dithiocarboxylate ligands were reacted as before to give $[Re(CO)_4(S_2CTR)]$ (Figure 1.17**B**) and this work was extended to include bithiophene. Bithiophene will lead to a greater polarization in the chain compared to thiophene. A weak point in this design is the many labile carbonyl ligands present in the complexes. However, luminescent rhenium(I) tricarbonyl complexes with long alkyl chains as spacers and terminal cyanobiphenyl groups displayed various mesophases[78]. Carbene ligands of the Fischer-type will also display strong polarization effects because of the very electron positive carbene-carbon atom coordinated to the metal. This effect is studied again by including bithiophene in the ligand. Until now, no carbene complexes displaying mesophases have been studied. To prevent mass loss by carbonyl elimination under thermal condition the very stable $Mn(\eta^5\text{-}C_5H_4Me)(CO)_2$ metal fragment was selected[79] (Figure 1.17**C**). The rod-like structure is induced by attaching alkyl chains to the carbene ligand. The carbene complexes are expected to have low melting points because of the substituted cyclopentadienyl ($[Mn(\eta^5\text{-}C_5H_4Me)(CO)_3]$ is an oil) ligand and are of interest to study.

REFERENCES

1. B. Wunderlich and J. Grebowicz, *Adv. Polym. Sci*., **1984**, 60, 2.
2. K. Lodewyckx, *Lanthanide-containing Liquid Crystals with Schiff's base ligands*, PhD thesis, Katholieke Universiteit Leuven, Belgium, **2003**.
3. P. J. Collings and M. Hird, *Introduction to Liquid crystals, Chemistry and Physics*, Taylor& Francis Ltd, London, **1997**.
4. P. Espinet, M. A. Esteruelas, L. A. Oro, J. L. Serrano and E. Sola, *Coord. Chem. Rev.*, **1992**, 117, 215.
5. D. Demus and L. Richter, *Textures of Liquid crystals*, Verlag Chemie, Weinheim, New York, **1984**.
6. G. W. Gray and J. W. Goodby, *Smectic Liquid Crystals*, Hill, Glasgow, London, **1984**.
7. A. M. Levelut, *J. Chim. Phys*., Paris, **1983**, 80,149.
8. S. Kumar, *Liquid crystals: experimental study of physical properties and phase transition*, University Press (Cambridge), **2001**.
9. P. J. Collings and S. Patel, *Handbook of Liquid Crystal Research*, University Press (Oxford), **1997**.
10. R. Van Deun, *Liquid Crystals with Lanthanides*, PhD thesis, Katholieke Universiteit Leuven, Belgium, **2001**.
11. http://plc.cwru.edu/tutorial/enhanced/files/lc/phase/phase.htm.
12. http://sharp-world.com/sc/library/lcd_e/s2_1_1e.htm.
13. http://dutch.phys.strath.ac.uk/CommPhys2002Exam/David_Wright/08-applications.htm.

14. J. W. Goodby and G. W. Gray, *Handbook of Liquid Crystals*, VCH, Weinheim, New York, **1999**.

15. A. Omenat and M. Ghedini, *J. Chem. Soc. Chem. Commun*., **1994**, 1309.

16. P. M. Maitlis, D. W. Bruce, R. Dhillion, D. A. Dunmur, F. P. Fanizzi, S. E. Hunt, R. Le Lagadec, E. Lalinde, R. Orr, J. P. Rourke, N. J. S. Salt, J. P. Stacey and P. Styring, *New J. Chem.*, **1990**, 14, 549.

17. S. A. Hudson and P. M. Maitlis, *Chem. Rev*., **1993**, 93, 861.

18. D. Vorlander, *Ber. Dtsch. Chem. Ges*., **1910**, 43, 3120.

19. D. Vorlander, *Z. Phys. Chem. Stochiom, Verwandtschaftsl*., **1923**, 105, 211.

20. A. Skoulios, *Ann. Phys*. Paris, **1978**, 3, 421.

21. J. Malthete and J. Billard, *Mol. Cryst., Liq. Cryst*., **1976**, 34, 117.

22. A. –M. Giroud and U. T. Muller-Westerhoff, *Mol. Cryst., Liq. Cryst*., **1977**, 41, 11.

23. D. W. Bruce, *Acc. Chem. Res*., **2000**, 33, 831.

24. D. W. Bruce, *Adv. Inorg. Chem.*, **2001**, 52, 151.

25. D. Fazio, C. Mongin, B. Donnio, Y. Galerne, D. Guillon and D. W. Bruce, *J. Mater. Chem*., **2001**, 11, 2852.

26. M. Benouazzane, S. Coco, P. Espinet, J. M. Martin-Alvarez and J. Barbera, *J. Mater. Chem*., **2002**, 12, 691.

27. T. I. Shabatina, E. V. Vovk, V. A. Timoshenko, Y. N. Morosov and G. B. Segreev, *Colloid Surface A*, **2002**, 198, 255.

28. C. K. Lai, C. H. Chang and C. H. Tsai, *J. Mater. Chem.*, **1998**, 8, 599.

29. S. T. Trzaska and T. M. Swager, *Chem. Mater*., **1998**, 10, 438.

30. S. T. Trzaska, H. X. Zheng and T. M. Swager, *Chem. Mater*., **1999**, 11, 130.

31. L. Diez, P. Espinet and J. A. Miguel, *J. Chem. Soc., Dalton Trans*., **2001**, 1189.

32. U. T. Muller-Westerhoff, A. Nazzal, R. J. Cox and A. M. Giroud, *Mol. Cryst., Liq. Cryst.,* **1980**, 56, 249.

33. H. Adams, N. A. Bailey, D. W. Bruce, R. Dhillon, D. A. Dunmur, S. E. Hunt, E. Lalinde, A. A. Maggs, R. Orr, P. Styring, M. S. Wragg and P. M. Maitlis, *Polyhedron*, **1988**, 7, 1861.

34. M. A. Guillevic, T. Gelbrich, M. B. Hursthouse and D. W. Bruce, *Mol. Cryst., Liq. Cryst*., **2001**, 362, 147.

35. M. Ghedini, D. Pucci, A. Crispini and G. Barberio, *Organometallics*, **1999**, 18, 2116.

36. A. Pegenau, T. Hegmann, C. Tschierske and S. Diele, *Chem. Eur. J*., **1999**, 5, 643.

37. A. M. Giroud-Godquin and P. M. Maitlis, *Angew. Chem. Int. Ed. Engl*., **1991**, 30,375.

38. C. Piechocki, J. Simon, A. Skoulios, D. Guillon and P. Weber, *J. Am. Chem. Soc*., **1982**, 104, 5245.

39. A. G. Gurek, V. Ahsen, F. Heinemann and P. Zugenmaier, *Mol. Cryst., Liq. Cryst*., **2000**, 75, 338.

40. K. Msayib, S. Makhseed and N. B. McKeown, *J. Mater. Chem*., **2001**, 11, 2784.

41. R. Naito, K. Ohta and H. Shirai, *J. Porphyrins Phthalocyanines*, **2001**, 5, 44.

42. J. C. Swarts, E. H. G. Langmer, N. Krokeide-Hove and M. J. Cook, *J. Mater. Chem.*, **2001**, 11, 434.

43. A. N. Cammidge and H. Gopee, *Chem. Commun.*, **2002**, 966.

44. J. Sleven, T. Cardinaels, C. Gorller-Walrand and K. Binnemans, *ARKIVOC*, **2003** (iv), 68.

45. D. W. Bruce, *J. Chem. Soc., Dalton. Trans.*, **1993**, 2983.

46. W. Liu and T. S. Shi, *Acta. Chim. Sin.*, **2001**, 59, 466.

47. M. Castella, F. Lopez-Calahorra and D. Velasco, *Liq. Cryst.*, **2002**, 29, 559.

48. R. Bai, S. Li and Y. F. Zou, *Liq. Cryst.*, **2001**, 28, 1873.

49. C. H. Lee and T. Yamamoto, *Bull. Chem. Soc. Japan*, **2002**, 75, 615.

50. S. Kumar, M. Manickem, S. K. Varshney, D. S. S. Rao and S. K. Prasad, *J. Mater. Chem.*, **2000**, 10, 2483.

51. B. Y. Tang, J. J. Ge and A. Q. Zang, *Chem. Mater.*, **2001**, 13, 78.

52. A. N. Cammidge and H. Gopee, *J. Mater. Chem.*, **2001**, 11, 2773.

53. I. D. Olenik, L. Spindler, M. Copic, H. Sawade, D. Kruerke and G. Heppke, *Phys. Rev. E.*, **2002**, 6501.

54. C. J. Bowlas, D. W. Bruce and K. R. Seddon, *Chem Commun.*, **1996**, 1625.

55. J. T. Hamill, C. Hardcre, M. Nieuwenhuyzen, K. R. Seddon, S. A. Thompson and B. Ellis, *Chem. Commun.*, **2000**, 1929.

56. A. I. Smirnova, D. Fazio, E. Fernandez Iglsias, C. G. Hall, D. Guillon, B. Donnio and D. W. Bruce, *Mol. Cryst., Liq. Cryst*., **2003**, 396, 227.

57. B. Donnio, B. Heinrich, H. Allouchi, J. Kain, S. Diele, D. Guillon and D. W. Bruce, *J. Am. Chem. Soc*., **2004**, 126, 15258.

58. F. H. Allen, O. Kennard, D. G. Watson, L. Brammer, A. G. Orpen and R. Taylor, *J. Chem. Soc., Perkin Trans*., **1987**, 2, S1.

59. R. Angelici, *Coord. Chem. Rev.,* **1990**, 105, 61.

60. S. Abe, M. Kijima and H. Shirakwa, *J. Mater. Chem*., **2000**, 10, 1509.

61. I.A. Levitsky, K. Kishikawa, S.H. Eichhorn and T.M. Swager, *J. Am. Chem. Soc*., **2000**, 122, 2474.

62. J.D. Bunning, J.L. Butcher, D.J. Byron, A.S. Matharu and R.C. Wilson, *Liq. Cryst*., **1995**,19, 693.

63. L-H. Wu, Y-C. Wang and C.S. Hsu, *Liq. Cryst*., **2000**, 27, 1503.

64. X.M. Dai, H. Narihiro, H. Goto, K. Akagi and H. Yokoyama *Synth. Met*., **2001**, 119, 397.

65. D. Delaere, M. T. Nguyen and L. G. Vanquickenborne, *J. Phys. Chem. A*, **2003**, 107, 838.

66. J. Roncali, *Hand book of conducting polymers 2nd Edn*., New York, **1998**.

67. C. Furlani and M. L. Luciani, *Inorg. Chem.*, **1968**, 7, 1586.

68. D. Coucouvanis and J. P. Fackler (jr), *J. Am. Chem. Soc*., **1967**, 89, 1346.

69. J. P. Fackler (jr), W. Seidel and J. A. Fetchin, *J. Am. Chem. Soc*., **1968**, 90, 2707.

70. J. P. Fackler (jr), *Inorg. Chem*., **2002**, 41, 6959.

71. H. Adams, A. C. Albeniz, N. A. Bailey, D. W. Bruce, A. S. Cherodian, R. Dhillon, D. A. Dunmur, P. Espinet, J. L. Feijoo, E. Lalinde, P. M. Maitlis, R. M. Richardson and G. Ungar, *J. Mater. Chem*., **1991**, 1, 843.

72. M. Bonamico, G. Dessy, V. Fares and L. Scaramuzza, *J. Chem. Soc., Dalton Trans*., **1975**, 2250.

73. M. Bonamico, G. Dessy and V. Fares, *J. Chem. Soc., Chem. Commun*., **1969**, 1106.

74. M. Bonamico, G. Dessy and V. Fares, *J. Chem. Soc., Dalton Trans.,* **1977**, 2315.

75. C. Bellito, G. Dessy and V. Fares, *Inorg. Chem*., **1985**, 24, 2815.

76. K. Umakoshi and Y. Sasaki, *Adv. Inorg. Chem*., **1994**, 40, 187.

77. K. Ohta, H. Ema, I. Yamamoto and K. Matsuzaki, *Liq. Cryst*., **1988**, 3, 1671.

78. T. Cardinaels, K. Driesen, T. N. Parac-Vogt, B. Heinrich, C. Bourgogne, D. Guillon, B. Donnio, and K. Binnemans, *Chem. Mater*., **2005**, 17, 6589.

79. U. Schubert, *Organometallics*, **1982**, 1, 1085.

Chapter 2

Nickel(II) complexes with thiophene-containing ligands

2.1 Introduction

Many classical inorganic nickel(II) complexes with rod-like structures and N and/or O donor-atom ligands, such as bidentate β-enaminoketones[1,2], tropolonates[3] and salicylaldimine[4] have been studied for their liquid crystalline properties. Disc-shaped nickel(II) mesogens have been reported with phthalocyanine[5,6] and alkoxy hydrazine[7] ligands.

An important class of nickel(II) complexes are those with sulfur donor-atoms such as thiols, dithiolene and dithiocarboxylate as ligands[8,9]. The chemistry of nickel(II) thiolate complexes has attracted attention and has been studied widely because of the identification of nickel in the active site of the enzyme hydrogenase in biological systems[10]. Since the colour remains an important issue in liquid crystalline displays the role of nickel(II) in liquid crystalline materials must not be underestimated for potential application[11,12]. The first mesogenic nickel(II) complexes were those with dithiolene ligands and were studied by Giroud and Muller-Westerhoff, in 1977[13].

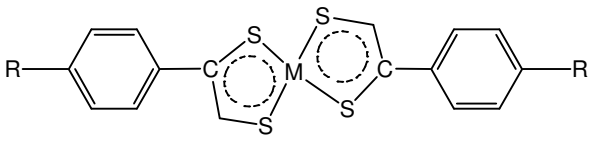

M = Ni, Pd, Pt

The first example of a nematogenic nickel(II) metallomesogen reported was a complex substituted with terminal butyl chains[13] (above). For compounds with longer alkyl chains, smectic mesomorphism was observed. The nickel(II) and platinum(II) complexes displayed enantiotropic mesophases, which were nematic for the shorter chains and smectic for the longer alkyl chains while the corresponding palladium complexes did not show any mesomorphic properties. As intermolecular forces play an important role in the mesophase character, the lack of mesomorphism may be due to the strong Pd-Pd bond.

In addition to the calamitic (rod-like) metallomesogens, Ohta *et al.*[14] reported disc-shaped metallomesogens for nickel and dithiolenes. Nickel(II) dithiolene with four 3,4-bis(dodecyloxy)phenyl substituents was shown by X-ray diffraction to give rise to a hexagonal disordered columnar (discotic) mesophase.

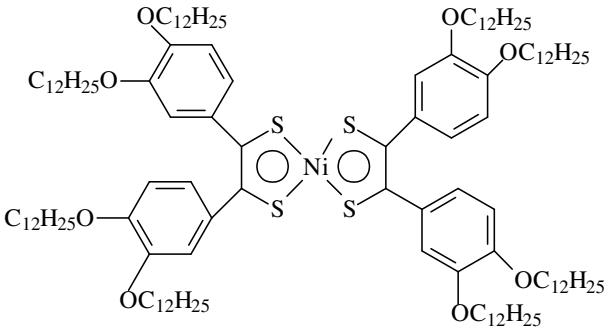

Of the piperazine dithiocarbamate complexes of palladium, nickel, copper and zinc only the nickel and copper derivatives showed liquid-crystalline behaviour[15]. Both the nickel and copper complexes showed similar phase behaviour for the

hexyloxy chain. On cooling from the isotropic liquid a highly birefringent, schlieren texture of smectic C was observed.

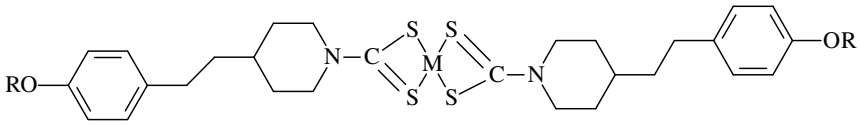

M = Pd, Ni, Cu, Zn

The mesogenic properties of bis(p-alkylphenyldithiolate) complexes of nickel(II) and platinum(II) were reported by Mueller-Westerhoff in 1980[16].

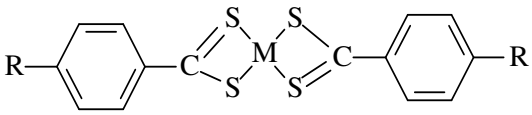

M = Ni, Pt; R = alkyl or alkyloxy substituents

In 1988 Adams *et al.*[17] synthesized the mesomorphic 4-alkyloxydithiobenzoate derivatives of Ni, Pd and Zn. The mesomorphism of nickel(II) and palladium(II) complexes were similar, showing smectic C phases for longer alkyl chains ($n \geq 8$). In general, the melting points of the palladium complexes were 20-30^{o}C higher than those of the nickel complexes, whereas clearing points were about 80^{o}C higher.

Adams *et al.*[18] as well as Ohta and co-workers[19] undertook detailed studies on the liquid crystalline properties of 4-alkyloxydithiobenzoate derivatives. The 4-alkyloxydithiobenzoates of Zn, Ni and Pd are highly dichroic and can be used in liquid crystal displays. The strongly coloured mesomorphic dithiolates prepared by Giroud and Muller-Westerhoff[16] were investigated as potential dyes in guest-host systems, by incorporation of the mesomorphic derivatives into nematic hosts[20]. The linear dichroism of the 4-alkyloxydithiobenzoates of nickel(II) was

also measured by the Sheffield group[21] in the nematic solvent and reported that those complexes were not suitable as dyes for displays.

In 1988 Ohta *et al*. employed alkyldithiocarboxylate as ligands to form dimeric nickel(II) complexes that exhibited monotropic smectic phases[22]. They also employed alkoxydithiocarboxylate to form monomeric nickel(II) complexes that exhibited double and triple melting behaviour. In nickel(II) and platinum(II) complexes the dispersion forces are more dominant and dissociation into the monomer is possible at the temperature of the mesophase.

Earlier literature (1963-1975) have revealed nickel(II) complexes (d^8 electron configuration) displaying a variety of coordination numbers and many different coordination modes for thiol, dithiocarboxylate, dithiocarbamate and trithiocarboxylate ligands[8]. Square-planar, tetrahedral, 5-coordinate, and octahedral geometries are known for nickel(II) with dithiocarboxylate ligands. It has been widely demonstrated that square-planar or square-pyramidal coordination leads to the appearance of liquid crystalline properties, whereas tetrahedral geometry usually inhibits mesophase formation. All the mesomorphic complexes are diamagnetic, which has been interpreted to indicate a square-planar coordination about the metal.

In this study the reactions of a series of 5-alkyl-2-thiophenedithiocarboxylates with nickel(II) chloride were investigated to see if the inclusion of thiophene in the chain would affect the outcome of the reactions and play a role in determining

the melting point behaviour and properties of mesophases. Reactions of dithiocarboxylates and derivatives were extensively studied and resulted in some fascinating chemistry and new structurally interesting complexes[8].

2.2 Results and discussion

2.2.1 Synthesis and characterization

Five complexes of the type $[Ni(S_2CTR)_2]$ (where T = 2,5-disubstituted thiophene, R = alkyl group; C_4H_9 (**1**), C_6H_{13} (**2**), C_8H_{17} (**3**), $C_{12}H_{25}$ (**4**), $C_{16}H_{33}$ (**5**)) were synthesized via a four-step reaction sequence as shown in Scheme 2.1.

The reactions with butyl lithium were carried out with nitrogen-saturated, dried solvents and in an inert atmosphere. The procedure that was used is similar to the one described by Brandsma[23] for the lithiation of thiophene. Step 1 involved the lithiation of thiophene on position 2 followed by the subsequent addition of alkyl bromide. In the second step 2-alkylthiophene was converted into 5-alkyl-2-thiophenedithiocarboxylic acid. It involved the lithiation of alkyl thiophene on position 5 followed by the addition of CS_2, resulting in a deep red colour. On further acidification with dilute hydrochloric acid, 5-alkyl-2-thiophenedithiocarboxylic acid was formed. Subsequently this acid was converted into the sodium salt by reacting with sodium methoxide, again in an inert atmosphere, in the third step. All the intermediates were isolated.

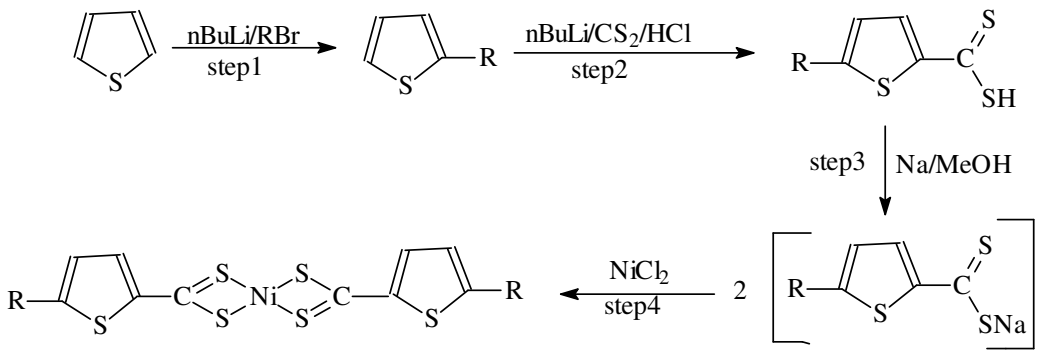

R = alkyl group; C_4H_9 (**1**), C_6H_{13} (**2**), C_8H_{17} (**3**), $C_{12}H_{25}$ (**4**), $C_{16}H_{33}$ (**5**)

Scheme 2.1

The final step was similar to that of Adams *et al.*[18] who prepared complexes with dithiobenzoate ligands. The addition of a pale green solution of nickel(II) chloride to a stirred solution of sodium 5-alkyl-2-thiophenedithiocarboxylate in water, lead to a change in the colour of the reaction mixture from dark red to blue-violet. The mixture was allowed to stir for 3 hours at room temperature to ensure completion of reaction. The product was precipitated by adding excess methanol and separated by filtration and dried. The colours of complexes **1** and **2** were blue whereas the colours of **3**-**5** were violet. Further purification was done on a silica gel column and the product was purified with hexane/CH_2Cl_2 (4:1) as the eluent. IR and NMR spectroscopy were used to characterize the complexes (**1-5**).

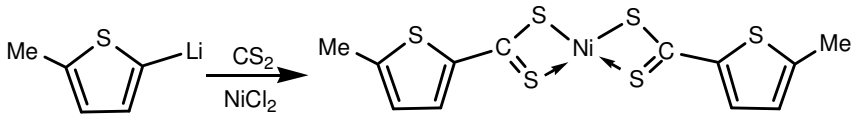

6

Scheme 2.2

In a second method (one-pot reaction), 2-methylthiophene was lithiated by butyl lithium at –20°C in THF. The colour of the solution immediately changed to orange on addition of the BuLi, but changed gradually to yellow after stirring for 30 minutes. The mixture was cooled to -50°C and carbon disulfide was added. The mixture became dark red in colour and was stirred for 30 minutes. Anhydrous nickel(II) chloride was added in small portions and the mixture was allowed to reach room temperature. The yellow solid material gradually dissolved on reacting and the solution changed first to green then to blue and thereafter to violet over a period of three hours. The blue-violet product was purified by filtration of the reaction mixture through a plug of silica gel, once the solvent was changed to dichloromethane and afforded **6** in very high yield (the yield was more than 80%). From this mixture it was possible to isolate both a blue and violet compound by column chromatography with mixtures of hexane and dichloromethane. The blue compound indicated by **6a** was less soluble in organic solvents compared with the violet compound indicated by **6b**. Spectroscopic data revealed that two different products or isomers were present in the reaction mixture.

In a third experiment, the blue complex **1a** was dissolved in THF and stirred at room temperature. A sample was taken after 1 hour and the ^{1}H NMR spectrum was recorded in deuterated chloroform. As stirring continued the colour of the reaction mixture gradually changed from blue to violet. After 12 hours the conversion was complete and only the violet complex (**1b**) could be isolated from the reaction mixture. A similar result was achieved after stirring **2a** for 10 hours. The blue compound converted into the violet compound and after further analysis of the products it was clear that the blue and violet complexes of **1** or **2** could be

isomers (the blue isomers were indicated as **1a** or **2a** and the violet ones as **1b** or **2b**).

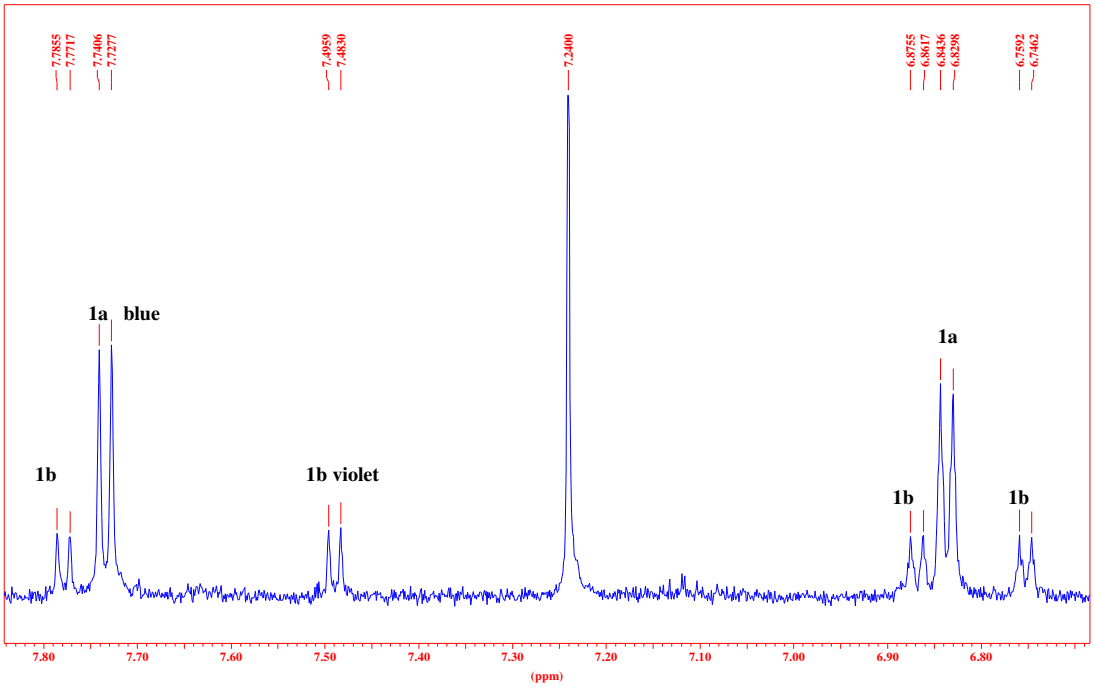

Figure 2.1 ^{1}H NMR spectrum in the thiophene region of **1** (**1a** and **1b**)

In the first method the conversion of the blue isomer into the violet isomer is very slow. In the second method the conversion is much faster, indicating that the solvent facilitates the conversion. THF is a reasonably strong coordinating solvent to transition metals and will assist in stabilizing intermediates during ligand displacement. Figure 2.1 represents the ^{1}H NMR spectrum of compound **1** (**1a** and **1b**) in the thiophene region after withdrawing a sample from the reaction mixture. The sample was taken after 1 hour stirring at room temperature in THF according to the third experiment above. The spectrum shows a mixture of two compounds in different concentrations as indicated by the two sets of resonances. It is

important to note the sharp signals of high resolution for the different protons in the ^{1}H NMR spectrum. This is indicative of diamagnetic and not paramagnetic complexes and implies that the nickel complexes could be square planar or maybe octahedral, but not tetrahedral.

In the first set of resonances, two strong doublets at 7.73 and 6.83 ppm appear in the thiophene region indicating two protons in different electronic environments. This is as a result of the two different substituents in the 2- and 5-positions of the thiophene ring. If **1** has two or more thiophene-containing ligands it means that they are all coordinated to the nickel in a similar fashion. The structures proposed in Figures 2.2 and 2.4 are possible structures that meet this requirement. Similar two-signal resonances were observed for all the blue isomers in the thiophene region of this study.

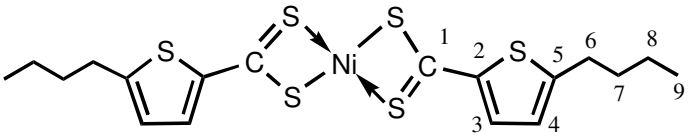

Figure 2.2 Proposed structure of the blue compound, **1a**, with atom numbering

Examples of complexes with two bidentate dithiocarboxylate or dithiocarbamates ligands surrounding one nickel(II) metal have been documented before and a crystal structure determination of $[Ni\{S_2CPh\}_2]$ revealed a flat, square-planar mononuclear nickel(II) complex[24].

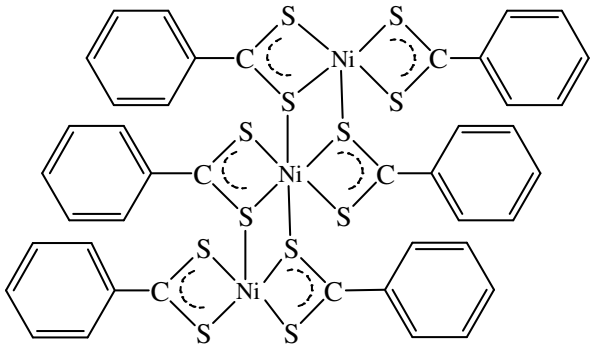

Figure 2.3 Intermolecular interactions between the nickel and sulfur atoms in the solid state of the mononuclear nickel(II) complexes[24]

Structural work confirmed some intermolecular sulfur-metal interaction between chains of square planar complexes for mononuclear [Ni(dithiobenzoate)$_2$] and [Pd(dithiobenzoate)$_2$] complexes in the solid state (Figure 2.3). This interaction will affect the coordination numbers and geometry of the nickel centres in the clusters of three mononuclear complexes. The carbon and the hydrogen attached to the carbons are numbered as shown in Figure 2.2. The carbon in the CS_2 unit is indicated as C1, this procedure of numbering atoms is in line with thiophene numbering schemes where S takes the 1-position. The nickel(II) complexes give deep blue solutions[24,25]. Similar complexes have been reported for diethyldithiocarbamates[26], xanthates[27] and dithiophosphates[28].

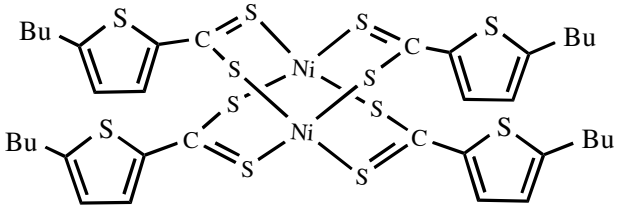

Figure 2.4 Structure of dimeric nickel(II) complexes with bridging R-CS_2 ligands

Another structural type to be considered for **1a** is a dinickel(II) structure with only bridging R-CS_2 ligands (Figure 2.4)[29]. Such a complex will also afford only two doublets of different chemical shifts in the ^{1}H NMR spectrum. Complexes of this kind are quite common and structural data were obtained from single crystal X-ray determinations of $[Ni_2\{S_2CCH_3\}_4]$[30] and $[Ni_2\{S_2CCH_2Ph\}_4]$[31,32]. These complexes were reported to have a red-brown colour in the solid state and in solution[30,32]. Based on the above information, the colours of the reported complexes and the spectral data, the blue isomers **1a**, **2a** and **6a** were assigned to be monomeric, square planar nickel(II) complexes with two terminal bidentate dithiocarboxylate ligands (see Figures 2.2 and 2.10).

Also visible in the thiophene region of the spectrum of **1** (**1a** and **1b**) in Figure 2.1 are four doublets of much weaker intensities. These resonances belong to the spectrum of a second compound, described as the violet compound. The four doublets indicate that there are two thiophene ligands in different electronic environments. Two possible monomeric forms of the complex with composition $[Ni\{S_2C\text{-thiophene-Bu}\}_2]$ can be considered, i.e. **1a** and **1a'** (Figure 2.5). It is known in carbene chemistry that complexes with thienyl substituents may display restricted rotation around the thienyl-carbene carbon bond, resulting in the formation of two isomers with different positions for the sulfur atoms in the thiophene rings[33]. This was ascribed to charge transfer from the thiophene ring via the π-system to the electrophilic carbene carbon atom. A similar situation may exist for an electrophilic carbon atom of a CS_2-unit coordinated to a transition metal and attached to the thiophene ring in **1**. In a square planar complex this will

result in the two sulfur atoms being on the same or on opposite sides of the molecule (Figure 2.5), representing a mixture of geometric isomers.

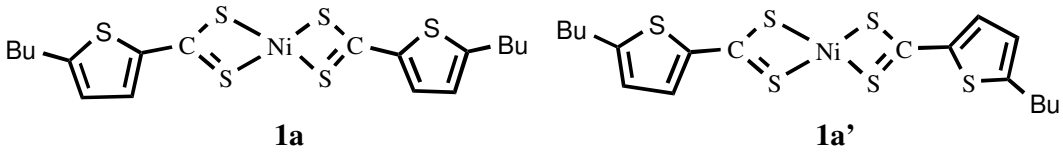

1a **1a'**

Figure 2.5 Mixture of geometrical isomers resulting from restricted rotation

This is not a satisfactorily explanation for the composition of **1b** for a number of reasons. The large differences in chemical shift values would rather indicate either different modes of co-ordination to the nickel(II) by the 2,5-Bu-thiophene-CS_2 ligand or two ligands of totally different composition. The intensities of the resonances of the four protons in the ^{1}H NMR spectrum of **1b** are exactly the same and that would indicate no preference for any one of the two isomers, which is unlikely. Spectra of pure samples of the blue compound, **1a/2a**, are without the violet component, **1b/2b**, and pure samples of the violet compound are without the blue component. Other arguments of importance against the existence of two isomers are different chemical shift values for the two sets of resonances, the large colour difference of the two isomers and an irreversible conversion reaction of the blue into the violet compound.

Many other possibilities exist for mono- and dimeric nickel(II) complexes with RCS_2 ligands and some of the most likely will now be considered and examined. If one of the coordinated sulfur atoms in the chelate ring would change from a thiol and thione to a thiol and thiophene-sulfur, two different types of sulfur donor ligands could be present in the complex (Figure 2.6).

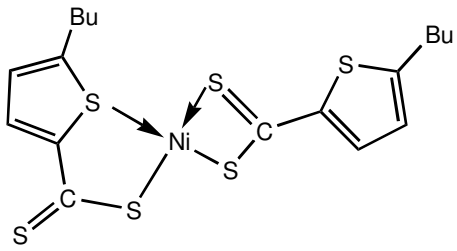

Figure 2.6 Complex with thioether-thiol and thioketone-thiol ligands

These different coordination modes will most definitely result in larger changes in the chemical shift values of the thiophene protons and could also explain the role of THF in the conversion of **1a** to **1b**. Five-membered chelate rings are more stable than four-membered chelate rings that could act as a driving force for the conversion. Arguments against such isomerization processes are the known, poor coordinating abilities of sulfur atoms in thiophene rings to transition metals[34]. This has been ascribed to the involvement of one of the sulfur lone pair electrons in the π-delocalization of electron density over the thiophene ring[35]. Also, in instances where coordination through the thiophene sulfur atom was observed, the sulfur would flip out of the plane of the ring, become sp^3-hybridize and in the process destroy the aromatic character of the thiophene ring[34]. This will result in proton chemical shifts of dienes that are found upfield from the aromatic region. This structural type was eliminated as a possible explanation of the spectral data of **1b** on the basis of the poor coordinating properties of a thiophene sulfur atom.

The conversion and spectroscopic results of **1b** can also be explained by the possibility of two mononuclear nickel(II) complexes forming a dimer by sharing dithiocarboxylate ligands, resulting in one bridging thiophene-containing ligand

for each similar terminal ligand. Two important structures can exist, one with a bridging dithiocarboxylate and the other with bridging sulfur ligands. Figures 2.7 and 2.8 present possible structures of the violet compounds **1b** based on these assumptions.

Structural properties of complexes containing bridging dithiobenzoate ligands in dimetal complexes have been observed for tetrahedrally coordinated Zn(II) and with mononuclear dithiocarbamates tetrahedrally coordinated to Zn(II), Cu(II) and Cd(II) metal centers[17,36].

Complexes of nickel(II) with both terminal and bridging CS_2-ligands and square planar coordination will result in two five-membered chelate rings being perpendicularly orientated if a nickel-nickel bond is assumed. The second isomer, the trans isomer, will have a flat square arrangement of eight atoms. This complex cannot exist because of the small bite angle required by the remaining terminal dithiocarboxylate ligands when forming four membered chelate rings with the nickel centres.

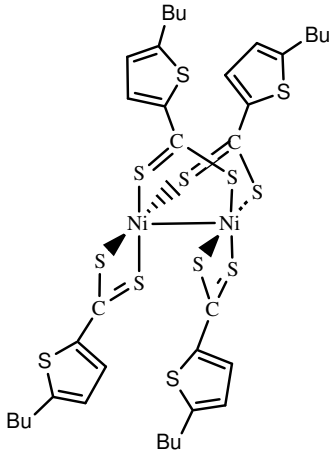

Figure 2.7 Proposed structure of the violet compound **1b**, with bridging CS_2-ligands

As far as we are aware no examples of such *cis*-nickel(II) complexes have been reported but a structure determination of a similar *cis*-[$Pt_2(\mu\text{-dtc})_2(dtc)_2$] (dtc = dithiocumato) complex revealed the coordination modes shown in Figure 2.7[37]. This is a very interesting structural type as on the one side of the complex with the terminal CS_2-ligands, the ligands will form two parallel chains, whereas, they will divert outwards from the metal-metal bond on the other side of the complex. The preferred structures for nickel(II) complexes with bidentate dithiocarboxylate ligands are mononuclear nickel(II) complexes with two terminal dithiocarboxylate ligands when a heteroatom or aryl substituent forms part of the ligands (Figure 2.2)[24] and four bridged dithiocarboxylate ligands when alkyl substituents are part of the ligands (Figure 2.4)[31]. The argument against this type of coordination of RCS_2 for **1b** is that it should generate very similar NMR data compared to **1a**.

Bridging S-ligands, on the other hand, form three membered rings and are again perpendicular in a square planar arrangement of S-ligands around the nickel (II) centers in **1b** (Figure 2.8)[38]. Examples of bridging mercaptide ligands (RS^-) of Ni(II) and terminal trithiocarboxylate ligands are found in literature[38]. The mercaptides form mostly as a result of CS_2 elimination from a trithiocarboxylate ligand and are excellent bridging ligands. As a result of the sp^2-thione carbon in **1b**, now part of the chain and free from being coordinated to the metal, a kink is formed in the chain. This and the orientations caused by substituents in the 2- and 5-positions of the thiophene ring (zig-zag), allows the chains to divert towards the other chains of the terminal CS_2-ligands to still afford a rod-like appearance.

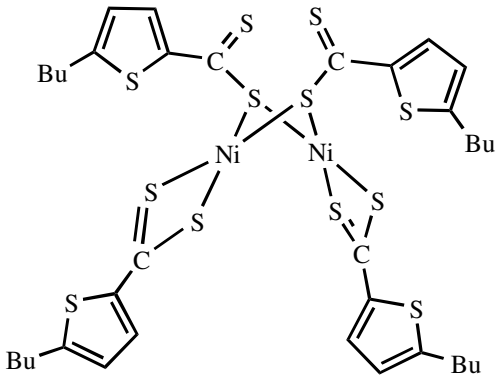

Figure 2.8 Proposed structure of the violet compound **1b**, with bridging S-ligands

Proposed mechanisms for the conversion of a monomer into a dimer for the two classes are presented in Schemes 2.3 and 2.4. The dimer is formed when two monomers interact in an intermolecular fashion. A lone pair of a coordinated sulfur atom of a ligand of the first complex attacks the nickel atom of the second complex and in the process detaches itself from the metal. The same process, but in a reversed way, happens from the second to the first nickel complex. In the process the sulfur atoms of both ligands will bridge two nickel-atoms and form two five- membered rings with two nickel and two sulfur atoms. One ligand remains coordinated to each nickel in the same way as found for the monomer.

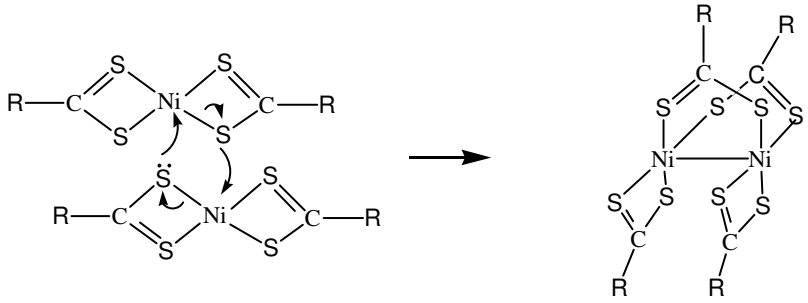

Scheme 2.3 Proposed mechanism for the dimerization of nickel(II) complexes with bridging dithiocarboxylate ligands

Even though it is well-known that trithiocarboxylates and dithiocarbamates would readily eliminate carbon disulphide to afford mercaptides or amines (under acidic conditions), we did not in the context of this project, found literature evidence of the elimination of carbon monosulfide from dithiocarboxylates to yield mercaptides. In this case (**1b**) it means that a sulfur atom will rather bridge and not use the available thione sulfur to form a five-membered chelate ring. It is worth mentioning that the coordinating properties of 2-aminocyclopentene-1-dithiocarboxylate were studied and revealed that bonding with metal ions occurred through the amino nitrogen and deprotonated thiol sulfur atoms leaving the thione uncoordinated[39]. Previous arguments of the coordinating abilities of thiophene sulfur atoms ruled out possible competition for a coordination site by this atom (Figure 2.6) as such was the case with amino-dithiocarboxylates. On the other hand, it was assumed that the nucleophilicity of a coordinated sulfur to nickel(II) was too low to compete with an available thione in the coordination to a second nickel(II) center.

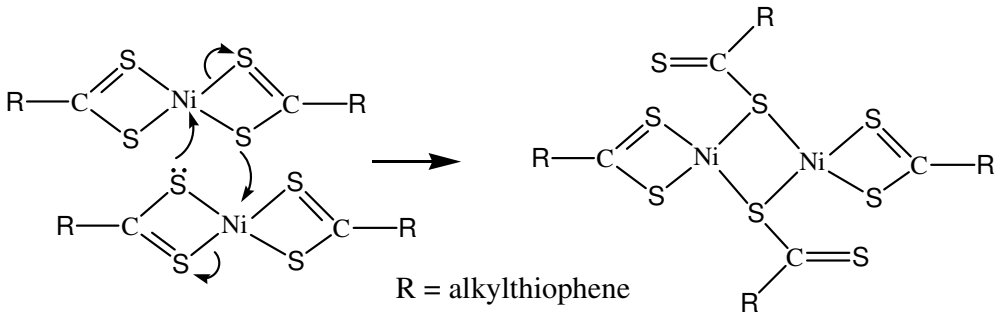

Scheme 2.4 Proposed mechanism for the dimerization of nickel(II) complexes with bridging thiol ligands

A more likely explanation can be found by considering a change in the coordination mode of one half of the RCS_2 ligands and thus affording ^1H NMR resonances of the same intensities. A very unexpected, but with well-characterized complex in literature deals with the conversion of one or both of the dithiocarboxylate ligands into a perthiocarboxylate ligand[40,41]. These complexes were originally incorrectly formulated as being disulphide bridged dinickel(IV) complexes with four terminally coordinated dithiocarboxylate ligands and each of the metals in an octahedral ligand environment[42]. It was later shown that these violet or dark red complexes, $[Ni(S_2CR)_2S]$, were in fact mononuclear nickel(II) complexes (Figure 2.9), displaying a four-membered dithiocarboxylato and a five-membered perthiocarboxylato chelate ring[43]. The formation of the sulfur inserted perthiocarboxylato ligand is facilitated by a sulfur source such as S_8 or anionic polysulphides and/or thermal reaction conditions[43-46]. This process can be reversed by abstracting a sulfur atom with PPh_3[45,46]. A further driving force for the S-insertion is the expansion of a four to a thermodynamically favoured five membered chelate ring.

The formation of violet vs blue compounds in this study was contributed not only by the properties of the solvent, but also by the length of the alkyl chain. Using the first method of synthesis the blue monomers are preferred for the shorter chains (C_4 and C_6) and the violet compounds for the longer chains (C_8, C_{12} and C_{16}). By stirring **1a** or **2a** in THF for less than one day the conversion into **1b** and **2b**, respectively, is completed. It should be reasonably easy to eliminate or prove that the mixed mononuclear perthiocarboxylate nickel(II) complexes as being

representative of **1b** – **6b.** This could be done on the basis of chemical analyses, mass spectrometry, literature surveys and spectroscopic methods (NMR and IR).

The atom-numbering scheme adopted in this dissertation for bridging dithiocarboxylate or perthiocarboxylate chelate rings differ from those of terminal dithiocarboxylate ligands only by the addition of an apostrophe to the atom number (Figure 2.9).

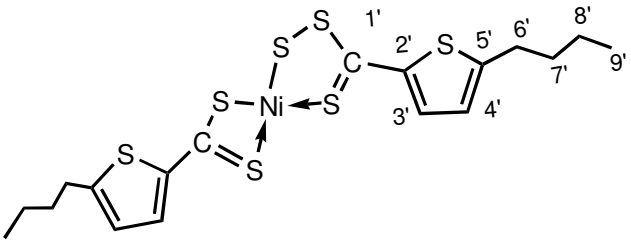

Figure 2.9 Proposed structure of a nickel(II) complex with mixed dithiocarboxylate and perthiocarboxylate ligands

Efforts to obtain single crystals from a wide range of solvents of any of **1b** – **6b**, were unsuccessful. Based on the physical and spectroscopic data and literature results it was concluded that **1b**-**6b** were the mononuclear nickel(II) complexes with perthio and dithiocarboxylate ligands as shown in Figure 2.9. Further confirmation of this structure for **1b** – **6b** was made by literature survey, the violet colour, chemical analyses, and the mass spectral and spectroscopic data. The only outstanding issue was the source of an additional sulfur for insertion. The formation of perthiocarboxylate complexes of nickel(II) have previously been

achieved by thermal conditions and the addition of polysulfides, elemental sulfur or by a photolytic procedure in dichloromethane or chloroform[45,46].

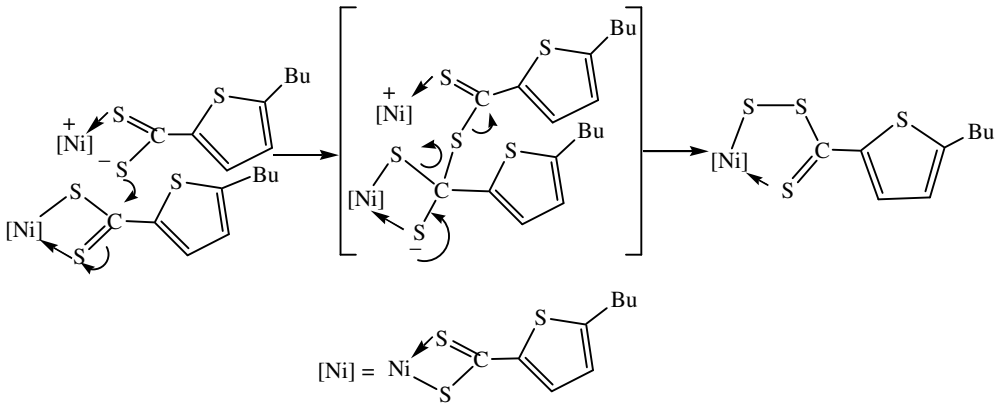

Scheme 2.5 Proposed mechanism for the formation of the mononuclear perthiocarboxylate complex

In this study it is unclear how the sulfur inserted ligand was formed under mild conditions, and in the absence of an oxidant. Studies involving the mechanism of the sulfur insertion process using labeled ^{34}S revealed that the sulfur atom is inserted between a C-S bond and not between a M-S bond[43,47]. Based on this a mechanism, insertion of a sulfur atom from one dithiocarboxylate molecule into a second one, to form perthiocarboxylate is presented in Scheme 2.5. It was previously noted that the temperature plays an important role for the transformation of a dithiocarboxylate to a perthiocarboxylate ligand, and in this study it can be assumed that the thiophene facilitated the sulfur inclusion under the mild reaction conditions. This could be achieved by the stabilization of the electrophilic CS_2-carbon in the intermediate by electron charge transfer from the thiophene ring. A further driving force is the greater stability of five-membered chelate rings compared to four-membered chelate rings. In conclusion, the

structures of the deep blue compounds **1a**, **2a** and **6a** and the violet compounds **1b**-**6b** are as shown in Figure 2.10.

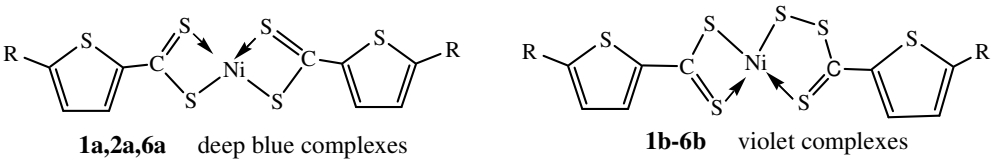

1a,2a,6a deep blue complexes **1b-6b** violet complexes

Figure 2.10 Structures of nickel(II) dithiocarboxylate complexes

Characterization of complexes:

The mass peak at m/z-value of 632 (^{58}Ni, 3%) corresponds to the mass of the molecule **3b** and represents the molecular ion, $[Ni(S_3CTR)(S_2CTR)]^+$ (R = C_8H_{17}). This can be seen as part of the isotope cluster indicated by a m/z-value of 633 in Figure 2.11 and confirm the assignments of **1b-6b**.

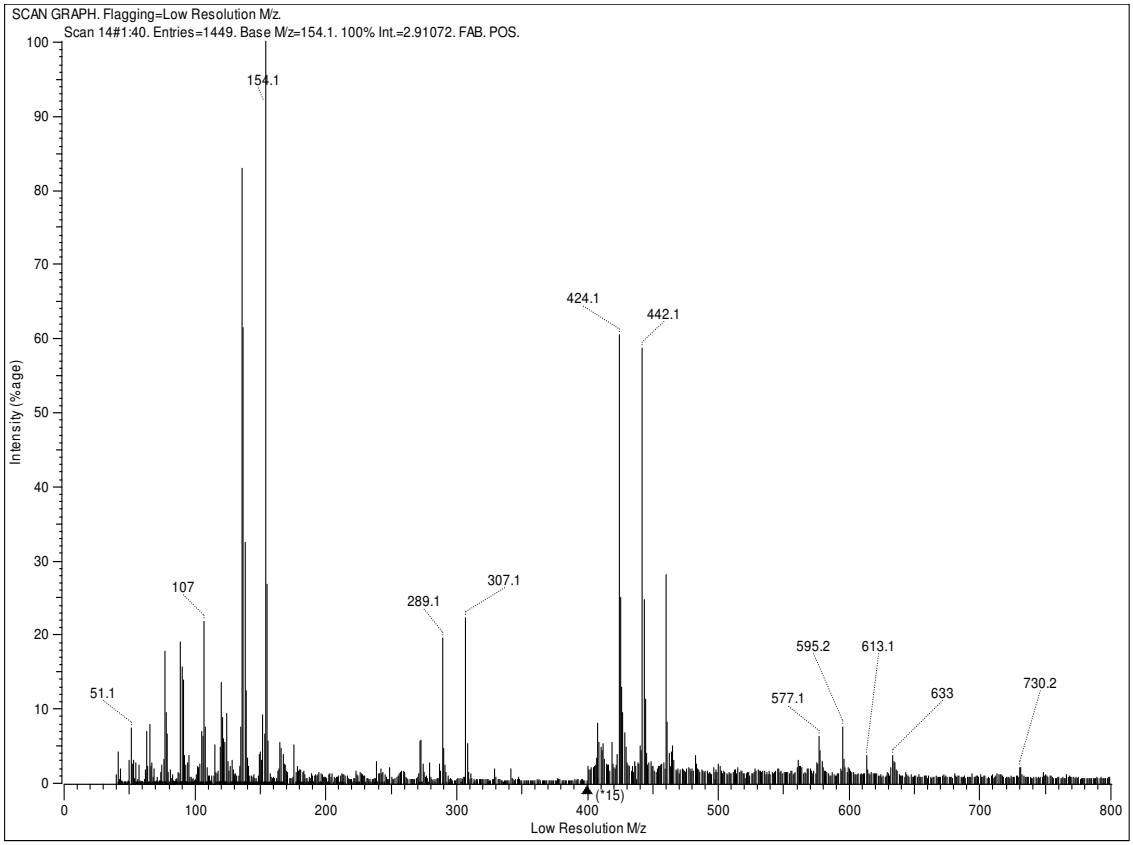

Figure 2.11 Mass spectrum of $[Ni(S_3CTC_8H_{17})(S_2CTC_8H_{17})]^+$**(3b)**

The stronger peaks in the ^1H NMR spectrum of bis(5-butyl-2-thiophenedithiocarboxylato)nickel(II), **1** (Figure 2.1) are two doublets, at chemical shift values of 7.73 and 6.83 ppm for the two protons H3 and H4 of the thiophene ring. The doublet at 7.73 ppm was assigned to H3 that is closer to the dithiocarboxylate (C1) substituent and affected more by the coordination of the sulfur atoms to the nickel. The signal of H3 is expected to be downfield because of the electron withdrawing nature of the dithiocarboxylate group compared to the doublet at 6.83 ppm assigned to H4 because of the alkyl chain in the 5-position.

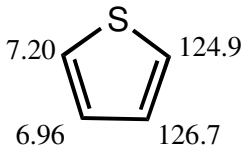

Figure 2.12 ^{1}H and ^{13}C NMR data (δ, ppm) for thiophene[48]

The value for H3 is significantly downfield from the corresponding value of thiophene. Figure 2.12 gives the ^{1}H and ^{13}C NMR chemical shifts for thiophene[48]. The reason for this large downfield shift of almost 1 ppm is the result of the electron-withdrawing CS_2-substituent that is further enhanced as a result of its coordination to the nickel(II) centre. The transfer of electron density from the thiophene ring to the nickel(II) center and the resulting deshielding of H3 is shown in Figure 2.13. The environment of H4 is less affected and this resonance is only marginally upfield because of the inductive effect of the alkyl chain.

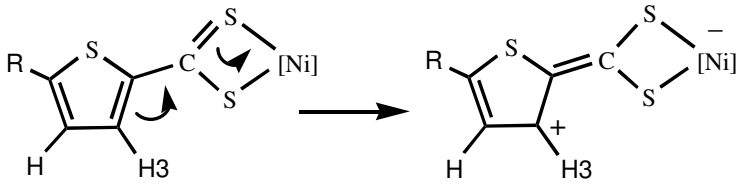

Figure 2.13 Charge delocalization from the thiophene ring to the nickel(II) center

The ^{1}H NMR spectrum of $[Ni(S_2CTC_6H_{13})_2]$ **2a** showed similar peaks to that of $[Ni(S_2CTC_4H_9)_2]$ **1a** and were assigned similarly.

Figure 2.1 shows the ^{1}H NMR spectrum in the thiophene region of **1** (**1a** and **1b**), pure samples of $[Ni(S_2CTR)_2]$ **1a** and $[Ni(S_3CTR)(S_2CTR)]$ **1b** (T = 2,5-disubstituted thiophene, R = C_4H_9) confirmed that this spectrum represents a mixture of the two compounds. The four doublets in the thiophene region of **1b**

support the structure of two different chemical environments for the thiophene-containing ligands. The chemical shifts were assigned based on the resonances observed for the monomer. Instead of the doublet at 7.73 ppm for the monomer **1a**, two doublets were formed, one slightly downfield at 7.78 ppm and the other one slightly upfield at 7.48 ppm. The latter was assigned to H3' of the perthiocarboxylate chelate ring as the introduction of an additional sulfur atom would weaken the effect of coordination to the metal. The other two doublets were at 6.86 ppm slightly downfield, and at 6.75 ppm, slightly upfield from the doublet of the monomer **1a** at 6.83 ppm, and were assigned to H4 and H4', respectively. The phenyl protons of the two types of ligands in $[Ni(S_3CPh)(S_2CPh)]$[43] also gave different chemical shifts and support the structural assignment of **1b.**

The ^{1}H NMR data of **1a**, **1b**, **2a**, **2b**, **3-5b**, **6a** and **6b** are given in Table 2.1. The ^{1}H NMR spectrum of **3b** is shown in Figure 2.14. The four doublets are at 7.77, 7.49, 6.86 and 6.75 ppm, respectively. Interestingly, the triplet of the CH_2 group attached to the thiophene of the octyl chain is also duplicated for the two types of ligands emphasizing the large differences in the coordination modes of the perthio- and dithio-carboxylato ligands.

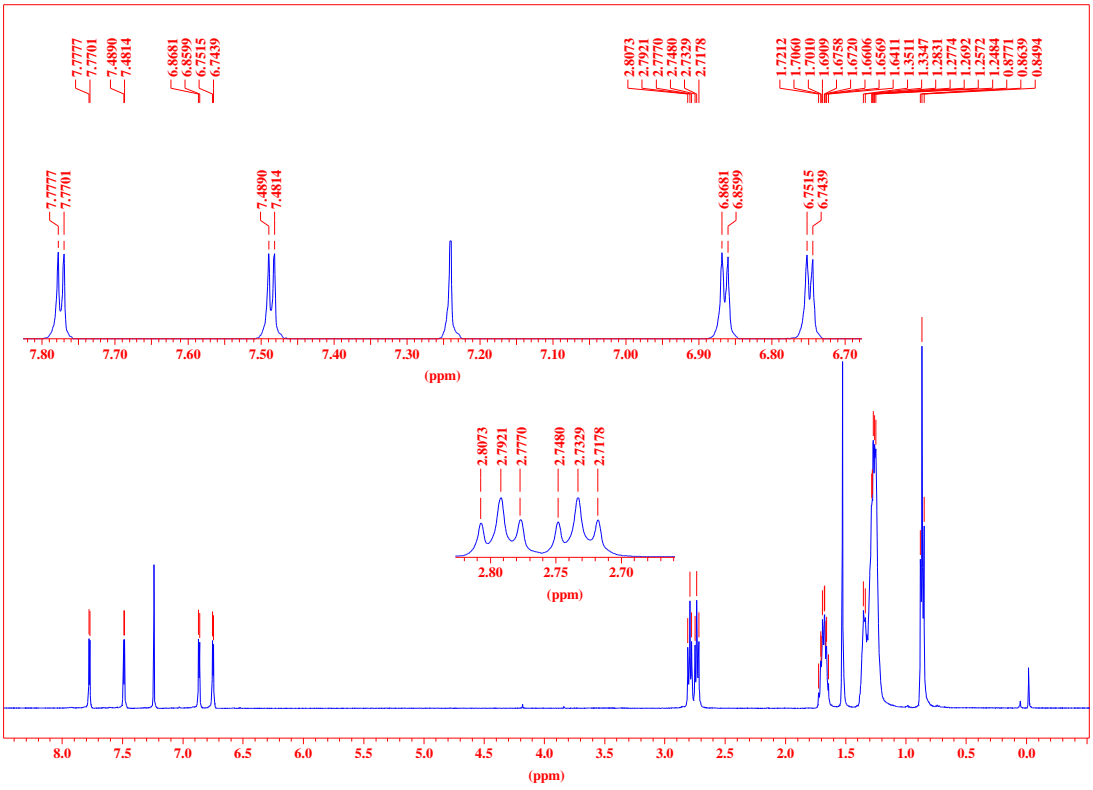

Figure 2.14 ^{1}H NMR spectrum of [Ni($S_3CTC_8H_{17}$)($S_2CTC_8H_{17}$)] **3b**

The resonances in the ^{13}C NMR spectra of **1**-**6b** were assigned based on a 2D HETCOR spectrum recorded for **3b.** The ^{13}C NMR spectrum of **3b** (Figure 2.15) showed the reasonances of CS_2 as one peak for **1a**, **2a** and **6a** and two peaks for **1-6b**. The lower chemical shift value was assigned to the CS_2 of the perthiocarboxylato ligand.

These resonances are typically at 228 ppm for identical dithiocarboxylate ligands and at 214 and 227 ppm for the complexes with mixed dithio- and perthiocarboxylate ligands. The thiophene resonances as well as the carbon atoms of the alkyl chain are also duplicated for the two different ligands in **1b** – **6b** and

are unique for both types of complexes. The ^{13}C NMR data of **1-6** is indicated in Table 2.1.

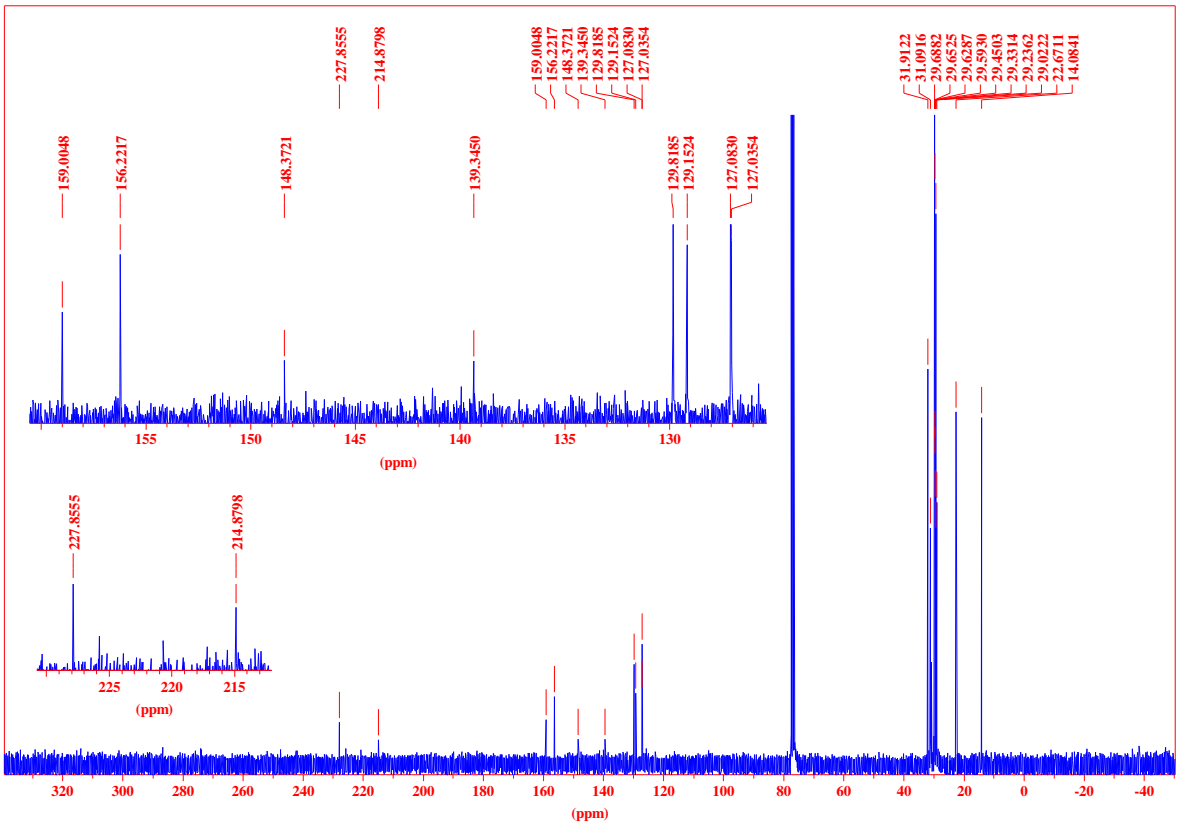

Figure 2.15 ^{13}C NMR spectrum of $[Ni(S_3CTC_8H_{17})(S_2CTC_8H_{17})]$ **3b**

The infrared spectra of all the complexes showed similar peaks. The spectrum of **1a**, $[Ni(S_2CTC_4H_9)_2]$ showed prominent peaks at 2918, 1458, 1375, 1049, 977 and 721 cm^{-1}. The peak at 2918 cm^{-1} was assigned for the CH_2-groups of the alkyl chain and the peak at 1458 cm^{-1} was assigned for the arene-carbon (C-C thiophene) stretching frequency. The peak at 1375 cm^{-1} was assigned for the terminal CH_3 group. The peaks at 1049 and 977 cm^{-1} were assigned for C-S stretching frequencies. Usually the stretching frequencies of the dithiocarboxylic

acid are around 1100 and 900 cm^{-1} for the C=S and C-S stretching frequencies[49,50], respectively and the Ni-S vibrations are found in the far infrared region around 350 cm^{-1} in nickel complexes[51]. The infrared spectral data for the complexes **1-6** is indicated in Table 2.1 and UV spectra of **1a** and **1b** are given in Figure 2.16.

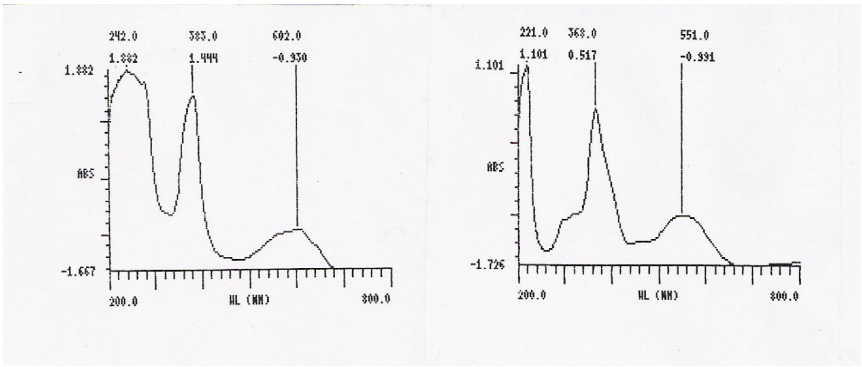

Figure 2.16 UV spectra of **1a** (blue) and **1b** (violet)

The d-d transition of nickel(II) in the blue complex is at 602 nm and the value is similar to that reported by Furlani[52] for monomeric dithiocarboxylate complexes of nickel(II). The d-d transition of nickel(II) in the violet complex is at 551 nm and is similar to that for a mixed dithiobenzoato and perthiobenzoato nickel(II) complex[19].

Chemical analysis of **3b** $Ni(S_2CTC_8H_{17})(S_3CTC_8H_{17})$ for molecular formula $NiC_{26}H_{38}S_7$, showed that the calculated values correspond to the found values. Theoretical values: C = 49.28%, H = 6.05% and S = 35.42%, Analytical values: C = 49.67%, H = 6.25% and S = 37.17%,

Table 2.1 Spectroscopic data of the complexes **1-6**

Complex	^{1}H NMR (δ/ppm in $CDCl_3$)	^{13}C NMR (δ/ppm in $CDCl_3$)	IR (ν/cm^{-1} in Nujol mol)
1a, R = C_4H_9	7.73 (d, 2H, H3, J=3.9), 6.83 (d, 2H, H4, J=3.6), 2.79 (t, 4H, H6, J=7.2), 1.66 (m, 4H, H7), 1.37 (m, 4H, H8), 0.92 (t, 6H, H9, J=7.2)	*S_2C (C1), 159.3 (C2), 148.8 (C5), 129,8 (C3), 127.0 (C4), 33.1, 30.8, 22.7, 13.6 (C6-C9)	2918 (vs), 1458 (vs), 1375 (s), 1049 (m), 977 (m), 721 (s)
1b	7.78 (d, 2H, H3, J=3.9), 7.49 (d, 2H, H3', J=4.1), 6.87 (d, 2H, H4, J=3.9), 6.75 (d, 2H, H4', J=3.9), 2.80 (t, 4H, H6, J=7.2), 2.74 (t, 4H, H6', J=7.2), 1.67 (q, 4H, H7, J=7.5'), 1.66 (q, 4H, H7', J=7.5), 1.40 (m, 4H, H8, J=7.4), 1.39 (m, 4H, H8', J=7.4), 0.93 (t, 6H, H9, J=7.2), 0.92 (t, 6H, H9', J=7.2)	227.9, 214.9 (C1 and C1'), 160.1, 158.2, 149.4, 148.6, 131.3, 129.8, 127.6, 127.2 (C2-C5 and C2'-C5'), 33.6, 31.4, 22.6, 13.9 (C6-C9 and C6`-C9`)	2921 (vs), 1461 (vs), 1375 (s), 1049 (m), 970 (m), 925 (w), 721 (s)
2a, R = C_6H_{13}	7.72 (d, 2H, H3, J=4.1), 6.82 (d, 2H, H4, J=3.9), 2.78 (t, 4H, H6, J=7.7), 1.68 (m, 4H, H7), 1.30 (m, 12H, H8-H10), 0.87 (t, 6H, H11, J=7.5)	*S_2C (C1), 159.4 (C2), 148.8 (C5), 129.6 (C3), 127.0 (C4), 31.4, 31.2, 29.7, 28.7, 22.5, 14.0 (C6-C11)	2920 (s), 1461 (vs), 1375 (s), 1050 (m), 978 (m), 721 (s)
2b	7.77 (d, 2H, H3, J=3.2), 7.48 (d, 2H, H3', J=3.2), 6.86 (d, 2H, H4, J=3.1), 6.75 (d, 2H, H4', J=3.1), 2.82 (dt, 8H, H6 and H6', J=7.2), 1.71 (m, 8H, H7 and H7'), 1.32 (m, 24H, H8-H10 and H8'-H10'), 0.91 (t, 12H, H11 and H11', J=7.2)	227.8, 214.8 (C1 and C1'), 159.0, 156.2, 147.4, 144.6, 139.3, 128.8, 127.1, 127.0 (C2-C5 and C2'-C5'), 30.8, 29.9, 28.9, 27.9, 21.6, 13.1 (C6-C11 and C6'-C11')	2920 (vs), 1460 (vs), 1375 (s), 1097 (m), 1050 (m) 978 (m), 720 (s)
3b, R = C_8H_{17}	7.77 (d, 2H, H3, J=4,0),	227.8, 214.8 (C1 and	2920 (vs),

	7.49 (d, 2H, H3', J=3.7), 6.86 (d, 2H, H4, J=3.8), 6.75 (d, 2H, H4', J=3.8), 2.79 (t, 4H, H6 , J=7.8), 2.74 (t, 8H, H6', J=7.2), 1.67 (m, 8H, H7 and H7`), 1.62 (m, 40H, H8-H12 and H8'-H12'), 0.87 (t, 12H, H13 and H13', J=6.5/7.2')	C1`), 159.0 , 156.2 (C2 and C2'), 148.4, 139.3 (C5 and C5'), 129.8, 129.1 (C3 and C5'), 127.1, 127.0 (C4 and C4'), 31.8, 31.1, 30.7, 29.7, 29.2, 29.0, 22.6, 14.1 (C6-C13 and C6'-C13')	1461 (vs), 1375 (s), 1067 (w), 1048 (m), 999 (m), 970 (m), 721 (s)
4b, R = $C_{12}H_{25}$	7.78 (d, 2H, H3, J=4.0), 7.48 (d, 2H, H3', J=3.9), 6.86 (d, 2H, H4, J=3.9), 6.75 (d, 2H, H4', J=3.9), 2.79 (t, 4H, H6, J=7.6), 2.73 (t, 4H, H6', J=7.5), 1.67 (m, 8H, H7 and H7`), 1.29 (m, 72H, H8-H16 and H8'-H16'), 0.87 (t, 12H, H17 and H17', J=7.2)	227.8, 214.8 (C1 and C1`), 159.0, 156.2, 148.4, 139.3, 129.8, 129.2, 127.1, 127.0 (C2-C5 and C2'-C5'), 31.9, 31.8, 31.4, 31.1, 30.7, 29.7, 29.6, 29.6, 29.5, 29.3, 29.1, 29.0, 22.7, 14.1 (C6-C17 and C6'-C17')	2921 (vs), 1460 (vs), 1375 (s), 1049 (m), 994 (w), 980 (m), 720 (s)
5b, R = $C_{16}H_{33}$	7.70 (d, 2H, H3, J=3.9), 7.48 (d, 2H, H3', J=3.9), 6.86 (d, 2H, H4, J=3.9), 6.75 (d, 2H, H4', J=3.9), 2.76 (dt, 8H, H6 and H6', J=7.8/7.5), 1.69 (m, 8H, H7 and H7'), 1.28 (m, 104H, H8-H20 and H8'-H20'), 0.86 (t, H21 and H21', J=6.5/7.0)	227.9, 214.9 (C1 and C1`), 159.0, 156.2, 139.3, 129.8, 129.2, 127.1, 127.0 (C2-C5 and C2'-C5'), 31.9, 31.1, 31.0, 30.7, 30.6, 30.2, 29.9, 29.8, 29.7, 29.7, 29.7, 29.6, 29.5, 29.4, 29.2, 29.2, 29.0, 22.7, 14.1 (C6-C21 and C6'-C21')	2922 (vs), 1458 (vs), 1375 (s), 1049 (m) 977 (m), 925 (w), 720 (s)
6a, R = CH_3	7.72 (d, 2H, H3, J=4.0), 6.82 (d, 2H, H4, J=3.9), 2.43 (s, 3H, Me)	228.0 (C1), 159.0, 139.3, 129.2, 127.1, (C2-C5), 14.1 (C6)	2919 (vs), 1460 (vs), 1375 (s), 1049 (m), 978 (m), 721 (s)
6b, R = CH_3	7.76 (d, 2H, H3, J=3.8),	227.9, 214.9 (C1 and	2920 (vs),

	7.47 (d, 2H, H3', J=3.6), 6.85 (d, 2H, H4, J=3.7), 6.74 (d, 2H, H4', J=3.6), 2.47 (s, 3H, Me), 2.43 (s, 3H, Me')	C1`), 159.0, 156.2, 140.1, 139.3, 129.8, 129.2, 127.1, 127.0 (C2-C5 and C2'-C5'), 14.2, 14.1 (C6 and C6`)	1458 (vs), 1375 (s) 1046 (m), 999 (w), 978 (m), 721 (s)

* not observed.

2.2.2 Thermal properties

Thermal properties of the complexes were investigated by using Differential Scanning Calorimetry (DSC) and Hot-stage Polarising Optical microscopy (POM).

All the complexes were subjected to thermal analysis by DSC. The scanning rate was 10^{o}C per minute. No double melting behaviour was observed for **1a, 1b**, **2a, 2b** and **5b** whereas double melting behaviour was observed for **3b** and **4b**. Two endothermic peaks could be observed at 77^{o}C and 88^{o}C for **3b** (Figure 2.17). The peak at 88^{o}C is compatible with the melting point and the peak at 77^{o}C is for crystal-to-crystal transition. The clearing point was not observed in the DSC. Complex **4b** also showed two endothermic peaks at 102^{o}C and 117^{o}C. Ohta and coworkers[53] suggested that the double melting behaviour of long-chain substituted compounds is a thermal behaviour close to mesomorphism.

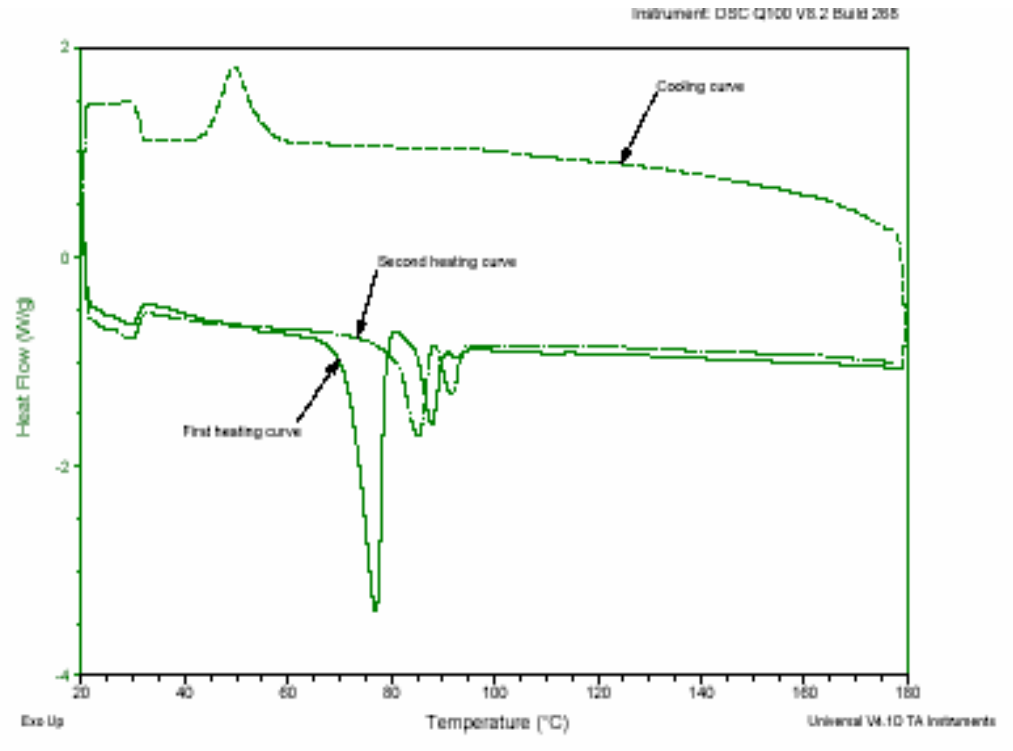

Figure 2.17 DSC thermogram of [Ni($S_3CTC_8H_{17}$)($S_2CTC_8H_{17}$)] **3b**

Complexes **3b**, **4b** and **5b** were also examined by Hot-stage Polarising Optical Microscopy. The complex **3b** (Figure 2.18) is an enantiotropic liquid crystal and it exhibits a nematic phase. Enantiotropic liquid crystal shows mesomorphism upon heating the solid as well as on cooling the isotropic liquid. The transition temperature of **3b** was between 92°C and 116°C.

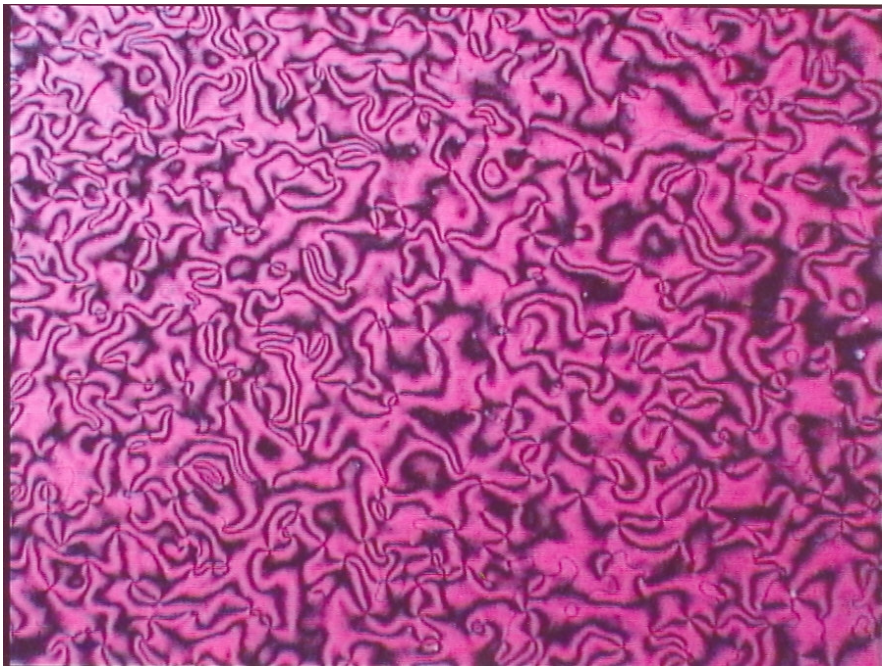

Figure 2.18 Nematic phase of [Ni($S_3CTC_8H_{17}$)($S_2CTC_8H_{17}$)] **3b** at 105°C (200 x magnification)

The optical texture of **3b** is similar to the nematic phase of 4-nonyloxybenzoic acid[54] described in chapter 1. Complex **4b** was a mixture of dark highly viscous liquid and opaque crystals. The liquid was not birefringent and therefore it was not a liquid crystal. The opaque crystals however melted to a nematic phase, but it was difficult to observe because of the presence of the other dark fluid phase. Complex **5b** directly melted to isotropic liquid without showing any mesophases. Transition temperatures of the complexes **1-5** are given in Table 2.2, and the dependence of the transition temperatures on the chain length is shown in Figure 2.19.

Table 2.2 Transition temperatures of **1-5**

Complex	Chain	Transition	Temperature (^{o}C)
1a	C_4H_9	$Cr \rightarrow I$	52
2a	C_6H_{13}	$Cr \rightarrow I$	65
3b	C_8H_{17}	$Cr \rightarrow N$ $N \rightarrow I$	92 116
4b	$C_{12}H_{25}$	$Cr \rightarrow N$ $N \rightarrow I$	102 117
5b	$C_{16}H_{33}$	$Cr \rightarrow I$	61

Cr = crystal, *N* = nematic phase, *I* = isotropic liquid

Complexes **1, 2** and **5b** directly melted to the isotropic liquids without passing through any mesophases. The transition temperature range for **3b** was between 92^{o}C-116^{o}C (*N*→*I*) whereas for benzene analogue[18] [Ni($S_3CBC_8H_{17}$)($S_2CBC_8H_{17}$), the range was between 126^{o}C-198^{o}C (*N*→*I*). The lower transition temperature observed for **3b** may be due to thiophene in the complex. It was reported[55] that thiophene systems have generally lower melting points than their benzene counter parts due to reduced packing efficiency in the molecules.

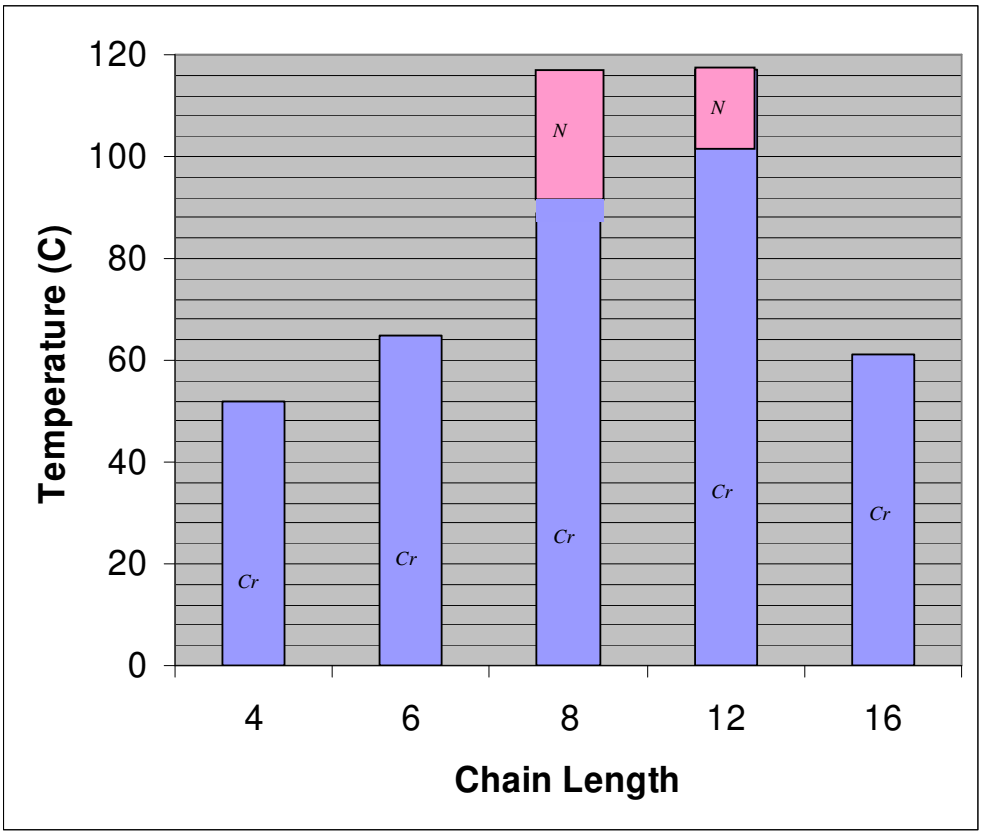

Figure 2.19 The dependence of the transition temperatures of the complexes on the alkyl chain length *(N = nematic , Cr = crystal)*

Complexes **1a, 1b, 2a, 2b** and **5b** had no mesogenic behaviour whereas complexes **3b** and **4b** showed nematic mesophases. The optimum chain length suitable for mesomorphism for the alkyl thiophene dithiocarboxylate complexes was C_8.

2.3 Experimental Section

Materials and instrumentation

All commercially available chemicals were used as received. Solvents were dried and distilled under nitrogen prior to use. Thiophene was purified as described by Spies and Angelici[56]. All reactions were performed in an inert atmosphere of either nitrogen or argon by using Schlenk techniques and vacuum-line. Column chromatography was carried out using silica gel.

Infrared spectra were recorded on a Perkin Elmer Spectrum 1000 FT-IR spectrophotometer. All NMR spectra were recorded in deuterated chloroform using the chloroform peak as standard on a Bruker ARX – 300 spectrometer. High-resolution mass spectra were recorded on a Finnegan 8200 spectrometer. UV- visible spectra were recorded on a Varian Cary 1E spectrometer.

Liquid-crystalline properties were examined on a Differential Scanning Calorimeter (DSC) Q 100 V8.2 Build 268 and Hot-stage Polarising Optical Microscope (POM) Olympus BX60 equipped with a Linkam THMS 600 hot stage and a Linkam TMS 93 Programmable temperature controller.

2.3.1 Synthesis

All the complexes were synthesized via a four-step reaction in a similar manner. A typical procedure for complex **1** is described.

Preparation of 2-butyl thiophene

The reaction was done in an inert atmosphere. The procedure which was used is similar to the one described by Brandsma[23]. n-Butyl lithium (15.6 ml, 25.0 mmol) was added to a mixture of THF (50.0 ml) and hexane (30.0 ml), which was cooled to -20°C. Thiophene (1.68 g, 20.0 mmol) was introduced over 10 minutes with cooling between 0°C and 10°C. The cooling bath was removed and allowed to rise to the room temperature. Butyl bromide (2.74 g, 20.0 mmol) was added in one portion without external cooling. The temperature of the solution was raised to 50°C and kept at this temperature for a further 30 minutes and after which 100 ml of ice water was added with vigorous stirring. Two separate layers were observed and the separation was done in air. After separation of the layers, two extractions with diethyl ether were carried out. The combined organic solutions were dried over anhydrous $MgSO_4$ and concentrated in a rotary evaporator and weighed. Yield = 2.38 g; 85%.

Preparation of 5-butyl-2-thiophenedithiocarboxylic acid ($C_4H_9TCS_2H$)

In the second step 2-butyl thiophene was converted into 5-butyl-2-thiophenedithiocarboxylic acid. The first part of the reaction was done in an inert atmosphere. n-Butyl lithium (12.5 ml, 20.0 mmol) was added to a solution of THF (50.0ml) and hexane (30.0 ml), which was cooled to -20°C. 2-butyl thiophene (2.38 g, 17.0 mmol) was introduced over 10 minutes with cooling between 0°C and 10°C. The cooling bath was removed and allowed to rise to room temperature and stirred for a further 10 minutes. The solution was cooled to 0°C and copper(I) bromide (0.1 g) was added. Carbon disulfide (1.29 g, 17.0

mmol) was added drop-wise to the stirred mixture. The colour of the reaction mixture changed to a deep-red colour. The cooling bath was removed and allowed to rise to the room temperature and stirring was continued for a further 1 hour. Ice water (100.0 ml) was added followed by dilute hydrochloric acid (20.0 ml, 1mol/dm^3). The next part was done in air. The organic layer was separated and extracted into diethyl ether (70.0 ml) and washed with 2 x 50.0 ml of water. The product was dried over $MgSO_4$ and the solvent removed *in vacuo*. Yield = 3.30 g; 89.8%.

Preparation of sodium-5-butyl-2-thiophenedithocarboxylate ($C_4H_9TCS_2Na$)

The reaction was done in an inert atmosphere. Sodium metal (0.35 g, 15.28 mmol) was added over 10 minutes to vigorously stirred methanol (50.0 ml). When all the sodium had dissolved, additional (20.0 ml) methanol was added. 5-Butyl-2-thiophenedithiocarboxylic acid (3.30 g, 15.28 mmol) was added over 5 minutes to the mixture and left stirring for 30 minutes. The solvent was removed *in vacuo*, leaving the sodium 5-butyl-2-thiophenedithiocarboxylate as an orange-brown solid. Yield = 3.09 g; 85%.

*Synthesis of Bis(5-butyl-2-thiophenedithiocarboxylato) nickel(II) [$Ni(S_2CTC_4H_9)_2$] (**1a**)*

The procedure was similar to that of Adams *et al.*[18], who prepared dithiobenzoate complexes. The reaction was done in air. To a stirred solution of sodium 5-butyl-2-thiophenedithiocarboxylate (1.55 g, 6.5 mmol) in water (25.0 ml) was added drop-wise a pale green solution of $NiCl_2.6H_2O$ (0.71 g, 3.0 mmol) in water (10.0

ml) at room temperature. The colour of the solution turned blue-violet and the mixture was left to stir for 3 hours. The mixture was concentrated to 25.0 ml on a rotary evaporator and 20.0 ml of methanol was added. The precipitate was separated by filtration and dried. The product was purified on a silica gel column and the desired product was extracted with hexane: CH_2Cl_2 (4:1) as the eluent. A blue powder was obtained on evaporation of the solvent. Yield = 0.49 g; 66%.

The synthetic route for the other four complexes was similar. The experimental data of the complexes **1-5** are summarized in Table 2.3.

Table 2.3 The experimental data of **1-5**

Complex	Amount of nickel(II) chloride added (mmol)	Amount of sodium salt (mmol)	Colour of the product	Yield (%)
1a	3.0	6.5	Dark blue solid	66
2a	2.0	5.0	Dark blue solid	58
3b	2.5	5.8	Violet powder	64
4b	2.2	5.0	Dark violet oily solid	48
5b	1.8	4.0	Dark violet oily solid	52

*Second method (one-pot reaction) for **6a** and **6b***

In a second method (one-pot reaction), 2-methylthiophene (1.96 g, 20.0 mmol) was lithiated by n-butyl lithium (13.8 ml, 22.0 mmol) at –20°C in THF. The

colour of the solution immediately changed to orange on addition of the BuLi, but changed gradually to yellow after stirring for 30 minutes. The mixture was cooled to -50° and carbon disulfide (1.52 g, 20.0 mmol) was added. The mixture became dark red in colour and was stirred for 30 minutes. Anhydrous nickel(II) chloride (1.30 g, 10.0 mmol) was added in small portions and the mixture was allowed to reach room temperature. The yellow solid material gradually dissolved on reacting and the solution changed first to green then to blue and thereafter to violet over a period of three hours. The blue-violet product was purified by filtration of the reaction mixture through a plug of silica gel once the solvent was changed to dichloromethane and afforded **6** in very high yield (the yield was more than 80%). From this mixture both blue and violet compounds were isolated by column chromatography with mixtures of hexane and dichloromethane as eluents.

Yield of **6a** (blue) = 1.22 g, 30%.

Yield of **6b** (violet) = 1.63 g, 40%.

2.4 Conclusion

The reactions of a series of 5-alkyl-2-thiophenedithiocarboxylates with nickel(II) chloride formed two types of complexes, mononuclear nickel(II) complexes with two terminal dithiocarboxylate ligands (blue) and mononuclear nickel(II) complexes with perthio- and dithiocarboxylate ligands (violet). The formation of violet vs blue compounds in this study was contributed not only by the properties of the solvent, but also by the length of the alkyl chain and the presence of thiophene in the chain. Using the first method of synthesis the blue monomers are preferred for the shorter chains (C_4 and C_6) and violet compounds for the longer

chains (C_8, C_{12} and C_{16}). It was previously noted[19] that the temperature plays an important role for the transformation of dithiocarboxylate to a perthiocarboxylate ligand. In this study it can be assumed that the thiophene facilitated the sulfur inclusion under the mild reaction conditions. The blue compounds are less soluble than the violet compounds. Thermal studies with DSC and POM showed that the complexes with C_8 and C_{12} alkyl chains are liquid crystals (metallomesogens). The mesomorphism of the two complexes was similar, as both complexes showed nematic phases. The dark colour of the complexes has made phase characterization very difficult. The transition temperatures of these complexes are lower than the benzene analogues[18] as predicted. Complexes **3b** and **4b** are the first examples of metallomesogens of nickel(II) complexes with 5-alkyl-2-thiophenedithiocarboxylate as ligands. In future, further work will be done on the optical and conducting properties of these complexes.

REFERENCES

1. Y. G. Galyametdinov, G. I. Ivanova and I. V. Ovchinnikov, *Zh. Obshch. Khim.*, **1991**, 61, 234.
2. C. P. Roll, A. G. Martin, H. Goerls, G. Leibeling, D. Guillon, B. Donnio and W. Weigand, *J. Mater. Chem*., **2004**, 14, 1722.
3. A. Mori, R. Mori, M. Takemoto, S. Yamamoto, D. Kuribayashi, K. Uno, K. Kubo and S. Ujiie, *J. Mater. Chem.*, **2005**, 15, 3005.
4. M. Marcos, P. Romero and J. L. Serrano, *J. Chem. Soc., Chem. Commun*., **1989**, 1641.
5. M. Hannack, A. Beck and H. Lehmann, *Synthesis*, **1987**, 703.
6. J. Sleven, T. Cardinaels, C. Gorller-Walrand and K. Binnemans, *ARKIVOC*, **2003** (iv) 68.
7. A. Bacchi, M. Carcelli, O. Francescangeli, F. Neve, P. Pelagatti and C. Pelizzi, *Inorg. Chem. Commun.*, **1999**, 2, 255.
8. D. Coucouvanis, *Progr. Inorg. Chem*., **1970**, 11, 233.
9. R.P. Burns, F.P. McCullong and C.A. McAuliffe, *Adv. Inorg. Rad. Chem.,* **1980**, 23, 211.
10. A. L. Fluharty, *Chemistry of the thiol group*, part 1 edited by S. Patai, John Wiley & sons, **1974**, 589.
11. P. Espinet, M.A. Esteruelas, L.A. Oro, J.L. Serrano and E. Sola, *Coord. Chem. Rev.,* **1992**, 117, 215.
12. D.W. Bruce, *J. Chem. Soc., Dalton Trans.,* **1993**, 2983.
13. A. M. Giroud and U. T. Muller-Westerhoff, *Mol. Cryst., Liq. Cryst*., **1977**, 41, 11.

14. K. Ohta, H. Hasebe, H. Ema, T. Fugimoto and I. Yamamoto, *J. Chem. Soc., Chem. Commun*., **1989**, 1610.

15. N. Hoshino-Miyajima, *J. Chem. Soc., Chem. Commun*., **1993**, 1442.

16. U. T. Muller-Westerhoff, A. Nazzal, R. J. Cox and A. M. Giroud, *Mol. Cryst., Liq. Cryst.,* **1980**, 56, 249.

17. H. Adams, N. A. Bailey, D. W. Bruce, R. Dhillon, D. A. Dunmur, S. E. Hunt, E. Lalinde, A. A. Maggs, R. Orr, P. Styring, M. S. Wragg and P. M. Maitlis, *Polyhedron*, **1988**, 7, 1861.

18. H. Adams, A. C. Albeniz, N. A. Bailey, D. W. Bruce, A. S. Cherodian, R. Dhillon, D. A. Dunmur, P. Espinet, J. L. Feijoo, E. Lalinde, P. M. Maitlis, R. M. Richardson and G. Ungar, *J. Mater. Chem*., **1991**, 1, 843.

19. K. Ohta, H. Ema, Y. Morizumi, T. Watanabe, T. Fugimoto and I. Yamamoto, *Liq. Cryst*., **1990**, 8, 311.

20. K. L. Marshall and S. D. Jacobs, *Mol. Cryst., Liq. Cryst*., **1988**, 159, 181.

21. D. W. Bruce, D. A. Dunmur, S. E. Hunt, P. M. Maitlis and R. Orr, *J. Mater. Chem*., **1991**, 1, 857.

22. K. Ohta, H. Emma, I. Yamamoto and K. Matsuzaki, *Liq. Cryst*., **1988**, 3, 1671.

23. L. Brandsma and H. D. Verkruijsse, *Preparative Polar Organometallic Chemistry Volume 1*, Springer Verlag, Heidelberg, **1987**, 124.

24. M. Bonamico, G. Dessy, V. Fares and L Scaramuzza, *J. Chem. Soc., Dalton Trans.,* **1975**, 2250.

25. C. Furlani and M.L. Luciani, *Inorg. Chem.,* **1968**, 7, 1586.

26. M. Bonamico and G. Dessy, *J. Chem. Soc.*(A), **1971**, 264.

27. F. Drawert, K.H. Reuther and F. Born, *Chem. Ber.*, **1960**, 93, 3056.

28. P. Porta, A. Scammellotti and N. Vinciguerra, *Inorg. Chem.,* **1968**, 7, 2625.

29. K. Umakoshi and Y. Sasaki, *Adv. Inorg. Chem.,* **1994**, 40, 187.

30. C. Bellitto, G. Dessy and V. Fares, *Inorg. Chem.,* **1985**, 24, 2815.

31. M. Bonamico, G. Dessy and V. Fares, *J. Chem. Soc., Chem. Commun.,* **1969,** 1106.

32. M. Bonamico, G. Dessy and V. Fares *J. Chem. Soc., Dalton Trans.,* **1977**, 2315.

33. Y.M. Terblans and S. Lotz, *J. Chem. Soc., Dalton Trans.,* **1997**, 2177.

34. R.J. Angelici, *Coord. Chem. Rev.,* **1990**, 105, 61.

35. T.B. Rauchfuss, *Prog. Inorg. Chem.,* **1991**, 39, 259.

36. A. Domenicano, L. Torelli, A. Vaciago and L. Zambonelli, *J. Chem. Soc.* (A), **1968**, 1351.

37. J.M. Burke and J.P. Fackler (jr), *Inorg. Chem.,* **1974**, 11, 4017.

38. A.C. Villa, A.G. Manfredotti, M. Nardelli and C. Pelizzi, *J. Chem. Soc., Chem. Commun.,* **1970**, 1322.

39. K. Nag and D.S. Joardar, *Inorg. Chim. Acta*, **1975**, 14, 133.

40. J.P. Fackler (jr) and D.Coucouvanis, *J. Am. Chem. Soc.*, **1967**, 89, 1745.

41. D.C. Fries and J.P. Fackler (jr) *J. Chem. Soc., Chem. Commun.,* **1971**, 276.

42. W. Hieber and R. Brück, *Z. Anorg. Allgem. Chem.,* **1952**, 269, 13.

43. D.Coucouvanis and J.P. Fackler (jr), *J. Am. Chem. Soc.*, **1967**, 89, 1346.

44. P. Fackler (jr), J.A. Fetchin and D.C. Fries, *J. Am. Chem. Soc.*, **1972**, 94, 7323.

45. J.P. Fackler (jr), J.A. Fetchin and J.A. Smith, *J. Am. Chem. Soc*., **1970**, 92, 2910.

46. J.P. Fackler (jr), D. Coucouvanis and J.A. Fetchin, W.C. Seidel, *J. Am. Chem. Soc*., **1968**, 90, 2784.

47. J.P. Fackler (jr) and J.A. Fetchin, *J. Am. Chem. Soc.,* **1970**, 92, 2912.

48. R.J. Abraham, J. Fischer and P. Lottus, "*Introduction to NMR Spectroscopy*", John Wiley&Sons, **1998,** 30.

49. M. L. Shankaranarayana and C. C. Patel, *Can. J. Chem*., **1961**, 39, 1633.

50. J. M. Burke and J. P. Fackler (jr), *Inorg. Chem*., **1972**, 11, 3000.

51. D. H. Busch, *Adv. Chem*., **1963**, 1, 37.

52. C. Furlani, O. Piovesana, A.A.G. Tomlinson, *J. Chem. Soc., Dalton Trans.,* **1972**, 212.

53. K. Ohta, A. Ishii, H. Muroki, I. Yamamoto and K. Matsuzaki, *Mol. Cryst. Liq. Cryst.,* **1985**, 116, 299.

54. R. Van Deun, *Liquid Crystals with Lanthanides*, PhD thesis, Katholieke Universiteit Leuven, Belgium, **2001**.

55. L. H. Wu, Y. C. Wang and C. S. Hsu, *Liq. Cryst*., **2000**, 27, 1503.

56. G. H. Spies and R. J. Angelici, *Organometallics*, **1987**, 6, 1902.

Chapter 3

Zinc(II) complexes with thiophene-containing ligands

3.1 Introduction

Complexes of zinc with sulfur ligands have been studied widely because of their biological importance and their use as accelerators in the vulcanization of rubber[1]. In addition, the model compound, $[Zn(S_2CPh)_2]$ and its derivatives are of interest in material science.

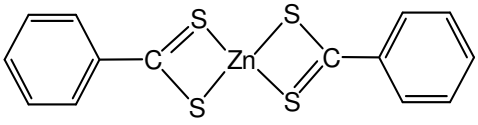

Figure 3.1 Tetrahedral $[Zn(S_2CPh)_2]$

Bonamico[2] suggested that, with the addition of p-alkyl or p-alkyloxy chains to the phenyl rings of $[Zn(S_2CPh)_2]$, rod-like molecules should result. In 1988 Adams *et al*.[3] synthesized the alkyloxy dithiobenzoate complexes of zinc, nickel and palladium and reported on their mesomorphic properties. Octyloxy dithiobenzoate complexes of zinc showed a nematic phase, while the nickel and the palladium analogues showed both nematic and smectic phases. X-ray determinations of single red crystals of octyloxy dithiobenzoate complexes of zinc showed that the molecules were dimeric, containing 8-membered $Zn_2S_4C_2$ rings, formed by the fusion of two ZnS_2C rings, and in which the geometry about zinc approximated to trigonal bipyramidal[4]. It was reported that EXAFS data for the octyloxy complex of zinc clearly indicated that the same structures are in the nematic mesophase as

in the red crystals. Thus the molecules are not tetrahedral about the metal, and the dimeric structure persists into the mesophase. It has already been noted that mesomorphism in metallomesogens seems to be incompatible with a tetrahedral geometry about the central metal[5].

Since 1985 many metallomesogens of zinc have been made with different ligands, monodentate (4-substituted pyridines)[5,6], bidentate (β-diketonates, dithiolenes, carboxylates, cyclometalated aromatic amines)[3-5,7], or polydentate (phthalocyanines[8-10], porphyrins[11,12]) and the mesomorphism of these complexes were examined. Some of the zinc complexes were not mesomorphic. Hoshino[13] ascribed the fact that the zinc analogues of the mesomorphic copper salicylaldimines were not liquid crystalline to the complexes being tetrahedral. A very important group of zinc complexes displaying liquid crystal properties is those with nitrogen donor atoms. These contain flat, macrocyclic rings acting as tetradentate ligands and two classes of importance are substituted porphyrins (Figure 3.2) and phthalocyanines (Figure 3.3). Bruce[12] reported calamitic liquid crystal phases for zinc(II) complexes of 5,15-disubstituted porphyrins.

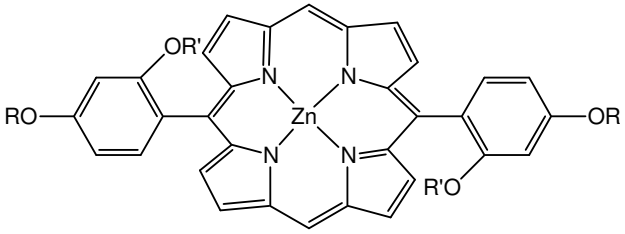

R = C_nH_{2n+1}, n = 8, 10, 12, 14, 16 (**A**); R = OR, R' = $S(O)_2C_6H_4$-p-NO_2(**B**)

Figure 3.2 Zinc complexes with porphyrin (**A**) and with lateral substituted (**B**) porphyrin ligands

The complexes showed smectic C phases, whereas uncoordinated porphyrins with their flat, disk-like geometries, normally display discotic phases[5]. In 1996 Wang and Bruce[14] showed that inherently disc-like porphyrins can be modified to be rod-like crystals with low melting points. This is achieved by using lateral substituents to prevent intermolecular π-π interactions. The thermal behaviour was investigated and it formed a nematic phase. The lateral group used was ortho-(para-nitrophenylsulphonyl)oxy group due to its strong electron-accepting ability.

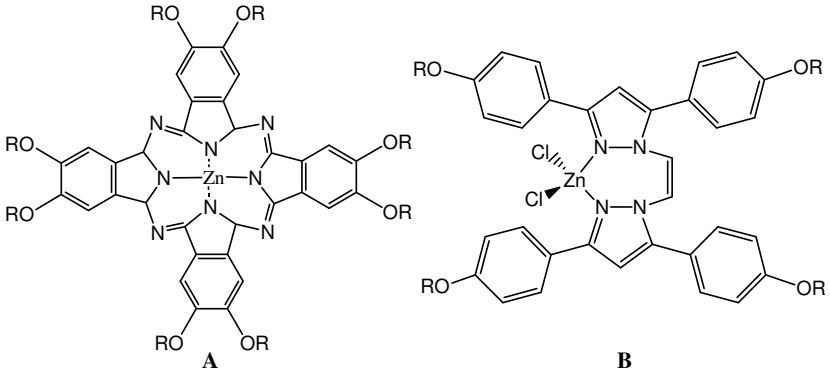

Figure 3.3 Zinc complexes with phthalocyanine (**A**) and pyrazolyl ligands (**B**)

Severs and co-workers[9] described the thermal behaviour of zinc phthalocyanines with eight peripheral dodecyloxy chains. Binnemans[10] reported the influence of the nature of the central metal ion on the transition temperatures of metal phthalocyanines with eight peripheral alkoxy chains. The melting points depended on the identity of the central metal ion and followed the order Ni(II) < (Cu(II) ≈ Co(II) < Zn(II) for increasing melting temperatures. Longer alkyloxy chains tend to lower the transition temperatures of the compounds. The melting points of these phthalocyanine complexes are in general higher than those of the corresponding metal-free phthalocyanines.

In the liquid crystalline zinc complexes described earlier, the geometry of the metal centre is either planar or trigonal bipyramidal[4-7]. Recently mesomorphism for zinc complexes have been reported regardless of the geometry (including tetrahedral) around the metal ion, with bis[3,5-bis(p-decyloxyphenyl)pyrazolyl]ethane[15] and hexacatenar 4,4'-disubstituted 2,2'-bipyridines[16] as ligands. Gimenez and coworkers[15] employed the idea of Date[17] that the controlled supramolecular assemblies possible with metal complexes can be obtained from suitable ligand design. The zinc complexes displayed enantiotropic smectic C and A phases. The molecular structure indicated that the zinc atom was in a tetrahedral environment of ligands, but the planes containing the pyrazole rings were arranged at angles of only 16^{o}, resulting in a macrostructure consisting of more or less planar layers.

In this study 5-alkyl-2-thiophenedithiocarboxylate complexes of zinc(II), analogues to the nickel(II) complexes described in chapter 2, were prepared and studied. Again small differences in structural features and electronic properties of the zinc complexes created by replacing a bridging phenyl by a thiophene unit were the main focus point. It was found that the presence of thiophene units helped to clear some of the confusion and irregularities in literature regarding the composition of nickel dithiocarboxylate complexes. Zinc dithiocarboxylate complexes were selected because of their close relationship with the metals Ni(II) and Cu(II) in their formation of stable complexes with S-donor ligands[3]. Zn(II) belongs to the d^{10}-configuration and affords, unlike Ni(II) (d^{8}) complexes, no

crystal field stabilization. The stability and the stereochemistry of a particular compound depends on the size and polarizing power of the Zn(II) cation and the steric requirements of the ligands.

3.2 Results and discussion

3.2.1 Synthesis and characterization

Five complexes of the type $[Zn(S_2CTR)_2]$ (where T =2,5-disubstituted thiophene unit, R = alkyl group; C_4H_9(**7**), C_6H_{13}(**8**), C_8H_{17}(**9**), $C_{12}H_{25}$,(**10**), $C_{16}H_{33}$(**11**)) were synthesized via a four-step reaction as shown in Scheme 3.1

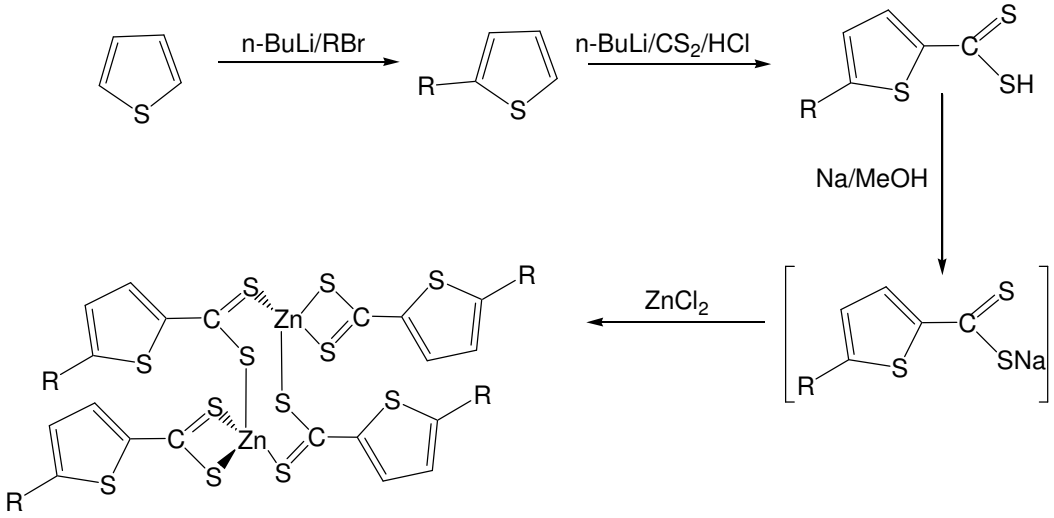

Scheme 3.1

The first three steps are similar to those described in chapter 2 for nickel(II) complexes. The sodium 5-alkyl-2-thiophenedithiocarboxylate compounds were synthesized according to literature procedures[18] as shown in Scheme 3.1. The first step involved the lithiation of thiophene at position 2 followed by the subsequent addition of alkyl bromide. In the second step, 2-alkyl thiophene was converted

into 5-alkyl-2-thiophenedithiocarboxylic acid. The first part of the reaction was done under an inert atmosphere. It involved the lithiation of alkyl thiophene at position 5 followed by the addition of CS_2. A deep red colour was observed on addition of CS_2. On further acidification with dilute hydrochloric acid, 5-alkyl-2-thiophenedithiocarboxylic acid was formed. Subsequently it was converted into the sodium salt by reacting with sodium methoxide.

The final step was similar to that used by Adams *et al.*[4] for the preparation of the corresponding dithiobenzoate complexes. On addition of a colourless solution of zinc chloride in water to a stirred solution of sodium 5-alkyl-2-thiophenedithiocarboxylate in water, the colour turned orange-brown and the reaction was allowed to stir for 3 hours at room temperature to ensure a complete reaction. The product was precipitated by adding excess methanol, separated by filtration and dried. Further purification was done on a silica gel column and the product was eluted with a mixture of hexane/dichloromethane (1:1) as eluent. IR and NMR spectroscopy were used to characterize the complexes. A structure determination (vide infra) revealed that two $[Zn(S_2CTR)_2]$ fused to afford a dizinc complex $[Zn_2(\mu\text{-}S_2CTR)_2(S_2CTR)_2]$.

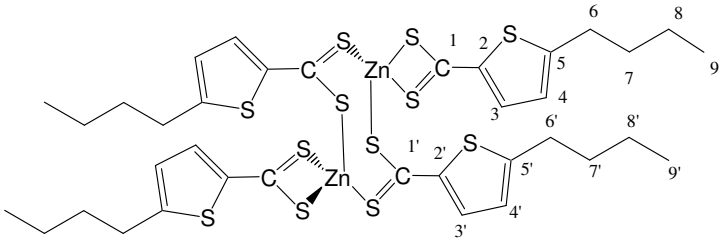

Figure 3.4

The carbon atoms are numbered starting with the carbon of CS_2 being C1 and numbering the hydrogen atoms with the same number as the carbons to which

they are attached. The bridging dithiocarboxylate ligands are numbered similarly but the atoms are indicated by adding apostrophes to the numbers.

The ^{1}H NMR spectrum of $[Zn_2(S_2CTC_4H_9)_4]$, **7** (Figure 3.5) displayed two doublets, at 7.87 ppm and 6.83 ppm in the arene region of the spectrum. The doublet signal at 7.87 ppm is assigned to H3 because it is closer to the dithiocarboxylate carbon (C1). The doublet signal at 6.83 ppm was assigned to H4 which is closer to the side of the alkyl (butyl) chain. The two doublets, which integrated for four hydrogen atoms, are indicative of two thiophene rings in a similar electronic environment. Hence, the terminal and bridging resonances in the ^{1}H NMR spectra coincides.

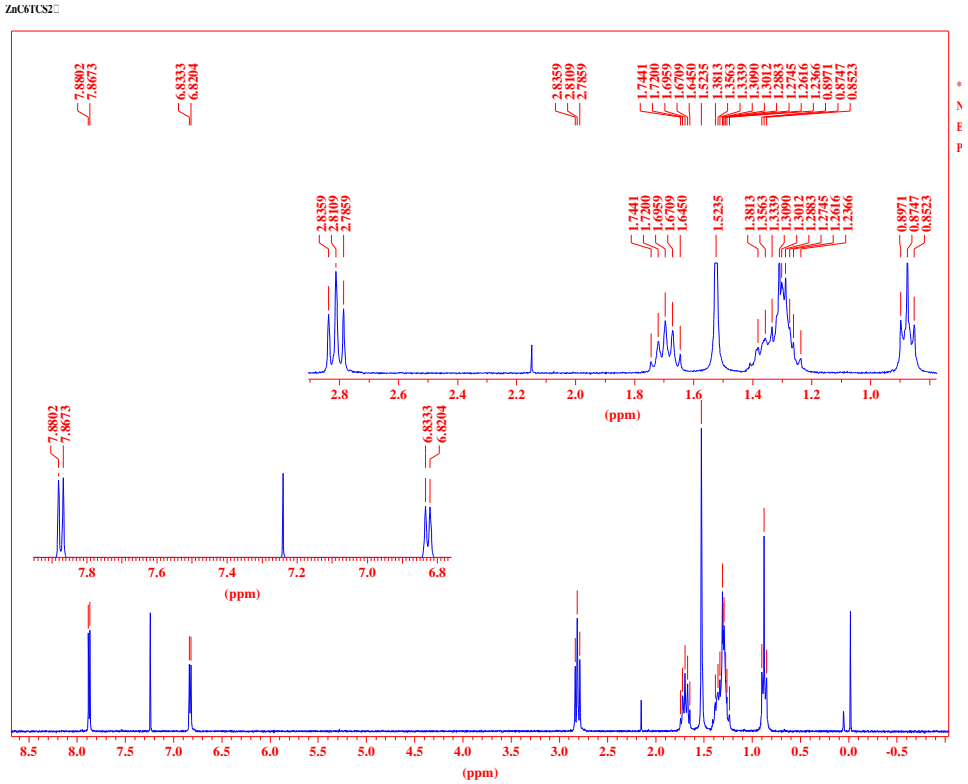

Figure 3.5 The ^{1}H NMR spectrum of $[Zn_2(S_2CTC_4H_9)_4]$ **7**

The signal at 2.82 ppm is assigned to the four protons of the two CH_2-groups attached to the two symmetrical thiophene rings. The multiplets at 1.66 and 1.42 ppm integrated for eight protons and represent the two middle CH_2-groups of the two butyl chains. The signal at 0.92 ppm integrated for six protons and was assigned to the two CH_3-groups at the end of the chains. The ^1H NMR spectra of all the complexes showed only two doublets in the arene region. The spontaneous insertion of a sulfur atom into the RCS_2-ligand in THF to give perthiocarboxylate ligands for the nickel(II) complexes was absent in the analogous zinc(II) complexes. However, similar insertions have been observed for zinc(II) benzenedithiocarboxylate complexes. The presence of the perthiocarboxylate ligands for nickel(II) complexes and absence thereof for zinc(II) complexes are ascribed to the electronic effects of the thiophene rings.

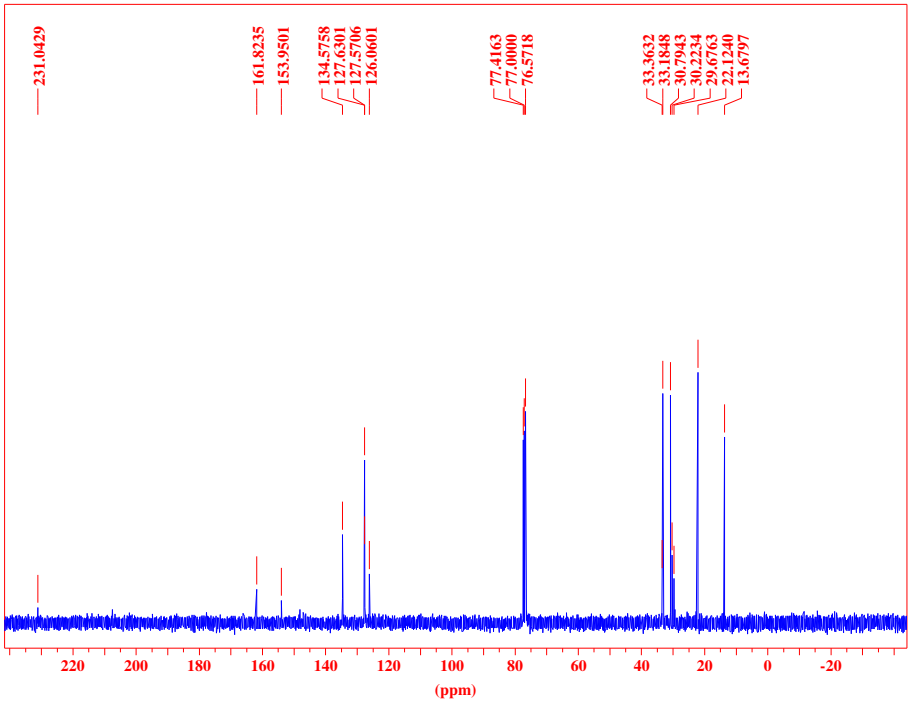

Figure 3.6 The ^{13}C NMR spectrum of $[Zn_2(S_2CTC_4H_9)_4]$ **7**

The ^{13}C NMR spectrum of $[Zn_2(S_2CTC_4H_9)_4]$, **7** (Figure 3.6) showed all the carbons of the thiophene rings, the butyl chains as well as that of the CS_2 chelate (C1). Again, no duplication of signals was observed, supporting the ^1H NMR data. None of the FAB mass spectra of any of the complexes gave a molecular ion peak or m/z-values assignable to fragment ions. The infrared spectra of all the complexes showed similar peaks. The infrared spectrum of $[Zn_2(S_2CTC_4H_9)_4]$, **7** showed prominent peaks at 2921, 1461, 1375, 1046, 980 and 721 cm^{-1}. The signal at 2921 cm^{-1} was assigned for the CH_2-groups of the alkyl chain and the peak at 1461 cm^{-1} was assigned for the arene-carbon (C-C thiophene) stretching frequency. The peak at 1375 cm^{-1} was assigned for the terminal CH_3 group. The peaks at 1046 and 980 cm^{-1} were assigned for C-S stretching frequencies of the dithiocarboxylate group. Usually the stretching frequencies of dithiocarboxylate complexes[19,20] are observed between 900 and 1100 cm^{-1}. The peak at 721 cm^{-1} was assigned for the arene C-H (thiophene). The infrared spectral values of **7-11** are given in Table 3.1.

Table 3.1 Spectral data of complexes **7-11**

Complex	^1H NMR (δ/ppm in $CDCl_3$)	^{13}C NMR (δ/ppm in $CDCl_3$)	IR (ν/cm^{-1} in Nujol)
$[Zn_2(S_2CTC_4H_9)_4]$ **7**	7.87 (d, 2H, H3, J=3.9), 6.83 (d, 2H, H4, J=3.6), 2.82 (t, 4H, H6, J=7.5), 1.66 (m, 4H, H7), 1.42 (m, 4H, H8), 0.92 (t, 6H, H9, J=7.2/7.5)	231.0 (C1), 161.8 (C2), 153.9 (C5), 134.6 (C3), 127.5 (C4), 33.2, 29.8, 22.1, 13.7 (C6-C9)	2921 (vs), 1461 (vs), 1375 (s), 1046 (m), 980 (m), 721 (s)
$[Zn_2(S_2CTC_6H_{13})_4]$ **8**	7.87 (d, 2H, H3, J=3.9), 6.83 (d, 2H, H4, J=3.9), 2.81 (t, 4H, H6, J=7.5), 1.69	207.0 (C1), 162.5 (C2), 148.7 (C5), 135.2 (C3), 128.0 (C4), 31.8, 31.5,	2921 (vs), 1458 (vs), 1375 (s), 1050 (m), 978

	(m, 4H, H7), 1.30 (m, 12H, H8-H10), 0.87 (t, 6H, H11, J=6.7)	31.4, 29.0, 22.9, 14.4 (C6-C11)	(m), 722 (s)
$[Zn_2(S_2CTC_8H_{17})_4]$ **9**	7.87 (d, 2H, H3, J=3.9), 6.82 (d, 2H, H4, J=3.9), 2.80 (t, 4H, H6, J=7.5/7.8), 1.69 (m, 4H, H7), 1.26 (m, 20H, H8-H12), 0.87 (t, 6H, H13, J=6.7/7.0)	207.5 (C1), 162.1 (C2), 148.3 (C5), 134.8 (C3), 127.6 (C4), 31.8, 31.1, 30.6, 29.2, 29.1, 29.0, 22.6, 14.0 (C6-C13)	2920 (vs), 1461 (vs), 1375 (s), 1048 (m), 970 (m), 721 (s)
$[Zn_2(S_2CTC_{12}H_{25})_4]$ **10**	7.85 (d, 2H, H3, J=3.9), 6.81 (d, 2H, H4, J=3.9), 2.79 (t, 4H, H6, J=7.5), 1.68 (m, 4H, H7), 1.23 (m, 36H, H8-H16), 0.85 (t, 6H, H17, J=6.2/7.0)	206.8 (C1), 161.6 (C2), 134.3 (C5), 128.8 (C3), 127.5 (C4), 35.7, 31.9, 31.1, 30.9, 29.7, 29.6, 29.4, 29.2, 29.0, 26.4, 22.7, 14.1 (C6-C17)	2921 (vs), 1460 (vs), 1375 (s), 1046 (m), 981 (m), 720 (s)
$[Zn_2(S_2CTC_{16}H_{33})_4]$ **11**	7.86 (d, 2H, H3, J=3.9), 6.82 (d, 2H, H4, J=4.1), 2.80 (t, 4H, H6, J=7.5), 1.67 (m, 4H, H7), 1.24 (m, 52H, H8-H20), 0.86 (t, 6H, H21, J=6.5/6.7)	207.4 (C1), 161.5 (C2), 153.9 (C5), 134.2 (C3), 127.5 (C4), 31.9, 31.3, 31.1, 30.8, 30.7, 30.5, 29.8, 29.7, 29.6, 29.5, 29.3, 29.2, 29.0, 26.4, 22.7, 14.1 (C6-C21)	2921 (vs), 1461 (vs), 1375 (s), 1049 (m), 977 (m), 721 (s)

The ^{1}H and ^{13}C NMR data of the complexes suggest that the complexes are either monomers or the chemical shifts of the terminal and bridging dithiocarboxylate ligands are the same in solution.

3.2.2 Molecular structure of $[Zn_2(S_2CTC_6H_{13})_4]$ (**8**)

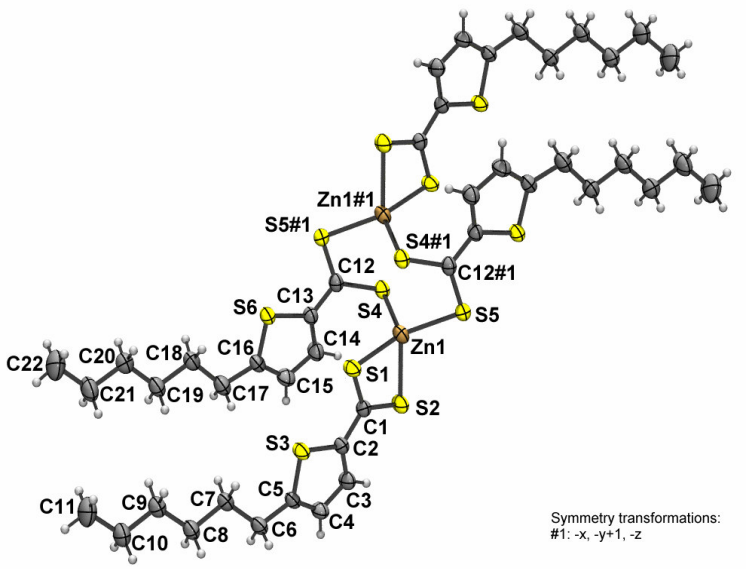

Figure 3.7 An ORTEP[21]+ POV-Ray[22] plot of the geometry of **8**

The molecular structure of **8** was determined by single crystal X-ray crystallography. Single crystals suitable for crystal structural determination were obtained by slow diffusion of hexane into a CH_2Cl_2 solution of **8** at room temperature. An ORTEP + POV-Ray plot of the geometry of **8** in Figure 3.7 and a computer generated model of **8** in figure 3.8 are given. Selected bond lengths are given in Table 3.2 and selected bond angles in Table 3.3.

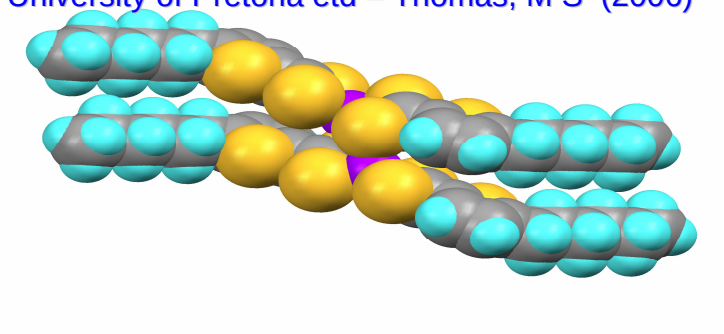

Figure 3.8 A computer generated model of **8**

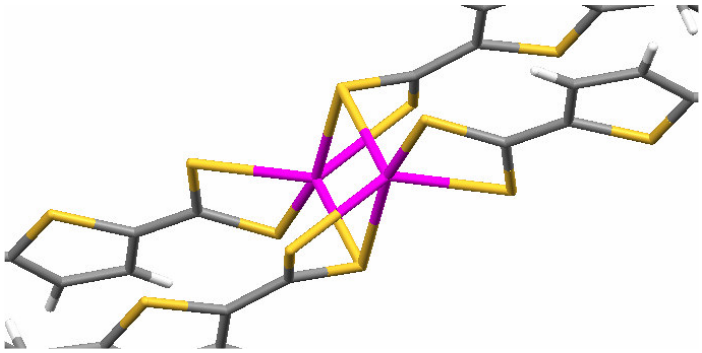

Figure 3.9 View of molecule showing the distorted trigonal bipyramidal arrangement of sulfur atoms around the zinc atoms

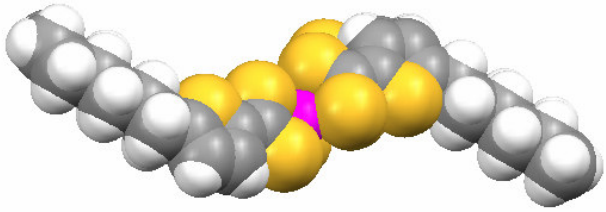

Figure 3.10 Side-on view showing the step-rod assembly of atoms as a result of the five-member thiophene rings

The structure of **8** can be compared to an analogous structure described for $[Zn_2(S_2CBC_8H_{17})_4]$ by Adams *et al.*[4]. Both structures display a dimeric assembly

with significant interaction between a sulfur of each monomer with the zinc metal of the other monomer in the solid state. As a result an eight-membered ring is formed with a chair conformation consisting of two zinc and two carbon atoms and four sulfur atoms. In the monomeric structure of $[Zn(S_2CPh)_2]^4$ or the dithiocarbamate $[Zn(S_2CNEt_2)_2]^4$ the zinc has a tetrahedral arrangement of ligands.

The molecular structure of **8** in the solid state is illustrated in Figure 3.7. Each molecule exists as a centrosymmetric dimer with the zinc atom in a five coordinated ligand environment with geometry that more closely resembles trigonal bipyramid (Figure 3.9). The dithiocarboxylate chelate ligands each bridge between an axial and an equatorial site with subtended angles of 67 or 75°. The remaining equatorial site is occupied by a sulfur already occupying an axial site of an adjacent, centrosymmetrically related, zinc co-ordination polyhedron. Four of the five zinc-sulfur bonds, excluding that to the axial bridging sulfur, S(4)#1, are short.

The distance between the zinc and axial bridging sulfur, S(4)#1, in structure **8** is 2.88Å, which is longer than the one reported for dithiobenzoate complexes, 2.83Å. The main difference between the overall shape of **8** compared to the linear structure of $[Zn_2(8\text{-odtb})_4]$ is the step-rod pattern that emerges for **8** in one plane whereas the p-benzene substituted octyloxy is linearly rod-shaped. This is a consequence of the five-member thiophene rings that cause a kink in the chains and can be seen in Figure 3.10. Figure 3.11 shows the packing of the lamellar rods and calamitic features.

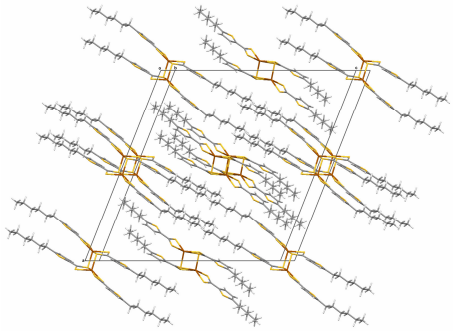

Figure 3.11 Shows the packing of the lamellar rods and calamitic features

Table 3.2 Selected bond lengths for **8**[a]

Atoms	Bond length (Å)	Atoms	Bond length (Å)
Zn(1)-S(4)#1	2.884(8)	[a]S(3)-C(2)	1.727(3)
Zn(1)-S(5)	2.354(8)	S(6)-C(16)	1.715(3)
Zn(1)-S(2)	2.454(8)	C(1)-C(2)	1.444(3)
Zn(1)-S(1)	2.369(7)	C(2)-C(3)	1.371(4)
Zn(1)-S(4)	2.392(8)	C(3)-C(4)	1.388(4)
S(1)-C(1)	1.701(3)	C(4)-C(5)	1.362(4)
S(2)-C(1)	1.690(3)	C(12)-C(13)	1.435(4)
S(4)-C(12)	1.723(3)	C(13)-C(14)	1.379(4)
S(5)-C(12)#1	1.683(3)	C(14)-C(15)	1.391(4)
S(3)-C(2)	1.727(3)	C(15)-C(16)	1.366(4)
S(6)-C(13)	1.729(3)	C(12)-S(5)#1	1.683(3)

[a] The corresponding bond lengths in thiophene are C(2)-S 1.714(1) Å, C(2)-C(3) 1.370(2) Å, C(3)-C(4) 1.423(2) Å[23]

Table 3.3 Selected bond angles for **8**

Atoms	Bond angle (°)	Atoms	Bond angle (°)
S(5)-Zn(1)-S(4)#1	67.62(2)	S(5)-Zn(1)-S(2)	111.59(3)
S(1)-Zn(1)-S(4)#1	96.96(3)	S(1)-Zn(1)-S(4)	117.86(3)
S(4)-Zn(1)-S(4)#1	82.43(3)	S(1)-Zn(1)-S(2)	74.74(3)
S(2)-Zn(1)-S(4)#1	167.72(3)	C(5)-S(3)-C(2)	92.31(13)
S(4)-Zn(1)-S(2)	109.35(3)	C(1)-S(1)-Zn(1)	83.99(9)
S(5)-Zn(1)-S(1)	134.47(3)	C(12)-S(4)-Zn(1)	98.94(9)
S(5)-Zn(1)-S(4)	102.78(3)	C(12)#1-S(5)-Zn(1)	93.72(9)

The bond lengths and bond angles of free thiophene[23] are compared with bond distances and angles of coordinated thiophene in **8**. The bond length of C-S increases slightly during coordination whereas the bond angle C(2)-S-C(5) remains the same. The bond length between carbon atoms on one side of the coordinated thiophene is smaller. In free thiophene the delocalization is within the ring whereas for **8** it is outwards towards the CS_2 ligand. This is manifested in the significantly shorter C(3)-C(4) bond distance in **8.** The distance of 1.44Å for C(1)-C(2) is shorter than the averaged distance for C-C (1.54Å) single bonds but longer than the averaged distance for C-C (1.34Å) double bonds. This may be due to the charge delocalization present in the thiophene ring in pi-contact with CS_2 and metal.

3.2.3 Thermal properties

The thermal properties of the complexes were preliminarily examined by Differential Scanning Calorimetry (DSC). The DSC thermogram reveals the presence of mesophases and liquid crystal phases by detecting the enthalpy change that is associated with a phase transition. Complexes **7**, **8** and **11** showed single sharp endothermic peaks whereas **9** and **10** showed two broad peaks, one small and one medium endothermic peak during melting. Ohta and coworkers[24] suggested that the double melting behaviour (two endothermic peaks) of long chain substituted compounds is a thermal behaviour close to mesomorphism. Figure 3.12 shows the DSC thermogram for $[Zn(S_2CTC_8H_{17})_2]$ **9**.

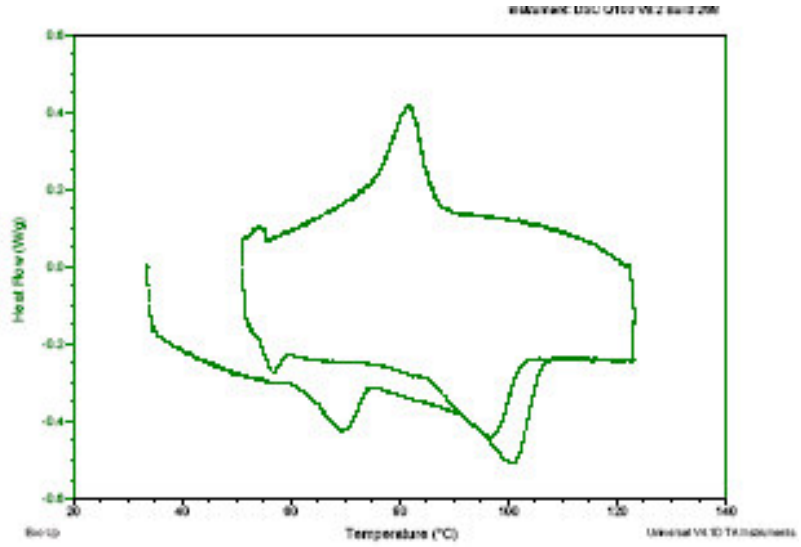

Figure 3.12DSC thermogram of **9**

Complex **9** showed two endothermic peaks, at 69°C and 102°C. The first peak at 69°C during the heating cycle is regarded as a crystal-crystal transition. The peak at 102°C is regarded as the melting point of the complex. Sometimes multiple endothermic events might represent transitions from one crystalline state to

another crystalline state, which occur when the substance exist in different molecular packing in the solid state at different temperatures[25]. Complex **10** also showed two endothermic peaks. The melting point peaks of **9** and **10** are broad whereas the melting point peaks of **7**, **8** and **11** are very sharp. The sharpness of the melting point gives an indication of the purity of the complex. Low molecular weight compounds with liquid crystalline properties are expected to have sharp melting points. The melting points of **7-11** from DSC are given in Table 3.4.

Table 3.4 Melting points of **7-11** complexes

Complex	Chain length	Melting point (^{o}C)
7	C_4H_9	132
8	C_6H_{13}	119
9	C_8H_{17}	102
10	$C_{12}H_{25}$	84
11	$C_{16}H_{33}$	52

The dependence of melting points of the complexes **7-11** on the chain length is depicted in Figure 3.13.

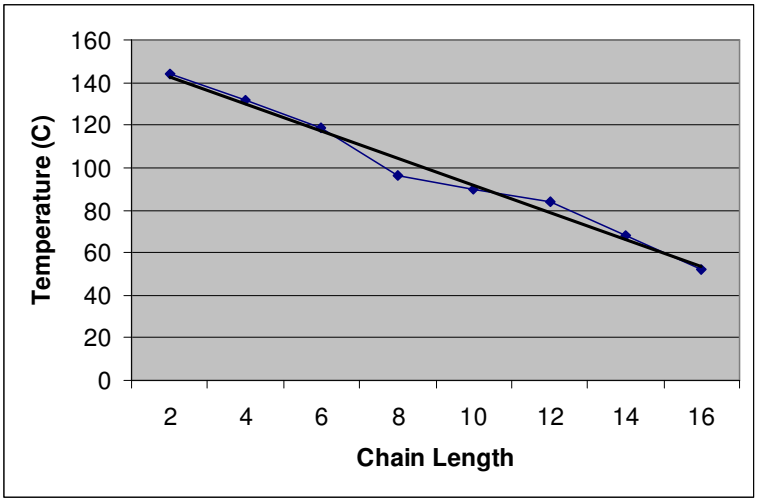

Figure 3.13 Dependence of the melting points of **7-11** on the chain length

The trend in the melting points is a steady decrease as the alkyl chain length of complexes increased (Figure 3.13). This trend was observed earlier for a homologous series of complexes that differ only in chain length[26]. The highest temperature 132°C for the shortest chain (C_4) and the lowest temperature 52°C for the longest chain (C_{16}) were observed. It is of interest to note that there is a linear decrease of melting points with increase in chain length. This has been ascribed to greater disorder caused by longer alkyl chains in the complexes.

Two complexes, one with sharp endothermic peak **11** and the other one **10** with two broad endothermic peaks were also examined by Hot-stage Polarising Optical microscopy. The complex **11** directly melted to the isotropic liquid without showing any mesophases. Complex **10**, when looking at the sample between crossed polarizers gave an impression that there is a mesophase present above 80°C. However, careful examination revealed that the birefringence observed was not due to a mesophase but due to tiny crystals floating in an isotropic melt. Cooling of the samples resulted in simple crystallization without forming any mesophases. Therefore complex **10** is not liquid crystalline.

3.3 Experimental

3.3.1 General

All commercially available chemicals were used as received. Solvents were dried and distilled under nitrogen prior to use. Thiophene was purified as described by Spies and Angelici[27]. All reactions were performed in an inert atmosphere of

either nitrogen or argon by using Schlenk techniques and vacuum-line. Column chromatography was carried out using silica gel.

Infrared spectra were recorded on a Perkin Elmer Spectrum 1000 FT-IR spectrophotometer. All NMR spectra were recorded in deuterated chloroform using the chloroform peak as standard on a Bruker ARX – 300 spectrometer.

Liquid-crystalline properties were examined on a Differential Scanning Calorimeter (DSC) Q 100 V8.2 Build 268 and Hot-stage Polarising Optical Microscope (POM) Olympus BX60 equipped with a Linkam THMS600 hot stage and a Linkam TMS93 Programmable temperature controller.

3.3.2 Structure determination of 8

A crystal of size 0.34 x 0.14 x 0.05 mm^3 was mounted in a sealed capillary tube for data collection. All geometric and intensity data were collected on a Siemens SMART diffractometer with a CCD detector.

3.3.3 Synthesis

All the complexes were synthesized via a four-step reaction in a similar manner. A typical procedure for complex **7** is described.

Preparation of 2-butyl thiophene

The procedure used is similar to the one described by Brandsma[18].The reaction was done in an inert atmosphere. n-Butyl lithium (15.6 ml, 25.0 mmol) was added to a mixture of THF (50.0 ml) and hexane (30.0 ml), which was cooled to -20^{o}C. Thiophene (1.68 g, 20.0 mmol) was introduced over 10 minutes with cooling

between 0°C and 10°C. The cooling bath was removed and allowed to rise to the room temperature. Butyl bromide (2.74 g, 20.0 mmol) was added in one portion without external cooling. The temperature of the solution was raised to 50°C and kept at this temperature for a further 30 minutes after which 100 ml of ice water was added with vigorous stirring. Two separate layers were observed and the separation was done in air. After separation of the layers, two extractions with diethyl ether were carried out. The combined organic solutions were dried over anhydrous $MgSO_4$ and concentrated in a rotary evaporator and weighed. Yield = 2.38 g; 85%.

Preparation of 5-butyl-2-thiophenedithiocarboxylic acid ($C_4H_9TCS_2H$)

In the second step 2-butyl thiophene was converted into 5-butyl-2-thiophenedithiocarboxylic acid. The first part of the reaction was done in an inert atmosphere. n-Butyl lithium (12.5 ml, 20.0 mmol) was added to a solution of THF (50.0ml) and hexane (30.0 ml), which was cooled to -20°C. 2-Butyl thiophene (2.38 g, 17.0 mmol) was introduced over 10 minutes with cooling between 0°C and 10°C. The cooling bath was removed and allowed to rise to room temperature and stirred for a further 10 minutes. The solution was cooled to 0°C and copper(I) bromide (0.1 g) was added. Carbon disufide (1.29 g, 17.0 mmol) was added drop-wise to the stirred mixture. The colour of the reaction mixture changed to a deep-red colour. The cooling bath was removed and allowed to rise to the room temperature and stirring was continued for a further 1 hour. Ice water (100.0ml) was added followed by dilute hydrochloric acid (20.0 ml, 1mol/dm^3). The next part was done in air. The organic layer was separated and

extracted into diethyl ether (70.0 ml) and washed with 2 x 50.0 ml of water. The product was dried over $MgSO_4$ and the solvent removed in *vacuo*. Yield = 3.30 g; 89.8%.

Preparation of sodium-5-butyl-2-thiophenedithiocarboxylate ($C_4H_9TCS_2Na$)

The reaction was done in an inert atmosphere. Sodium metal (0.35 g, 15.28 mmol) was added over 10 minutes to vigorously stirred methanol (50.0 ml). When all the sodium had dissolved, additional (20.0 ml) methanol was added. 5-Butyl-2-thiophenedithiocarboxylic acid (3.30 g, 15.28 mmol) was added over 5 minutes to the mixture and left stirring for 30 minutes. The solvent was removed *in vacuo*, leaving the sodium 5-butyl-2-thiophenedithiocarboxylate as an orange-brown solid. Yield = 3.09 g; 85%.

Synthesis of bis(5-butyl-2-thiophenedithiocarboxylato)zinc(II) [$Zn_2(S_2CTC_4H_9)_4$]

The procedure was similar to that of Adams *et al*[4], who prepared dithiobenzoate complexes. The reaction was done in air. To a stirred solution of sodium 5-butyl-2-thiophenedithiocarboxylate (1.55 g, 6.5 mmol) in water (25.0 ml) was added drop-wise a colourless solution of $ZnCl_2$ (0.41 g, 3.0 mmol) in water (10.0 ml) at room temperature. The colour of the solution turned orange-brown and the mixture was left to stir for 3 hours. The mixture was concentrated to 25.0 ml on a rotary evaporator and 20.0 ml of methanol was added. The precipitate was separated by filtration and dried. The product was an oily solid. The product was purified on a silica gel column with hexane as the initial eluent and the first and second fraction on evaporations obtained as an oily red liquid. The desired

product was eluted from the column with hexane:CH_2Cl_2 (1:1). An orange powder was obtained on evaporation of the solvent. Yield = 0.49 g, 33%.

Five complexes of the type bis(5-alkyl-2-thiophenedithiocarboxylato)zinc(II) were synthesized by varying the alkyl chain, C_4H_9, C_6H_{13}, C_8H_{17}, $C_{12}H_{25}$ and $C_{16}H_{33}$. All the complexes were isolated as solids. The experimental results of complexes **7-11** are given in Table 3.5.

Table 3.5 Experimental results of **7-11** complexes

Complex	Colour	Mass (g)	Yield (%)
7	Orange	0.49	33
8	Orange	0.76	46
9	Reddish-orange	0.79	52
10	Dark orange	0.82	38
11	Dark orange	0.79	32

3.4 Conclusion

The reactions of a series of 5-alkyl-2-thiophenedithiocarboxylates with zinc(II) chloride formed zinc(II) complexes with terminal dithiocarboxylate ligands. The colour of the products is orange or dark orange. The zinc complexes are less soluble than the nickel analogues. A X-ray structure determination of complex **8** showed it to be dimeric, containing 8-membered $Zn_2S_4C_2$ rings, formed by the fusion of two ZnS_2C rings, and in which the geometry of sulfur about zinc approximated to trigonal bipyramidal with Zn-S intermolecular bond distance of

2.39 Å, being of the same order as Zn-S intramolecular bond distance of 2.33 – 2.77 Å. The X-ray structure is similar to the one for zinc bis[4-alkyloxy)dithiobenzoates described by Adams *et al.*[4]. Zinc alkyloxydithiobenzoate complexes are rod-shaped whereas the zinc thiophenedithiocarboxylate complex, **8** displays a step in its rod shape. Complexes **7-11** did not show any mesomorphic properties whereas zinc bis alkyloxy dithiobenzoates are reported to be mesomorphic[3]. It was reported that the dimeric structure persisted into the mesophase for the alkyloxydithiobenzoate complexes. The X-ray crystal structure of **8** showed that the distance between the zinc and the axial bridging sulfur, S(4)#1, is greater than in the zinc bis alkyloxy dithiobenzoates. Only EXAFS studies can confirm whether the dimeric structure retained during the melting process of **9** and **10.** It was reported that if the molecular forces are too strong, or if they are too weak, no mesophases will appear even if the molecular geometry is favourable for liquid crystalline properties[3]. Complexes **9** and **10** did not have liquid crystalline properties.

REFERENCES

1. P. A. Cotton and G. Wilkinson, *Advanced Inorganic Chemistry,* Fifth edition, John Wiley & sons Inc., **1988**, 608.
2. M. Bonamico, G. Dessy, V. Fares and L. Scaramuzza, *J. Chem. Soc., Dalton Trans*., **1972**, 2515.
3. H. Adams, N. A. Bailey, D. W. Bruce, R. Dhillon, D. A. Dunmur, S. E. Hunt, E. Lalinde, A. A. Maggs, R. Orr, P. Styring, M. S. Wragg and P. M. Maitlis, *Polyhedron*, **1988**, 7, 1861.
4. H. Adams, A. C. Albeniz, N. A. Bailey, D. W. Bruce, A. S. Cherodian, R. Dhillon, D. A. Dunmur, P. Espinet, J. L. Feijoo, E. Lalinde, P. M. Maitlis, R. M. Richardson and G. Ungar, *J. Mater. Chem*., **1991**, 1, 843.
5. A-M. Giroud-Godquin and P. M. Maitlis, *Angew. Chem., Int. Ed. Engl*., **1991**, 30, 375.
6. E. Terazzi, J.-M. Benech, J.-P. Rivera, G. Bernardinelli, B. Donnio, D. Guillon and C. Piguet, *J. Chem. Soc., Dalton Trans*., **2001**, 769.
7. B. A. Gregg, M. A. Fox and A. J. Bard, *J. Chem. Soc., Chem. Commun*., **1987**, 1134.
8. D. Guillon, A. Skoulios, C. Piechocki, J. Simon and P. Weber, *Mol. Cryst., Liq. Cryst*., **1983**, 100, 275.
9. L. M. Severs, A. E. Underhill, D. Edwards, P. Wight and D. Thetford, *Mol. Cryst., Liq. Cryst*., **1993**, 234.
10. J. Sleven, T. Cardinaels, C. Gorller-Walrand and K. Binnemans, *ARKIVOC*, **2003** (iv) 68.

11. K. Ohta, G. J. Jiang, M. Yokoyama, S. Kusabayashi and H. Mikawa, *Mol. Cryst., Liq. Cryst*., **1981**, 66, 283.

12. D. W. Bruce, D. A. Dunmur, L. S. Santa and M. A. Wali, *J. Mater. Chem*., **1992**, 2, 363.

13. N. Hoshino, R. Hayakawa, T. Shibuya and Y. Matsunaga, *Inorg. Chem*., **1990**, 29, 5129.

14. Q. M. Wang and D. W. Bruce, *Tetrahedron Letters*, **1996**, 37, 7641.

15. R. Gimenez, A. B. Manrique, S. Uriel, J. Barbera and J. L. Serrano, *Chem. Commun*., **2004**, 2064.

16. G. Barberio, A. Bellusci, A. Crispini, M. Ghedini, A. Golemme, P. Prus and D. Pucci, *Eur. J. Inorg. Chem.*, **2005**, 181.

17. W. Date, E. Fernandez Iglesias, K. E. Rowe, J. M. Elliott and D. W. Bruce, *Dalton Trans*., **2003**, 1914.

18. L. Brandsma and H. D. Verkruijsse, *Preparative Polar Organometallic Chemistry, Volume 1*, Springer Verlag, Heidelberg, **1987**, 124.

19. M. L. Shankaranarayana and C. C. Patel, *Can. J. Chem*., **1961**, 39, 1633.

20. J. M. Burke and J. P. Fackler (jr), *Inorg. Chem.*, **1972**, 11, 3000.

21. L. J. Farrugia, *J. Appl. Crystallogr*., **1997**, 30, 565.

22. The POV-Ray Team, POV-Ray 2004, URL: http://www.pov-ray.org./download/.

23. S. A. Cooke, J. H. Holloway and A. C. Legon, *Chem. Phys. Lett.*, **1998**, 298, 151.

24. K. Ohta, A. Ishii, H. Muroki, I. Yamamoto and K. Matsuzaki, *Mol. Cryst., Liq. Cryst.,* **1985**, 116, 299.

25. T. Seshadri and H. –J. Haupt, *J. Mater. Chem*. **1998.**, 8, 1345.

26. L. Jongen, K. Binnemans, D. Hinz and G. Meyer, *Mater. Sci Eng.*, **2001**, C18, 199.

27. G. H. Spies and R. J. Angelici, *Organometallics*, **1987**, 6, 1902.

Chapter 4

Rhenium(I) complexes with thiophene-containing ligands

4.1 Introduction

Organometallic liquid crystals have only recently come to the foreground and various metals such as Fe[1-7], Rh[8], Mn[9,10], Pt[11], Pd[11,12], etc. have been studied and displayed liquid crystalline properties. Problems associated with organic ligands are often the lability and instability of the metal carbon bond under thermal conditions. Planar or linear complexes are favoured as they could be used to mimic anisotropic rods or discs. In some instances the chains will be attached to a π-bonded arene ligand and in other examples to metal carbon bonds (Figure 4.1).

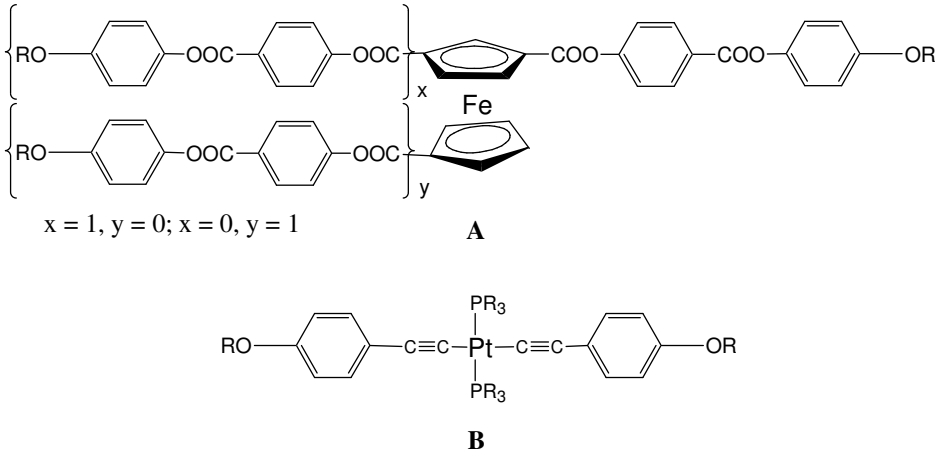

Figure 4.1 Calamitic organometallic liquid crystals

In the previous chapters' synthesis of nickel and zinc complexes, classical examples of inorganic compounds were discussed. In this section examples of

organometallic compounds of rhenium(I) with the same type of ligands were investigated. The coordination environment of ligands at the metal centre for nickel and zinc complexes is either square-planar or tetrahedral/trigonal bipyramidal. For many years, the mesomorphic properties of calamitic metal-containing liquid crystals[13] have mostly been associated with square planar or linear coordination at the metal centre. Thermotropic, calamitic mesophases of manganese(I) and rhenium(I) complexes of orthometalated imines were observed for the first time in 1994 by Bruce and co-workers[14]. The coordination geometry at the metal centre of these complexes was octahedral. It was reported that at least four aromatic rings in the organic backbone were necessary to preserve the overall molecular anisotropy to obtain the calamitic mesophases. Other orthometallated complexes of Mn(I) and Re(I) reported recently are with diazabutadiene[9,10,15,16] and 2,2'-bipyridine[14,17]. The carbonyl ligands have been omitted in Figure 4.2.

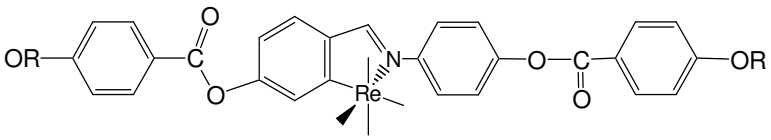

Figure 4.2 Orthometallated imine complexes of rhenium

Liquid crystals rely on the presence of anisotropic dispersion forces to stabilize their mesophases, and these arise from a shape anisotropy of the molecules, generally coupled with a significant anisotropy of polarisability. The addition of two extra ligands to the highly anisotropic coordinated planar, four-coordinate metal centre may generate octahedral coordination with reduced overall anisotropy[18]. In these complexes the rhenium is anchored in the centre of the

molecule by two nitrogen donor ligands and with the chain structure extending on both sides. The carbonyl ligands are omitted in Figure 4.3.

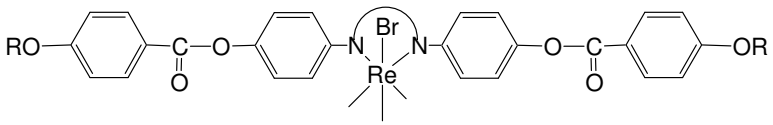

Figure 4.3 Diazabutadiene and bipyridine complexes of rhenium

Halotricarbonyl(α-diimine)rhenium complexes have been reported as efficient photosensitizers for energy and electron transfer[19]. Luminescence properties have been detected in *fac*-[ReX(α-diimine)$(CO)_3$] complexes where X can be varied from the simple halo and cyano group to organic ligands such as pyridine and acetylide[19,20]. Complexes of diazabutadienes with $ReBr(CO)_3$ have been reported as luminescent organometallic liquid crystals[21]. Binnemans and his co-workers synthesized the bromotricarbonyl rhenium(I) complexes by coupling mesogenic 4-cyanobiphenyl groups with a long alkyl spacer to a substituted imidazo[4,5-f]-1,10- phenanthroline, which acts as the coordinating group[22]. The mesophases of the complexes were nematic, smectic or lamello-columnar phases, depending on the position and number of 4-cyanobiphenyl groups.

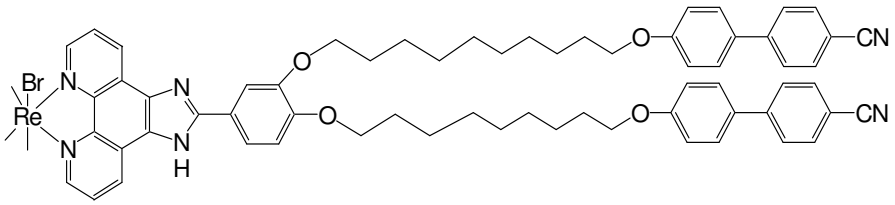

Figure 4.4 Luminescent rhenium(I) liquid crystals

The rhenium(I)-containing metallomesogens showed moderate transition temperatures and they were strongly luminescent, both in the solid state and in solution. In these complexes the rhenium is on one side of the chain structure.

In this study, 5-alkyl-2-thiophene- or bithiophenedithiocarboxylate complexes of rhenium(I) tetracarbonyl were synthesized and their structural features and potential liquid-crystalline properties investigated. Instead of arene rings thiophene rings are incorporated with the idea of modifying the structural features slightly and facilitating charge transfer processes and polarization effects.

4.2 Results and discussion

4.2.1 Synthesis and characterization

Complexes of the type $[Re(CO)_4(S_2CTR)]$ (where R = H, T = thiophene (**12**), R = CH_3 , T = bithiophene (**13**), R = $C_{14}H_{29}$, T = thiophene (**14a**), R = $C_{14}H_{29}$, T = bithiophene (**14b**)) were synthesized via a three-step reaction sequence.

During the first-step bromopentacarbonylrhenium, $[ReBr(CO)_5]$ was prepared by the reaction of dirheniumdecacarbonyl, $[Re_2(CO)_{10}]$ with bromine under a stream of nitrogen at room temperature (equation (1))[23].

$$[Re_2(CO)_{10}] + Br_2 \xrightarrow{\text{hexane}} 2[ReBr(CO)_5] \qquad (1)$$

In the second step pentacarbonyl(trifluoromethanesulfonato)rhenium(I), $[Re(CO)_5(O_3SCF_3)]$ was prepared from $[ReBr(CO)_5]$ (equation (2))[24].

$$[ReBr(CO)_5] + AgO_3SCF_3 \xrightarrow{CH_2Cl_2} [Re(CO)_5(O_3SCF_3)] + AgBr \qquad (2)$$

Silver(I) trifluoromethanesulfonate, $Ag(O_3SCF_3)$ was added to a dichloromethane solution containing $[ReBr(CO)_5]$ and stirring continued for 2 hours at room temperature. The fluffy AgBr precipitate was removed by filtration through a fine Schlenk frit to yield a clear solution. The volume of the solution was reduced under vacuum, allowed to warm to room temperature and freshly distilled hexane was added and the solvents were removed slowly in vacuum to precipitate $[Re(CO)_5(O_3SCF_3)]$ as a white powder.

In the third step, the 5-alkyl-2-thiophenedithiocarboxylate ion was prepared *in situ*, as described[25] in the previous chapter, and $[Re(CO)_5(O_3SCF_3)]$ added (equation (3)).

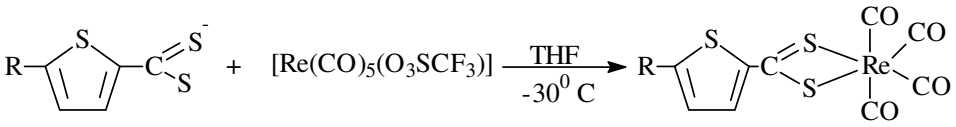

(3)

The colour of the mixture turned red, solvents were removed and the purification was done on a silica gel column. The complexes were characterized by NMR and IR spectroscopy and the data confirmed the assigned structures of the complexes.

The ^1H NMR spectrum of $[Re(CO)_4(S_2CC_4H_2SCH_3)$, **13** (Figure 4.5) showed two signals in the arene region of the spectrum, a doublet at 7.63 ppm and a multiplet at 6.82 ppm. Both integrated for one proton (the signal at 5.27 ppm should be discarded as it represents some dichloromethane in the sample).

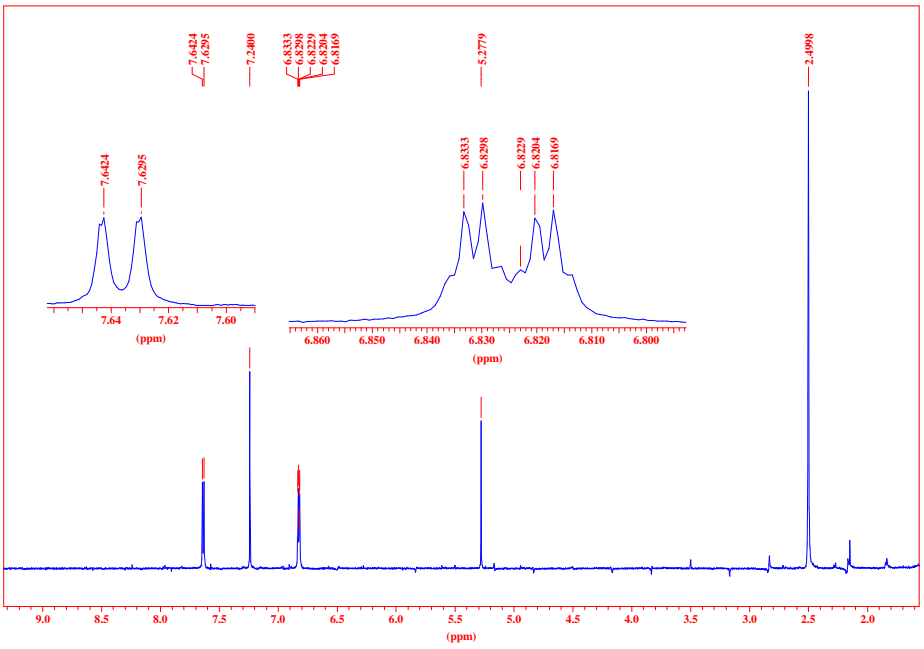

Figure 4.5 ^{1}H NMR spectrum of $[Re(CO)_4(S_2CTCH_3)]$ (**13**)

These protons, H3 and H4, are assigned to the protons of the thiophene ring. The resonances at 6.82 ppm is broadened because of the J_4 coupling with the protons of the methyl group. A singlet at 2.50 ppm, integrating for three protons, was assigned to the methyl group attached to the thiophene ring. Assignments of the protons in **12** were not unambiguous because of signals overlapping.

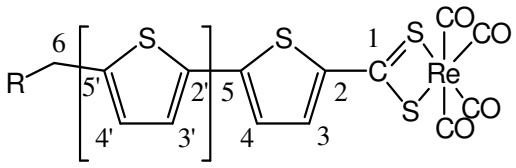

Figure 4.6 Structure of complexes with atomic numbering scheme used

The ^{13}C NMR of **14b** showed signals for all the carbon atoms in the structure and is depicted in Figure 4.7. The peak at 242.6 ppm in **13** was assigned to the carbons

of the carbonyl ligands, but was not observed in the spectra of **14a** and **14b**. The signal at 185.5 ppm is assigned to the CS_2 carbon, C1 and is close to the value reported for CS_2 carbon at 192.3 ppm in the solvent CS_2[26]. The thiophene carbons are readily assigned both from signal intensity and their chemical shift values at 152.7, 151.7, 128.6 and 127.5 ppm, repectively. Whereas the methyl carbon C6 in **13** is at 16.2 ppm, eleven chemical shift values of the total of fourteen carbons in the chain of **14b** were resolved. It is clear from the spectrum that overlapping of signals occurred in the 29.7 ppm region. The spectral data of **12**, **13, 14a** and **14b** are summarized in Table 4.1.

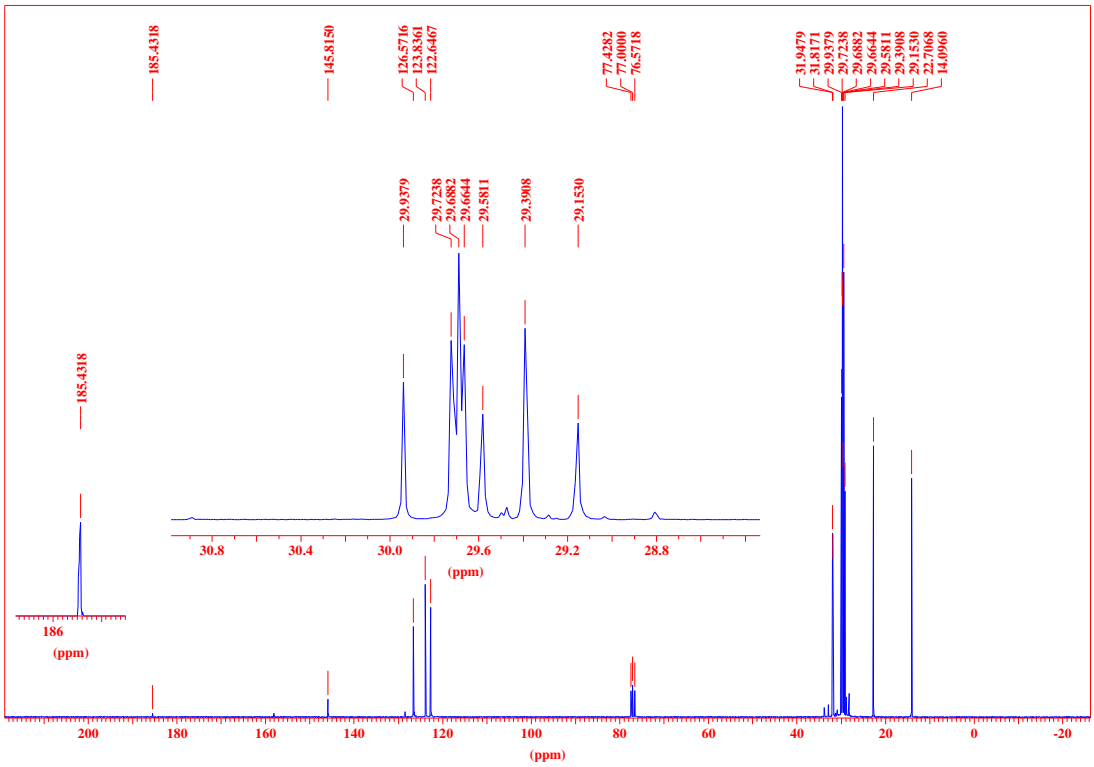

Figure 4.7 ^{13}C NMR spectrum of $[Re(CO)_4(S_2CTTC_{14}H_{29})]$ (**14b)**

Table 4.1 NMR and IR data of complexes **12-14**

Complex	^{1}H NMR (δ/ppm and *J*/Hz in $CDCl_3$)	^{13}C NMR (δ/ppm in $CDCl_3$)	IR[a] (ν/cm^{-1} in hexane)
12	7.16 (d, 2H, H3 and H4, *J* = 4.0), 7.14 (d, 2H, H3' and H4', *J* = 4.0), 6.97 (d, 1H, H5', *J* = 4.4)	240.0 (CO), 185.6 (CS_2), 141.1, 137.9 (C2, C5), 128.2 (C2' and C5'), 124.8 (C3 and C4), 124.2 (C3' and C4').	2099 (m), 2007 (s), 1995 (s), 1961 (s).
13	7.63 (d, 1H, H3, *J* = 3.9), 6.82 (m, 1H, H4), 2.5 (s, 3H, H6).	242.6 (CO), 185.5 (CS_2), 152.7 (C2), 151.7 (C5), 128.6 (C3), 127.5 (C4), 16.2 (C6)	2104 (m), 2010 (s), 1996 (s), 1959 (s).
14a	7.1 (d, 1H, H3 J = 4.0), 6.79 (m, 1H, H4), 2.84 (t, 2H, CH_2, H6, *J* = 7.5), 1.73 (m, 2H, H7), 1.32 (m, 22H, H8-H18), 0.92 (t, 3H, H19, *J* = 7.2).	CO*, 185.4 (CS_2), 145.8 (C2), 126.6, 123.8 and 122.6 (C3-C5), 31.9 (C6), 21.8, 29.9, 29.7, 29.6, 29.5, 29.4, 29.2 and 22.7 (C7-C18), 14.1 (C19)	2101 (m), 2007 (s), 1995 (s), 1961 (s).
14b	7.71 (d, 1H, H3, *J* = 4.1), 7.36 (d, 1H, H4, J = 4.4), 7.19 (d, 1H, H3', *J* = 4.1), 7.06 (t, 1H, H4', *J* = 4.4),), 2.84 (t, 2H, CH_2, H6, *J* = 7.5), 1.73 (m, 2H, H7), 1.32 (m, 22H, H8-H18), 0.92 (t, 3H, H19, *J* = 7.2).	CO*, 185.6 (CS_2, C5), 156.5 (C2), 153.4 (C5), 146.9 (C2'), 129.0 (C5'), 128.5, 127.6, 126.4, 124.7 (C3. C4, C3', C4'), 41.4 (C6), 31.9, 31.8, 29.9, 29.7, 29.6, 29.6, 29.4, 29.2, 22.7 (C7-C18), 14.1 (C19).	2101 (m), 2007 (s), 1996 (s), 1960 (s).

* not observed

The infrared spectra of the complexes have the typical pattern of four carbonyl ligands displaying C_{2v} symmetry and are representative of *cis*-$[M(CO)_4L_2]$ complexes. The spectrum of **13** (Figure 4.8) showed peaks at 2104 ($A_1^{(1)}$), 2010 ($A_1^{(2)}$), 1996 (B_1) and 1959 B_2) cm^{-1} of similar intensities.

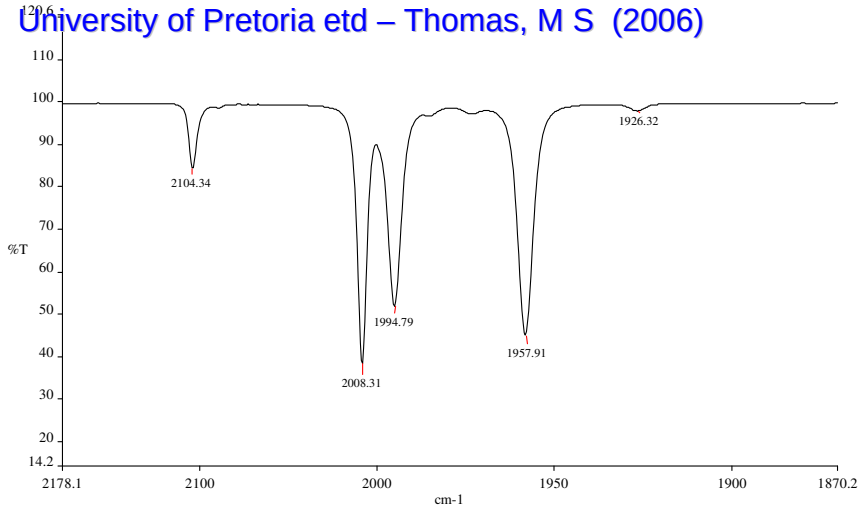

Figure 4.8 IR spectrum of $[Re(CO)_4(S_2CTCH_3)]$ (**13**)

4.2.3 Molecular Structure

The molecular structure of **12** was determined by single crystal X-ray crystallography and confirmed to have a cis-$[Re(S_2CTR)(CO)_4]$ arrangement of ligands. Single crystals suitable for crystal structural determination were obtained by slow diffusion of hexane into a dichloromethane solution of **12** at room temperature. The structure of **12** supported the spectroscopic data. The molecular structure of **12** is shown in Figure 4.9.

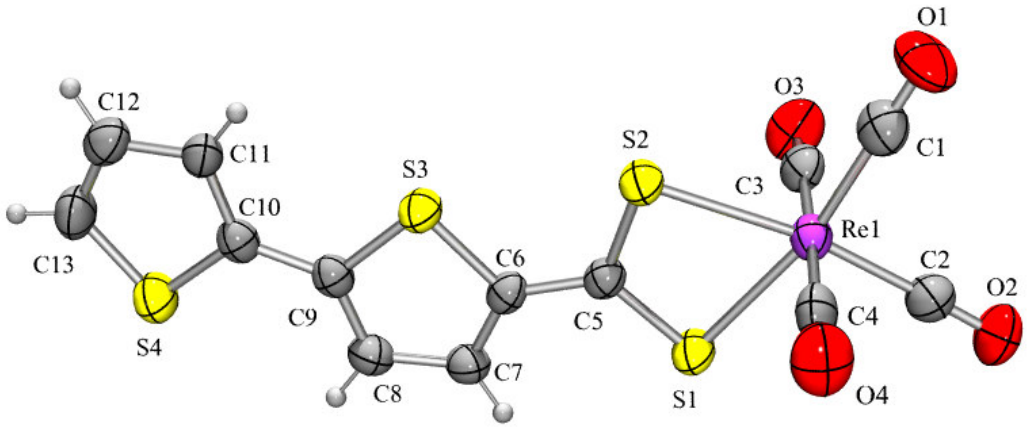

Figure 4.9 An ORTEP[27]+ POV- Ray[28] plot of the geometry of **12**

The Re-S distances are almost the same. Re(1)-S(1) is 2.512 Å whereas Re(1)-S(2) is 2.497 Å. This is also true for the C-S bond lengths of the carbon disulfide moiety, indicating delocalization of electron density over the chelate ring. The Re-C bond distances of the carbonyl ligands *trans* to the sulfur donor atoms are the same and significantly shorter than the other Re-C (carbonyl) distances. This is indicative of the poorer π-acceptor properties of the sulfur ligands compared to the carbonyl ligands. Selected bond lengths and angles are given in Table 4.2 and 4.3 respectively. The sulfur atoms in the thiophene rings of bithiophene are on opposite sides with respect to one another in the dithiocarboxylate ligand. Compared to bond distances of free thiophene (see chapter 3) the C-S distances are longer and represent less π-delocalization in the thiophene ring. Delocalization towards the coordinating CS_2 moiety on the outside of the ring is also important. Interestingly, the formal single bond in the thiophene rings in **12** is shorter than normal C-C single bonds or the corresponding distance in the free thiophene.

Table 4.2 Selected bond lengths for **12**

Atoms	Bond length (Å)	Atoms	Bond length (Å)
Re(1)-C(1)	1.942(6)	Re(1)-C(2)	1.943(6)
Re(1)-C(3)	1.993(6)	Re(1)-C(4)	1.998(6)
Re(1)-S(1)	2.512(1)	Re(1)-S(2)	2.497(1)
S(1)-C(5)	1.701(4)	S(2)-C(5)	1.692(5)
C(5)-C(6)	1.435(6)	C(9)-C(10)	1.437(7)
C(6)-S(3)	1.733(4)	C(10)-S(4)	1.721(5)
C(9)-S(3)	1.729(5)	C(13)-S(4)	1.693(6)

C(6)-C(7)	1.368(6)	C(10)-C(11)	1.398(7)
C(7)-C(8)	1.409(7)	C(11)-C(12)	1.429(8)
C(8)-C(9)	1.374(6)	C(12)-C(13)	1.348(8)

Table 4.3 Selected bond angles for **12**

Atoms	Bond angle (^{o})	Atoms	Bond angle (^{o})
C(1)-Re(1)-C(2)	91.5(2)	C(1)-Re(1)-C(3)	89.6(2)
C(1)-Re(1)-C(4)	91.9(2)	C(2)-Re(1)-C(3)	91.2(2)
C(2)-Re(1)-C(4)	89.9(2)	C(3)-Re(1)-C(4)	178.1(2)
O(1)-C(1)-Re(1)	178.5(6)	O(2)-C(2)-Re(1)	178.4(6)
O(3)-C(3)-Re(1)	178.2(5)	O(4)-C(4)-Re(1)	177.4(6)

4.2.2 Thermal properties

Thermal properties of the complexes were studied by using thermo-gravimetric analysis, TGA. All the complexes **12**, **13**, **14a** and **14b** decomposed before melting. The TGA spectrum of **12** (Figure 4.10) showed some decomposition between 155-160^{o}C, that is ascribed to the elimination of carbonyl ligands. As a result no mesophases were present in any of the compounds.

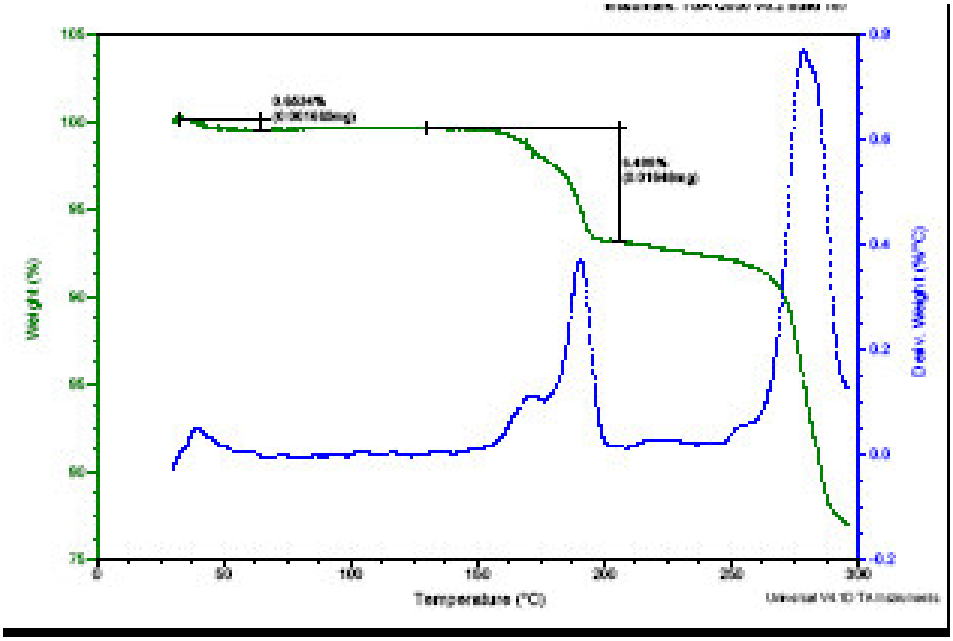

Figure 4.10 TGA spectrum of **12**

4.3 Experimental Section

General

Hexane and tetrahydrofuran were distilled over sodium and benzophenone prior to use, and dichloromethane was stored over calcium chloride. All chemicals were used as received unless otherwise specified. All reactions were performed in an inert atmosphere of either nitrogen or argon by using Schlenk techniques and vacuum-line. Column chromatography was carried out using silica gel.

Infrared spectra were recorded on a Perkin Elmer Spectrum 1000 FT-IR spectrometer. All NMR spectra were recorded in deuterated chloroform using the chloroform peak as standard on a Bruker ARX-300 spectrometer.

Thermal properties were studied on thermogravimetric analysis instrument TGA.

A crystal of size 0.34 x 0.10 x 0.06 mm^3 of **12** was mounted in a sealed capillary tube for data collection. All geometric and intensity data were collected on a Siemens SMART diffractometer with a CCD detector.

4.3.1 Synthesis

All the complexes were synthesized via a three-step reaction in a similar manner. A typical procedure for complex **13** is described.

Preparation of bromopentacarbonylrhenium, [$ReBr(CO)_5$]

Hexane (30.0 ml freshly distilled) was transferred to a 50.0 ml Schlenk flask equipped with a Teflon-coated stir bar. Dirheniumdeccacarbonyl, [$Re_2(CO)_{10}$] (6.50 g, 10.0 mmol) was added under a stream of N_2, and bromine (1.70 g, 11.0 mmol) was added to the solution by means of a syringe and immediately a precipitate was formed in the flask. Stirring was continued for 30 min, and almost all of the orange colour disappeared. Volatiles were removed under continuous vacuum at room temperature and a white powder was obtained. The white powder was transferred to a sublimator and sublimed at 85-90^oC. Yield = 3.65 g (90.0%).

Preparation of pentacarbonyl(trifluoromethanesulfonato)-rhenium(I), [*$Re(CO)_5(O_3SCF_3)$*]

Freshly sublimed bromopentacarbonylrhenium (3.25 g, 8.0 mmol) was placed in a 50.0 ml Schlenk flask along with a Teflon-coated stirring bar under an atmosphere of nitrogen. Dichloromethane (40.0 ml freshly distilled from P_4O_{10} under nitrogen) was added through a septum by syringe, and the solution was stirred

until all the $Re(CO)_5Br$ was dissolved. From a Schlenk addition tube 2.31 g (9.0 mmol) of $Ag(O_3SCF_3)$ was added under a purge of N_2, and stirring was continued for 2 hours at room temperature. The $Ag(O_3SCF_3)$ was weighed under subdued light and the reaction flask was wrapped with foil to exclude room light just before the addition of silver triflate. The fluffy AgBr precipitate was formed and removed by filtration through a fine Schlenk frit to yield a clear solution. The volume of the solution was reduced under vacuum, allowed to warm to room temperature and freshly distilled hexane was added and the solvents were removed slowly in vacuum to precipitate $[Re(CO)_5(O_3SCF_3)]$ as a white powder. Yield = 3.17 g (78%).

Preparation of tetracarbonyl-5-methyl-2-thiophenedithiocarboxylatorhenium(I) $[(CO)_4Re(S_2CC_4H_2SCH_3)]$

In the third step the 5-methyl-2-thiophenedithiocarboxylate ion was prepared in situ as described by Brandsma[25] in the previous chapter. A hexane solution which contained 0.32 g (2.0 mmol) of the 5-methyl-2-thiophenedithiocarboxylate ion was cooled to -30°C and 0.95 g (2.0 mmol) of $[Re(CO)_5(O_3SCF_3)]$ was added. The cold bath was removed and the mixture was left stirring for 2 hours. The colour of the mixture turned red. Solvents were removed and the purification was done on a silica gel column and the product was extracted with hexane/dichloromethane 4:1 as the eluent. Yield = 0.52 g (55%). The complexes **12, 14a** and **14b** were prepared similarly. See Table 4.4.

Table 4.4 Experimental results of **12-14** complexes

Complex	Colour	Mass (g)	Yield (%)
12	Red	0.67	62
13	Orange	0.52	55
14a	Orange	0.56	43
14b	Red	0.68	46

4.4 Conclusion

The complexes are not suitable as liquid crystals since the complexes decomposed before melting. From the TGA studies, it is clear that the carbonyl ligands are eliminated at lower temperatures.

REFERENCES

1. J. Bhatt, B. M. Fung, K. M. Nicholas and C. –D. Poon, *J. Chem. Soc., Chem. Commun.,* **1988**, 1439.
2. L. Ziminski and J. Malthête, *J. Chem. Soc., Chem. Commun*., **1990**, 1495.
3. R. Deschenaux and J. Santiago, *J. Mater. Chem*., **1993**, 3. 219.
4. H. Stegemeyer, R. Meister, U. Hoffmann, A. Sprick and A. Becker, *J. Mater. Chem*., **1995**, 5, 2183.
5. K. Yang and R. P. Lemieux, *Mol. Cryst., Liq. Cryst*., **1995**, 260, 247.
6. D. Vizitiu, B. J. Halden and R. P. Lemieux, *Chem. Commun*., **1997**, 1123.
7. D. Vizitiu, C. Lazar, B. J. Halden and R. P. Lemieux, *J. Am. Chem. Soc*., **1999**, 121, 8229.
8. J. P. Rourke, D. W. Bruce and T. B. Marder, *J. Chem. Soc., Dalton Trans*., **1995**, 317.
9. D. W. Bruce and X. -H. Liu, *J. Chem. Soc., Chem. Commun*., **1994**, 729.
10. X. -H. Liu, M. N. Abser and D. W. Bruce, *J. Organomet. Chem*., **1998**, 551, 271.
11. D. W. Bruce, E. Lalinde, P. Styring, D. A. Dunmur and P. M. Maitlis, *J. Chem. Soc., Chem. Commun*., **1986**, 581.
12. J. Barberá, P. Espinet, E. Lalinde, M. Marcos and J. L. Serrano, *Liq. Cryst*., **1987**, 2, 833.
13. D. W. Bruce, *J. Chem. Soc., Dalton Trans*., **1993**, 2983.
14. K. E. Rowe and D. W. Bruce, *Mol. Cryst., Liq. Cryst*., **1999**, 326, 15.
15. D. W. Bruce and X. -H. Liu, *Liq. Cryst*., **1995**, 18, 165.
16. X. -H. Liu, I. Manners and D. W. Bruce, *J. Mater. Chem*., **1998**, 1555.

17. K. E. Rowe and D. W. Bruce, *J. Chem. Soc., Dalton. Trans*., **1996**. 3913.

18. M. S. Wrighton and D. L. Morse, *J. Am. Chem. Soc*., **1974**, 96, 998.

19. A. J. Lees, *Chem. Rev*., **1987**, 87, 711.

20. V. W. W. Yam, V. C. Y. Lau and K. K. Cheung, *Organometallics*, **1995**, 14, 2749.

21. S. Morrone, G. Harrison and D. W. Bruce, *Adv. Mater*., **1995**, 7, 665.

22. T. Cardinaels, K. Driesen, T. N. Parac-Vogt, B. Heinrich, C. Bourgogne, D. Guillon, B. Donnio, and K. Binnemans, *Chem. Mater*., **2005**, 17, 6589.

23. M. H. Quick and R. P. Angelici, *Inorg. Synth*., **1979**, 19, 160.

24. S. P. Schmidt, W. C. Trogler and F. Basolo. *Inorg. Synth*., **1985**, 23, 41.

25. L. Brandsma and H. D. Verkruijsse, *Preparative Polar Organometallic Chemistry, Voulume 1*, Springer Verlag, Heidelberg, **1987**, 124.

26. M. Hesse, H.Meier, B. Zeeh, *Spektroskopische Methoden in der Organischen Chemie*, Georg Thieme Verlag, Stuttgart, **1984**, 201.

27. L. J. Farrugia, *J. Appl. Crystallogr*., **1997**, 30, 565.

28. The POV-Ray Team, POV-Ray 2004, URL: http://www.pov-ray.org./download/.

Chapter 5

Carbene complexes of Manganese(I) with thiophene-containing ligands

5.1 Introduction

Complexes containing metal-carbon double bonds are generally referred to as metal-carbene or metal-alkylidene complexes[1-3]. Applications of carbene complexes in organic syntheses have been widely employed and recognized for their usefulness[4-10], but very few studies directed towards material properties of carbene complexes have been recorded. The reason for this is that carbene complexes were traditionally seen as very unstable compounds and researchers rather looked at them as reaction intermediates. Today we know that many carbene complexes in transition metal chemistry are as stable as their counterparts displaying phosphine or other classical inorganic ligands. They have an additional advantage as they possess the capability of bringing in electronic contact the transition metal with a conjugated fragment that forms part of a substituent on the carbene carbon atom. Binuclear organometallic complexes in which the metal centres are connected by a conjugated bridge have attracted a lot of interest as potential molecular wires[11,12]. The only drawback to this approach is that connecting chains of carbon tend to be unstable at the sites of bond unsaturation. Thiophene and polythiophenes or their derivatives, on the other hand, have been identified as molecules with potential electro-optical properties and form part of some of the most stable molecular switching devices discovered to date[13]. For many years we have pursued the chemistry of mono- or binuclear transition metal carbene complexes where one of the substituents would contain a thiophene or

thiophene derivative[14-17]. One of the obvious possible applications for carbene complexes with thiophene derivatives is constructing materials with non-linear optical and liquid crystalline properties[18].

Among the stable and isolable organometallic compounds containing transition metals, Fischer-type carbene complexes have recently become very popular[19]. In Fischer carbene complexes at least one of the organic substituents will have a heteroatom with lone pair electrons. The carbene carbon atom is strongly electrophilic and will use the transition metal and/or the heteroatom to stabilize this center.

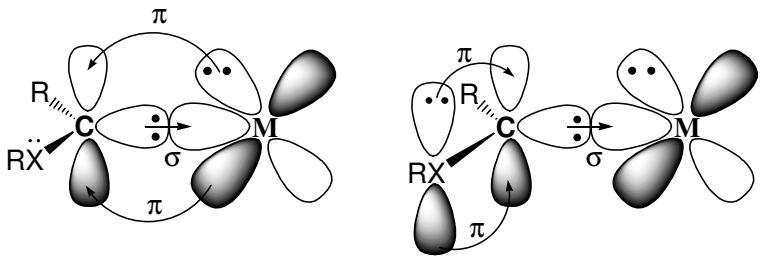

Figure 5.1 Electron distribution and bonding in Fischer carbene complexes

Fischer carbene ligands have empty p-orbitals perpendicular to the plane of the sp^2-orbitals and as a result, can act as a connector of π-electron conjugation from the metal to a conjugated chain or unit via the carbene carbon. Charge transfer is possible in a large segment of the complex and can be fine-tuned by carefully selecting the transition metal and the conjugated substituent on the carbene carbon. Molecules with large π systems and, in particular, organometallic complexes have been extensively used in attempts to obtain materials with non-linear optical (NLO) properties. It has been shown that organometallic complexes that contain thiophene moieties contribute to the enhancement of such properties[20-27]. Attention in this field has more recently been directed to "push-pull" molecules because transition metals introduce new

variables such as their different oxidation states, differences in the nature and number of the ligands that allow the modulation of their electron-withdrawing or releasing properties and optimization of their interaction with the π-spacer in order to create the best non-linear response[28].

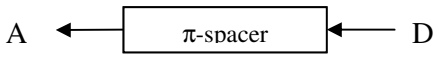

Figure 5.2 Push-Pull structures

Non centro-symmetric molecules are good candidates for second order non-linear activity and, in particular, large first β hyperpolarisabilty can be observed in conjugated poly-unsaturated organic molecules in which a π-system connects electron-donating **D** to accepting **A** groups. Fischer-type carbene complexes have recently become serious contenders as compounds exhibiting NLO-properties (Figure 5.2). Licandro and coworkers[29] reported and exploited the push-pull nature of pentacarbonyl(metal) carbene complexes. The $M(CO)_5$(carbene-carbon) moiety behaved as a strong electron-withdrawing group that is similar to a Lewis acid leading to polarization in the carbene substituent.

The aim was to synthesize carbene complexes of manganese(I) with thiophene or bithiophene containing-ligands and to test their liquid crystalline properties. We chose [Mn(η^5-C_5H_5)$(CO)_2$(carbene)] as our model compound as it is known to give very stable carbene complexes[30]. Important is the limiting of the number of carbonyl ligands as they could affect the melting behaviour of the compound adversely. We selected to use methylcyclopentadienyl instead of cyclopentadienyl as ligand that will lower and affect the temperature range of the melting process. The geometry around

the metal centre is pseudo tetrahedral, but diamagnetic which could also be of interest. Incorporation of a polarizable component is achieved by using 2-alkyl substituted thiophene carbene substituents. In 1994 Bruce[31] reported the liquid crystalline complexes of octahedral manganese(I). The complexes described were the first examples of calamitic (rod-like) liquid crystalline metal complexes containing manganese with octahedral coordination.

5.2 Results and discussion

5.2.1 Synthesis and characterization

Carbene complexes of manganese(I), of the type [MnMeCp(CO)$_2${C(OEt)TR}] (where T = 2,5-disubstituted thiophene, C_4H_2S (**a**) or bithiophene, $C_8H_4S_2$ (**b**) and R = H (**15**), C_6H_{13} (**16**),$C_{12}H_{25}$ (**17**), $C_{16}H_{33}$(**18**)) have been prepared.

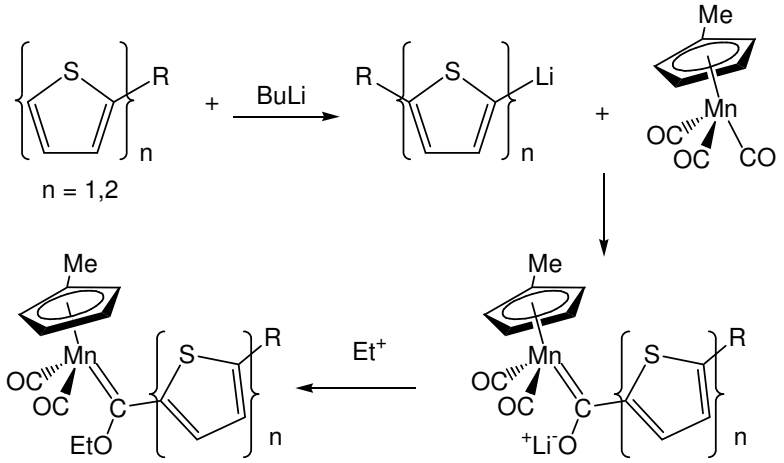

n = 1: R = H **15a**; C_6H_{13} **16a**; $C_{12}H_{25}$ **17a**; $C_{16}H_{33}$ **18a**.
= 2: R = H **15b**; C_6H_{13} **16b**; $C_{12}H_{25}$ **17b**; $C_{16}H_{33}$ **18b**.

Scheme 5.1

Alkyl thiophene or bithiophene derivatives were dissolved in THF and reacted in the cold under argon-atmosphere with BuLi dissolved in hexane. After the reaction

mixture was cooled to -40°C, [$MnMeCp(CO)_3$] was added. The mixture was first stirred in the cold and then for a further period at room temperature. The solvent was removed from the dark-red solution and the residue was re-dissolved in dichloromethane and alkylated in the cold with a solution of Et_3OBF_4. The reaction mixture was filtered through a plug of silica gel and thereafter chromatographed on silica gel by using hexane/dichloromethane (4:1) solution. The first yellow band was unreacted alkyl thiophene followed by a red-brown band, the desired product. The product was recovered from the solvent in high yield (about 70%). The complexes **15a-17a** were oils, whereas complex **18a** was a solid with melting point 31-32°C. The complexes **15b-17b** were solids, but **18b** was an oil. Once purified, NMR and IR spectroscopy and mass spectrometry were used to characterize the complexes **15a-18a** and **15b-18b**.

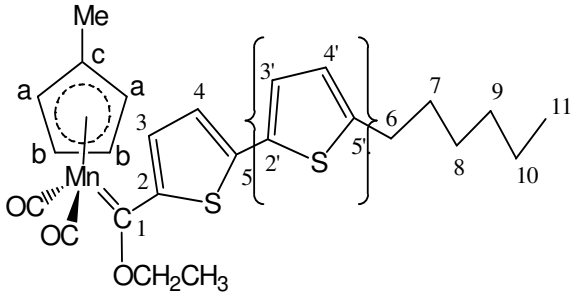

Figure 5.3 Atomic numbering of **16a/b**

In this chapter Figure 5.3 shows how the different atoms are numbered in the text for the different compounds. The cyclopentadienyl carbons are indicated by a, b and c, the second thiophene ring in the bithiophene complexes takes the same numbering sequence than the thiophene complexes but with primed numbers and the alkyl chains are numbered starting with carbon 6 and following the numerical order.

The ^1H NMR spectra of the thiophene (T) complexes **15a**-**18a** displayed resonances of much poorer resolution compared to the bithiophene (TT) analogues **15b**-**18b** and

it was not possible to get good coupling data for the thiophene complexes. The complex [MnMeCp(CO)$_2${C(OEt)TC$_6$H$_{13}$}] (T = thiophene, C$_4$H$_2$S) (**16a**) showed two broad singlets at 7.70 and 6.73 ppm for the two protons H3 and H4 of the thiophene ring. By contrast the spectrum of **17b** shown in Figure 5.4 displayed four well-resolved doublets (7.81, 7.12, 6.94 and 6.69 ppm) in the arene region. These patterns of chemical shifts for **16a**-**18a** and **16b**-**18b** are expected for 2,5-disubstituted thiophene and 2,5'-disubstituted bithiophene complexes, respectively. The carbene carbon in the 2-position is a strong electron-withdrawing substituent and H3/H3' will be shifted downfield compared to an alkyl chain, which is electron-donating on the other side of the thiophene ring, and H4/H4' will appear upfield. Compared to uncoordinated thiophene where H3 and H4 are found at chemical shift values of 6.96 ppm (chapter 2), H3 in the carbene complexes is downfield by *ca* 0.7 ppm and H4 upfield by *ca* 0.2 ppm.

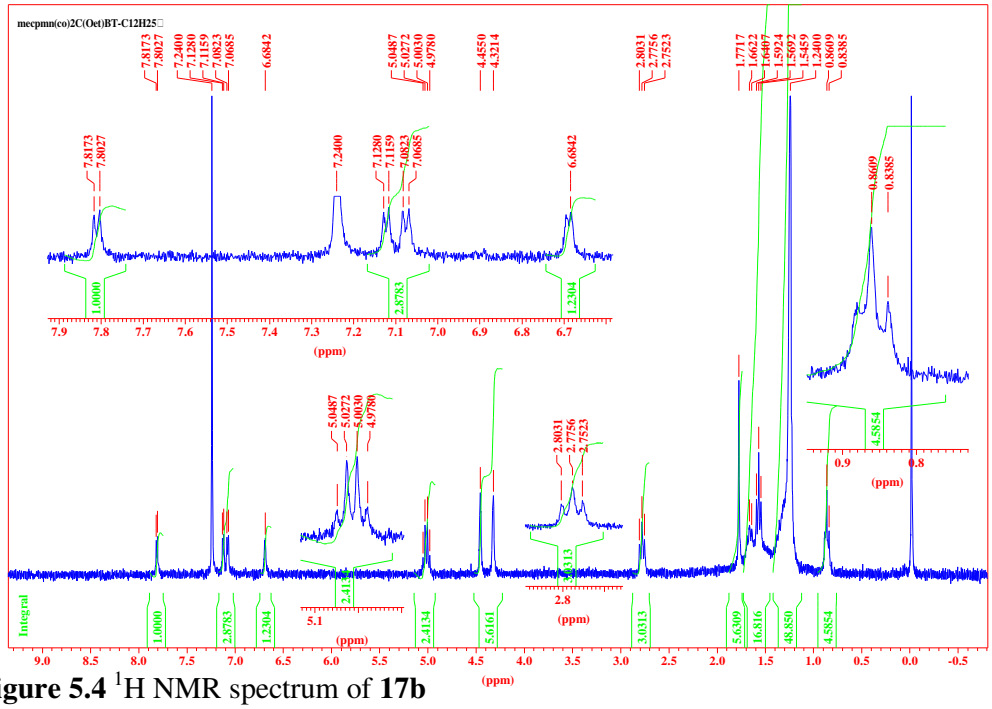

Figure 5.4 ^{1}H NMR spectrum of **17b**

The NMR data of the complexes are summarized in Tables 5.1 and 5.2. The chemical shifts of the methylene resonances of the ethoxy substituents of the carbene ligands afford characteristic quartets at 5.0 ppm, which compare well with values reported in the literature[14]. The resonances of the cyclopentadienyl protons a and b appear as two singlets around 4.4 ppm in the spectra and the alkyl chains start downfield for H6 as a triplet at *ca* 2.8 ppm (H6), then shows a broadened quintet at *ca* 1.65 ppm (H7, not always resolved) slightly upfield from the Cp methyl substituent at *ca* 1.75 ppm. The methyl group of the ethoxy substituent is next around 1.6 ppm followed by a strong multiplet at 1.5-1.2 ppm representing the rest of the alkyl chain which ends with a triplet for the last carbon of the chain at *ca* 0.85 ppm.

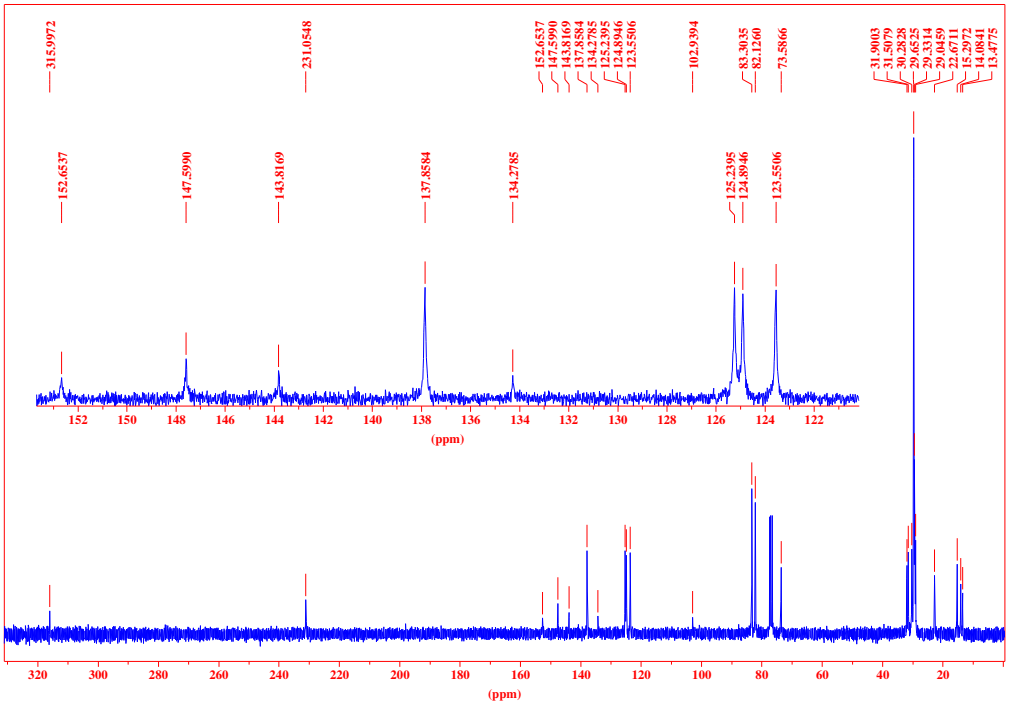

Figure 5.5 ^{13}C NMR spectrum of **17b** with an expanded view of the bithiophene region

The ^{13}C NMR spectrum of **17b** (Figure 5.6) clearly indicated the carbene carbon, the carbonyl ligands, the carbons of the bithiophene ring and also accounts for all the other carbon atoms in the structure. The spectrum depicted the carbene carbon C1 at 316.0 ppm and Mn-$(CO)_2$ at 231.1 ppm, respectively. In the bithiophene region all eight signals were resolved and from peak intensities it is possible to divide the chemical shifts in four quartenary and four CH resonances (see expansion in Figure 5.6). Moving further upfield, one could readily assign the c and a chemical shifts (figure 5.3) of the cyclopentadienyl ring and the carbene methylene carbon of the ethoxy substituent moved slightly upfield from the deuterated solvent resonances.

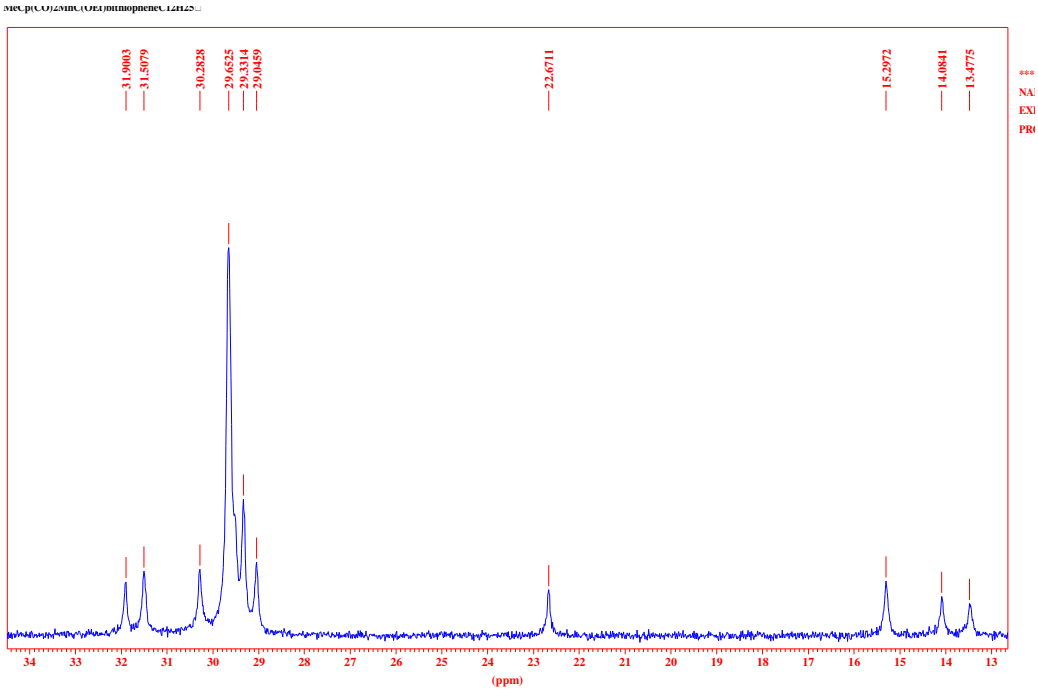

Figure 5.6 ^{13}C NMR spectrum of **17b** in the alkyl region

The alkyl chain is represented by 8 signals for the 12 carbon atoms with some overlapping at 29.0 ppm. The sequence for the methyl chemical shifts (ppm) is: EtO of carbene > Alkyl chain end > Cp substituent, based on the results of the ^{13}C NMR

spectra of [Mn(MeCp)(CO)$_3$], ethoxy carbene complexes[32] and the alkylthiophene substrates.

Table 5.1 Spectral data for the thiophene complexes, **15a-18a**

Complex	^{1}H NMR (δ/ppm and *J*/Hz in $CDCl_3$)	^{13}C NMR (δ/ppm in $CDCl_3$)	IR[a] (ν/cm^{-1} in hexane) M(CO)$_2$
15a	8.03 (s, 1H, H3), 7.26 (s, 2H, H4 and H5), 5.22 (s, 2H, OCH_2), 4.63 (s, 2H, Hb (Cp)), 4.56 (s, 2H, Ha (Cp)), 1.98 (t, 3H, Cp-CH_3 *J* = 7.0), 1.78 (t, 3H, CH_3 (OEt)), *J* = 7.2).	319.2 (C1, carbene), 231 (CO-Mn), 156.0 (C2), 135.9 (C5), 132.5 (C3), 128.0 (C4), 103.3 (Cc (Cp)), 84.0, 82.8 (Cb and Ca (Cp)), 75.2, 15.8 (O$\underline{C}H_2\underline{C}H_3$) 13.5 (Cp-$CH_3$).	1947 (vs), 1889 (vs)
16a	7.78 (s, 1H, H3), 6.81 (s, 1H, H4), 5.02 (s, 2H, OCH_2), 4.48(s, 2H, Hb of Cp) 4.35 (s, 2H, Ha of Cp) 2.78 (t, 2H, H6, *J* = 7.0), 1.60 (s, 6H, Cp-CH_3 and CH_3 (OEt)), 1.33 (m, 10H, H7-H10), 0.90 (t, 3H, H11, *J* = 7.2).	317.4 (C1, carbene), 231.2 (CO-Mn), 153.4 (C2), 137.3 (C5), 125.6 (C3), 125.0 (C4), 102.6 (Cc (Cp)), 83.2, 82.8 (Cb and Ca (Cp)), 73.5, 15.3 (O$\underline{C}H_2\underline{C}H_3$), 13.5 (Cp-$CH_3$), 31.5, 31.2, 30.6, 28.8, 22.5, 14.2 (C6-C11).	1943 (vs), 1886 (vs)
17a	7.77 (s, 1H, H3), 6.81 (s, 1H, H4), 5.03 (s, 2H, OCH_2), 4.48 (s, 2H, Hb (Cp)), 4.36 (s, 2H, Ha (Cp)), 2.80 (t, 2H, H6, *J* = 7.0), 2.20 (s, 3H, Cp-CH_3), 1.62 (t, 3H, CH_3 (OEt) *J* = 7.0), 1.32 (m, 20H, H7-H16), 0.97 (t, 3H, H17, *J* = 7.2).	317.4 (C1, carbene), 231.4 (CO-Mn), 153.9 (C2), 137.73 (C5), 126.1 (C3), 125.7 (C4), 102.8 (Cc (Cp)), 83.6, 82.4 (Cb and Ca (Cp)), 73.9, 15.7 (O$\underline{C}H_2\underline{C}H_3$), 14.1 (Cp-$CH_3$), 32.3, 31.7, 30.9, 30.0 (vs), 23.1, 14.4 (C6-C17).	1943 (vs), 1886 (vs)
18a	7.79 (s, 1H, H3), 6.80 (s, 1H, H4), 5.02 (s, 2H, OCH_2), 4.45 (s, 2H, Hb (Cp)), 4.33 (s, 2H, Ha (Cp)), 2.77 (s, 2H, H6), 1.79 (s, 3H, Cp-CH_3), 1.67 (s, 2H, H7), 1.57 (t, 3H, CH_3 (OEt),1.27 (m, 26H, H8-H20), 0.89 (t, 3H, H21,	317.6 (C1, carbene), 231.2 (CO-Mn), 153.5 (C2), 137.3 (C5), 126.2 (C4), 125.6 (C3), 102.7 (Cc (Cp)), 83.2, 82.0 (Cb and Ca (Cp)), 73.5, 15.5 (O$\underline{C}H_2\underline{C}H_3$), 13.5 (Cp-$CH_3$), 31.9, 31.2, 30.5, 29.6	1943 (vs), 1886 (vs)

	J = 7.2)	(vs), 22.6, 14.4 (C6-C21).	

[a] carbonyl region

Table 5.2 Spectral data for the bithiophene complexes, **15b-18b**

Complex	^{1}H NMR (δ/ppm and J/Hz in $CDCl_3$)	^{13}C NMR (δ/ppm in $CDCl_3$)	IR[a] (ν/cm^{-1} in hexane)
15b	7.81 (d, 1H, H3, J= 4.3), 7.29 (d, 1H, H4, J = 3.6), 7.14 (s, 2H, H3' and H4'), 7.02 (d, 1H, H5', J = 3.6), 5.02 (s, 2H, OCH_2), 4.46 (s, 2H, Hb (Cp)), 4.33 (s, 2H, Ha (Cp)), 1.78 (s, 3H, Cp-CH_3), 1.57 (s, 3H, CH_3 (OEt)).	319.4 (C1, carbene), 230.7 (CO-Mn), 157.3 (C2), 137.5 (C3), 145.8 (C5), 143.3 (C2'), 128.2 (C5'), 126.1 (C3'), 125.0 (C4), 124.3 (C4'), 97.5 (Cc (Cp)), 83.4 (Cb (Cp)), 82.3 (Ca (Cp), 73.7 (O$\underline{C}H_2$), 15.3 ($\underline{C}H_3$ (OEt)), 13.5 (Cp-$\underline{C}H_3$)	1945 (vs), 1888 (vs)
16b	7.81 (d, 1H, H3, J = 4.2), 7.12 (d, 1H, H4, J = 3.6), 6.94 (d, 1H, H3', J = 4.2), 6.69 (d, 1H, H4', J = 3.6), 5.02, d, 2H, OCH_2, J = 7.2), 4.46 (s, 2H, Hb (Cp)), 4.33 (s, 2H, Ha (Cp)), 2.78 (t, 2H,H6, J = 7.0), 2.29 (t, 3H, Cp-CH_3, J = 7.0), 1.67 (t, 3H, CH_3 (OEt), J = 7.0), 1.25 (m, 8H, H7-H10), 0.87 (t, 3H, H11, J = 6.7).	317.1 (C1, carbene), 231.0 (CO-Mn), 143.8 (C2), 137.9 (C5), 124.9 (C4), 129.9 (C2'), 128.9 (C5), 126.0 (C3'), 125.3 (C5'), 123.6 (C4'), 103.0 (Cc (Cp)), 83.7 (Cb (Cp)), 82.5 (Ca (Cp)), 73.9 (O$\underline{C}H_2$), 15.6 ($\underline{C}H_3$ (OEt), 13.4 (Cp-$\underline{C}H_3$), 31.9, 31.5, 30.3, 28.7, 22.6, 14.5 (C6-C11).	1944 (vs), 1887 (vs).
17b	7.81 (d, 1H, H3, J = 4.4), 7.11 (d, 1H, H4, J = 3.6), 7.07 (d, 1H, H3', J = 4.2), 6.68 (d, 1H, H4', J = 3.6), 5.02 (s, 2H, OCH_2, J=7.0), 4.45 (s, 2H, Hb (Cp)), 4.32 (s, 2H, Ha (Cp)), 2.77 (t, 2H, H6, J = 7.0), 1.77 (s, 3H, Cp-CH_3), 1.56 (t, 3H, CH_3 (OEt), J = 7.0), 1.24 (m, 20H, H7-H16), 0.85 (t, 3H, H17, J = 6.7).	316.0 (C1, carbene), 231.1 (CO-Mn), 152.7 (C2), 147.6 (C5), 143.8 (C2'), 137.9 (C3), 134.3 (C5'), 125.2 (C4), 124.9 (C3'), 123.9 (C4'), 102.9 (Cc (Cp)), 83.3, (Cb (Cp)), 82.1 (Ca (Cp)), 73.5 (O$\underline{C}H_2$), 15.3 ($\underline{C}H_3$ (OEt)), 13.5 (Cp-$\underline{C}H_3$), 31.9, 31.5, 30.3, 29.7, 29.3, 29.0, 22.7, 14.1 (C6-C17).	1944 (vs), 1887 (vs).
18b	7.81 (d, 1H, H3, J = 3.9), 7.12 (d,	317.7 (C1, carbene), 231.7	1943 (vs), 1887

	1H, H4, *J* = 3.6), 7.07 (d, 1H, H3', J = 4.0), 6.69 (d, 1H, H4', *J* = 3.6), 5.02 (s, 2H, OCH_2, *J* = 7.7), 4.46 (s, 2H, Hb (Cp)), 4.32 (s, 2H, Ha (Cp)), 2.78 (t, 2H, H6, *J* = 7.0), 1.77 (s, 3H, Cp-CH_3), 1.65 (t, 3H, CH_3 (OEt), *J* = 7.7) 1.28 (m, 28H, H7- H20), 0.86 (t, 3H, H21, *J* = 6.7).	(CO-Mn), 153.2 (C2), 152.9 (C5), 144.8 (C2'), 137.6 (C3), 135.3 (C5'), 125.1 (C4), 124.7 (C3'), 123.6 (C4'), 102.5 (Cc (Cp)), 83.3 (Cb (Cp)), 82.1 (Ca (Cp)), 76.6 ($O\underline{C}H_2$), 15.4 ($\underline{C}H_3$ (OEt)), 13.7 (Cp-$\underline{C}H_3$), 31.9, 31.6, 31.5, 30.3, 30.1,29.7, 29.6, 29.5,29.4, 28.7, 22.7, 22.6, 14.1 (C6-C21).	(vs).

[a] carbonyl region

The IR spectrum of **16a** showed two very strong bands at 1943 and 1886 cm^{-1} for the terminal CO ligands. This corresponds to the two infrared vibrations, ν_{sym} and ν_{asym} of the $M(CO)_2$ class of carbonyl complexes. The ^{13}C NMR chemical shifts for the carbons of the carbonyl ligands are typical for cyclopentadienylmanganese complexes with two carbonyl ligands[33].

The complexes were also studied by fast atom bombardment (FAB) mass spectrometry. All the spectra of the complexes showed a peak corresponding to the m/z-value of the molecular ion (M^+). The parent peak in FAB-MS of **18a** was m/z = 554 (7.5%). The m/z = 498 (100%) peak corresponding to M^+-2CO is the principal ion peak in the spectra. Fragment ions with m/z-values corresponding to $[M(MeCp)]^+$ and $[M(MeCp)(carbene)]^+$ are present in most spectra whereas $[M(carbene)]^+$ and $[M(CO)_2]^+$ are not represented. The fragmentation of parts of the carbene ligand was also observed. Based on these observations it is possible to assign a general fragmentation route for the complexes.

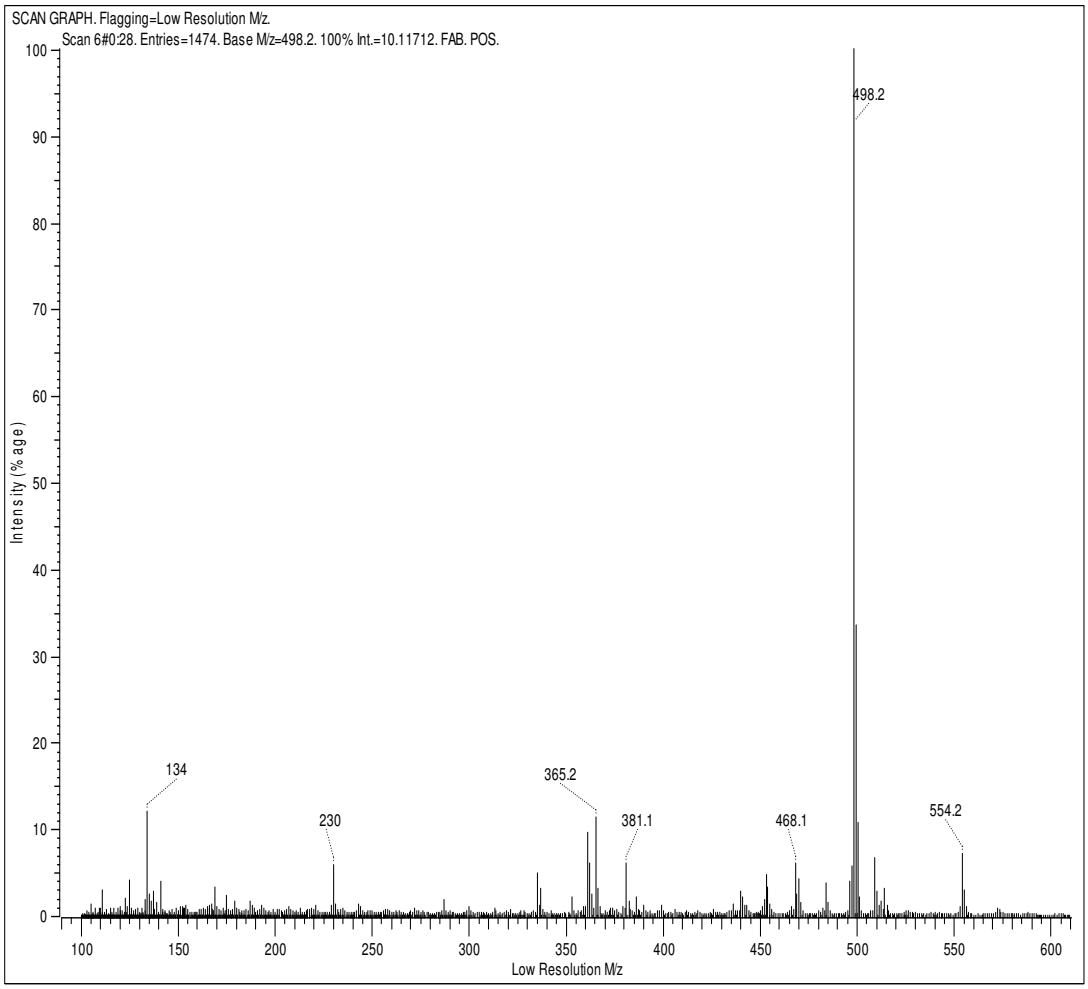

Figure 5.7 Mass spectrum of **18a**

All the other complexes fragmented in a similar manner. The mass spectral data of the complexes **15a-18a** are given in Table 5.3.

Table 5.3 Mass spectral data of **15a-18a** and **15b-18b**

Complex	Molecular formula	Parent peak (M^+)	Principal peak (M^+–2CO)	$[MnMeCp]^+$ fragment (134)
15a	$MnC_{15}H_{15}O_3S$	330 (30%)	274 (100%)	134 (13%)
16a	$MnC_{21}H_{27}O_3S$	414 (18%)	358 (100%)	134 (9%)
17a	$MnC_{27}H_{39}O_3S$	498 (12%)	442 (100%)	134 (8%)
18a	$MnC_{31}H_{47}O_3S$	554 (7.5%)	498 (100%)	134 (13%)

15b	$MnC_{19}H_{17}O_3S_2$	412 (20%)	356 (100%)	134 (12%)
16b	$MnC_{25}H_{29}O_3S_2$	n.o.[a]	440 (4%)	134 (9%)
17b	$MnC_{31}H_{41}O_3S_2$	580 (13%)	524 (100%)	134 (7%)
18b	$MnC_{35}H_{49}O_3S_2$	636 (8%)	580 (100%)	134 (8%)

[a]n.o. not observed.

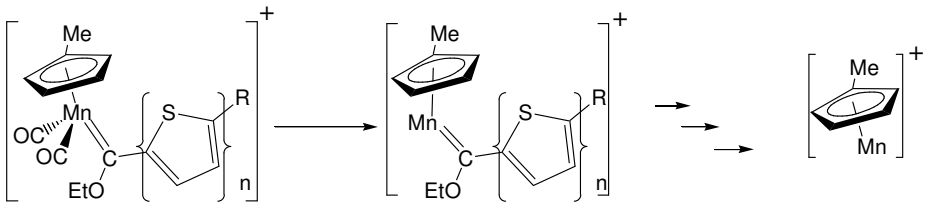

Figure 5.8 important fragmentations of ions in mass spectra

5.2.2 Thermal properties

The TGA measurements showed a decrease (weight loss) at about 50°C, indicating the loss of CO groups from the complex. Therefore the complexes are not stable at moderate temperatures and are not suitable for testing the liquid-crystalline properties.

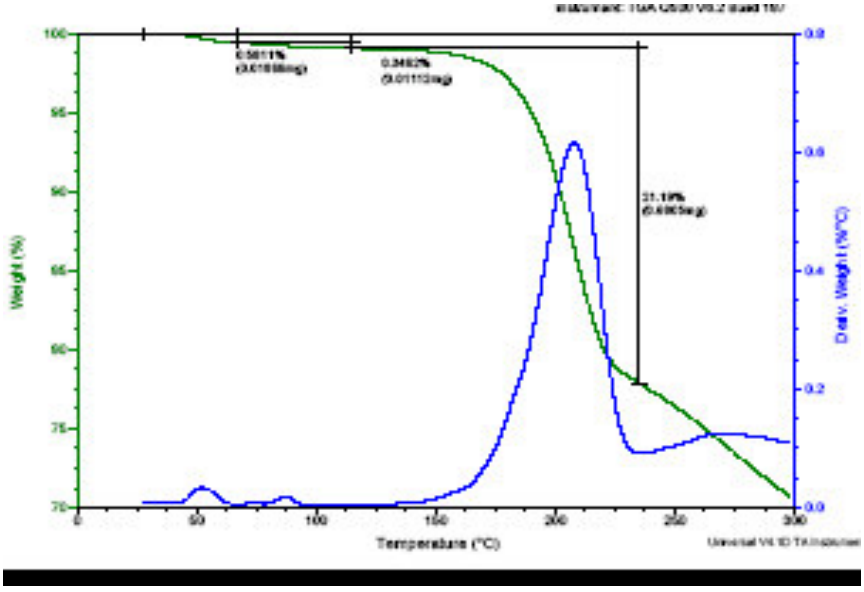

Figure 5.9 TGA spectrum of **18a**

5.3 Experimental Section

Thiophene and bithiophene were lithiated according to the procedure reported by Brandsma[33].

Synthesis

A general procedure for all the reactions in a general format is given.

2.0 mmol of the thiophene, alkylthiophene, bithiophene or alkylbithiophene was dissolved in THF (30.0 ml) and cooled to -15°C under Argon atmosphere. 1.60 M solution of butyl lithium (1.25 ml, 2.0 mmol) in hexane was added and the mixture stirred for 40 minutes. The reaction was cooled to -40°C and [$MnMeCp(CO)_3$] (0.44 g, 2.0 mmol) was added. The mixture was stirred in the cold for 30 minutes and for a further 1 hour at room temperature during which the colour of the solution changed from light orange to dark red. The solvent was removed under reduced pressure. The residue was re-dissolved in dichloromethane (30.0 ml), cooled to -30°C and alkylated with a dichloromethane solution of Et_3OBF_4 (0.38 g, 2.0 mmol). The solution was stirred for 30 minutes in the cold and for a further 1 hour at room temperature. The reaction mixture was filtered through a plug of silica gel and the solvent was removed under reduced pressure. The residue was chromatographed on silica gel by using hexane/dichloromethane (4:1) solution. The first yellow band was unreacted thiophene, alkylthiophene, bithiophene or alkylbithiophene, followed by the brown band, which contained the major product. On evaporation of the solvent, the product was obtained and for the solids, recrystalization from dichloromethane-hexane mixtures, pure complexes could be obtained.

Table 5.4 Experimental results of **15a-18a** and **15b-18b**

Complex	Mass of 2 mmol substrate (g)	State of the product	Melting point (^{o}C)	Mass product(g)	Yield (%)
15a	0.17	Oil	----------	0.51	78
16a	0.34	Oil	----------	0.56	68
17a	0.50	Oil	----------	0.54	55
18a	0.62	Solid	31-32	0.72	65
15b	0.33	Solid	63-65	0.53	65
16b	0.50	Solid	57-59	0.39	40
17b	0.67	Solid	48-49	0.56	48
18b	0.78	Oil	----------	0.58	46

5.4 Conclusion

The complexes showed a weight loss before reaching their melting points. Therefore the complexes are not suitable for testing their liquid crystalline properties.

REFERENCES

1. F.A.Cotton, C.M.Lukehart, *Prog. Inorg. Chem.*, **1972,** 489.

2. K.H.Dötz, H.Fischer, P.Hofmann, F.R.Kreissl, U.Schubert, K.Weiss, *Transition metal carbene complexes*, (Ed.: VCH Verlag Chemie) Weinheim **1983**.

3. R.R. Schrock, *Acc. Chem. Res.,* **1979**, 12, 98.

4. L.S. Hegedus, *Transition Metals in the Synthesis of Complex Organic Molecules* University Science Books, Mill Valley, California **1994**.

5. W.D. Wulff, *Organometallics,* **1998**, 17, 3116.

6. A. De Meijer, H. Schriver, M. Deutch, *Angew. Chem. Int. Ed. Engl.,* **2000**, 39, 3964.

7. J. Barluenga, *Pure Appl. Chem.,* **1999**, 71, 1453.

8. K.H. Dötz, P. Tomuschat, *Chem. Soc. Rev.*, **1999**, 28, 187.

9. R. Aumann, R. Frohlich, J. Prigge, O. Meyer, *Organometallics,* **1999**, 18, 1369.

10. Series of articles by various authors in *Tetrahedron,* **2000**, 56, 4859.

11. U.H.F. Bunz, *Angew. Chem., Int. Ed. Engl.,* **1996**, 35, 968.

12. F. Paul, C. Lapinte, *Coord. Chem. Rev.,* **1998**, 178-180, 431.

13. G. M. Tsivigoulis and J.–M. Lehn, *Angew. Chem. Int. Ed. Engl*., **1995**, 34, 1119.

14. Y.M. Terblans, H.M. Roos, S. Lotz, *J. Organomet. Chem.,* **1998**, 566,133.

15. M. Landman, H. Görls, S. Lotz, *J. Organomet. Chem.,* **2001,** 617-618, 280.

16. M. Landman, H. Görls, S. Lotz, *Eur. J. Inorg. Chem.,* **2001**, 233.

17. C. Crause, H. Görls, S. Lotz, *Dalton Trans.,* **2005**, 1649.

18. H. S. Nalwa, *Appl. Organomet. Chem*., **1991**, 5, 349.

19. E.O. Fischer, *Angew. Chem.,* **1974**, 86, 651.

20. N. J. Long, *Angew. Chem. Int. Ed. Engl*., **1995**, 34, 21.

21. K. J. Drost, V. P. Rao and A. K.-Y. Jen, *J. Chem. Soc., Chem. Commun*., **1994**, 369.

22. V. P. Rao, A. K.-Y. Jen, K. Y. Wong and K. J. Drost, *Tetrahedron Lett*., **1993**, 34, 1747.

23. A. K.-Y. Jen, V. P. Rao, K. Y. Wong and K. J. Drost, *J Chem. Soc., Chem. Commun*., **1993**, 90.

24. S. A. Jenekhe, W. C. Chen, S. Lo and S. R. Flom, *Appl. Phys. Lett*., **1990**, 57, 126.

25. Y. Wei, R. Hariharan and R. Bakthavatchalam, *J. Chem. Soc., Chem. Commun*., **1990**, 1161.

26. J. Lewis, N. J. Long, P. Raithby, G. P. Shields, W. Y. Wong and M. Younus, *J. Chem. Soc., Dalton Trans*., **1997**, 4283.

27. I.-Y. Wu, J. T. Lin, J. Luo, C.-S. Li, C. Tsai, Y. S. Wen, C.-C. Hsu, F.-F. Yeh and S. Liou, *Organometallics*, **1997**, 17, 2188.

28. G. Roth, H. Fischer, T. Meyer-Friedrichsen, J. Heck, S. Houbrechts and A. Persoons, *Organometallics*, **1998**, 17, 1511.

29. E. Licandro, S. Maiorana, A. Papagni, P. Hellier, L. Capella, A. Persoons and S. Houbrechts, *J. Organomet. Chem.*, **1999**, 583, 111.

30. U. Schubert, *Organometallics,* **1982**, 1, 1085.

31. W. Bruce and X. -H. Liu, *J. Chem. Soc., Chem. Commun*., **1994**, 729.

32. B.E. Mann, *Adv. Organomet. Chem.*, **1974**, 12, 135.

33. L. Brandsma and H. D. Verkruijsse, *Preparative Polar Organometallic Chemistry, Volume 1*, Springer Verlag, Heidelberg, **1987**, 124.

Appendix 1

Crystal data and structure refinement for **8**

Table 1. Crystal data and structure refinement for Zntiof.

Identification code	zntiof_abs	
Empirical formula	$C_{44}\ H_{60}\ S_{12}\ Zn_2$	
Formula weight	1104.54	
Temperature	293(2) K	
Wavelength	0.71073 Å	
Crystal system	Monoclinic	
Space group	C 2/c	
Unit cell dimensions	a = 29.1118(19) Å	a= 90º
	b = 6.4571(4) Å	b= 112.5790(10)º.
	c = 28.8391(19) Å	g = 90º.
Volume	5005.6(6) $Å^3$	
Z	4	
Density (calculated)	1.465 Mg/m^3	
Absorption coefficient	1.490 mm^{-1}	
F(000)	2304	
Crystal size	0.34 x 0.14 x 0.05 mm^3	
Theta range for data collection	2.53 to 26.50º.	
Index ranges	-36<=h<=14, -7<=k<=7, -35<=l<=35	
Reflections collected	12744	
Independent reflections	4712 [R(int) = 0.0354]	
Completeness to theta = 25.00º	99.5 %	
Absorption correction	Semi-empirical from equivalents	
Max. and min. transmission	0.928 and 0.734	
Refinement method	Full-matrix least-squares on F^2	
Data / restraints / parameters	4712 / 0 / 382	
Goodness-of-fit on F^2	1.082	
Final R indices [I>2sigma(I)]	R1 = 0.0324, wR2 = 0.0718	
R indices (all data)	R1 = 0.0582, wR2 = 0.0838	
Extinction coefficient	0	
Largest diff. peak and hole	0.272 and -0.401 e.$Å^{-3}$	

Table 2. Atomic coordinates (x 10^4) and equivalent isotropic displacement parameters ($Å^2$x 10^3) for Zntiof. U(eq) is defined as one third of the trace of the orthogonalized U^{ij} tensor.

	x	y	z	U(eq)
Zn(1)	491(1)	2776(1)	329(1)	47(1)
S(1)	1116(1)	3935(1)	1089(1)	43(1)
S(2)	794(1)	-360(1)	836(1)	48(1)
S(3)	1786(1)	2517(1)	2214(1)	43(1)
S(4)	-359(1)	3361(1)	209(1)	41(1)
S(5)	446(1)	2323(1)	-498(1)	44(1)
S(6)	220(1)	6496(1)	1646(1)	43(1)
C(1)	1141(1)	1401(4)	1259(1)	35(1)
C(2)	1451(1)	749(4)	1761(1)	35(1)
C(3)	1528(1)	-1214(5)	1957(1)	42(1)
C(4)	1847(1)	-1275(5)	2459(1)	42(1)
C(5)	2022(1)	612(4)	2660(1)	38(1)
C(6)	2374(1)	1098(5)	3184(1)	45(1)
C(7)	2367(1)	3315(5)	3355(1)	43(1)
C(8)	2712(1)	3652(5)	3899(1)	47(1)
C(9)	2726(1)	5858(5)	4075(1)	51(1)
C(10)	3058(2)	6189(6)	4618(1)	62(1)
C(11)	3080(2)	8401(8)	4791(2)	83(1)
C(12)	-270(1)	5216(4)	665(1)	36(1)
C(13)	-37(1)	4650(4)	1185(1)	36(1)
C(14)	45(1)	2690(5)	1390(1)	45(1)
C(15)	310(1)	2714(5)	1907(1)	49(1)
C(16)	438(1)	4649(5)	2107(1)	42(1)
C(17)	743(2)	5185(5)	2642(1)	55(1)
C(18)	774(1)	7455(5)	2782(1)	45(1)
C(19)	1104(1)	7831(5)	3329(1)	50(1)
C(20)	1140(1)	10073(5)	3483(1)	53(1)
C(21)	1466(2)	10440(6)	4028(1)	66(1)
C(22)	1486(2)	12655(8)	4195(2)	86(1)

Table 3. Bond lengths [Å] and angles [°] for Zntiof.

Zn(1)-S(5)	2.3543(8)	C(10)-H(10B)	0.95(4)
Zn(1)-S(1)	2.3697(7)	C(11)-H(11A)	0.93(5)
Zn(1)-S(4)	2.3924(8)	C(11)-H(11B)	0.97(4)
Zn(1)-S(2)	2.4540(8)	C(11)-H(11C)	0.96(4)
Zn(1)-S(4)#1	2.8840(8)	C(12)-C(13)	1.435(4)
S(1)-C(1)	1.701(3)	C(12)-S(5)#1	1.683(3)
S(2)-C(1)	1.690(3)	C(13)-C(14)	1.379(4)
S(3)-C(5)	1.721(3)	C(14)-C(15)	1.391(4)
S(3)-C(2)	1.727(3)	C(14)-H(14)	0.98(3)
S(4)-C(12)	1.723(3)	C(15)-C(16)	1.366(4)
S(5)-C(12)#1	1.683(3)	C(15)-H(15)	0.88(3)
S(6)-C(16)	1.715(3)	C(16)-C(17)	1.497(4)
S(6)-C(13)	1.729(3)	C(17)-C(18)	1.513(4)
C(1)-C(2)	1.444(3)	C(17)-H(17A)	0.98(4)
C(2)-C(3)	1.371(4)	C(17)-H(17B)	0.98(4)
C(3)-C(4)	1.388(4)	C(18)-C(19)	1.519(4)
C(3)-H(3)	0.89(3)	C(18)-H(18A)	0.98(3)
C(4)-C(5)	1.362(4)	C(18)-H(18B)	0.98(3)
C(4)-H(4)	0.90(3)	C(19)-C(20)	1.507(5)
C(5)-C(6)	1.498(4)	C(19)-H(19A)	1.00(3)
C(6)-C(7)	1.517(4)	C(19)-H(19B)	0.94(4)
C(6)-H(6A)	0.95(3)	C(20)-C(21)	1.511(4)
C(6)-H(6B)	0.94(3)	C(20)-H(20A)	0.93(3)
C(7)-C(8)	1.519(4)	C(20)-H(20B)	0.99(4)
C(7)-H(7A)	0.96(3)	C(21)-C(22)	1.503(6)
C(7)-H(7B)	1.00(3)	C(21)-H(21A)	1.10(4)
C(8)-C(9)	1.507(4)	C(21)-H(21B)	0.92(5)
C(8)-H(8A)	1.05(3)	C(22)-H(22A)	0.91(5)
C(8)-H(8B)	0.97(3)	C(22)-H(22B)	0.98(5)
C(9)-C(10)	1.505(4)	C(22)-H(22C)	0.87(5)
C(9)-H(9A)	1.02(3)		
C(9)-H(9B)	0.97(3)	S(5)-Zn(1)-S(1)	134.47(3)
C(10)-C(11)	1.507(6)	S(5)-Zn(1)-S(4)	102.78(3)
C(10)-H(10A)	0.99(4)	S(1)-Zn(1)-S(4)	117.86(3)

S(5)-Zn(1)-S(2)	111.59(3)	C(8)-C(7)-H(7A)	110.1(17)
S(1)-Zn(1)-S(2)	74.74(3)	C(6)-C(7)-H(7B)	108.4(17)
S(4)-Zn(1)-S(2)	109.35(3)	C(8)-C(7)-H(7B)	111.9(17)
S(5)-Zn(1)-S(4)#1	67.62(2)	H(7A)-C(7)-H(7B)	104(2)
S(1)-Zn(1)-S(4)#1	96.96(3)	C(9)-C(8)-C(7)	113.9(3)
S(4)-Zn(1)-S(4)#1	82.43(3)	C(9)-C(8)-H(8A)	109.9(17)
S(2)-Zn(1)-S(4)#1	167.72(3)	C(7)-C(8)-H(8A)	107.5(17)
C(1)-S(1)-Zn(1)	83.99(9)	C(9)-C(8)-H(8B)	113.6(18)
C(1)-S(2)-Zn(1)	81.59(9)	C(7)-C(8)-H(8B)	105.6(19)
C(5)-S(3)-C(2)	92.31(13)	H(8A)-C(8)-H(8B)	106(2)
C(12)-S(4)-Zn(1)	98.94(9)	C(10)-C(9)-C(8)	114.1(3)
C(12)#1-S(5)-Zn(1)	93.72(9)	C(10)-C(9)-H(9A)	108.4(18)
C(16)-S(6)-C(13)	92.21(13)	C(8)-C(9)-H(9A)	110.5(18)
C(2)-C(1)-S(2)	119.9(2)	C(10)-C(9)-H(9B)	106.9(18)
C(2)-C(1)-S(1)	120.67(19)	C(8)-C(9)-H(9B)	112.8(18)
S(2)-C(1)-S(1)	119.44(15)	H(9A)-C(9)-H(9B)	104(2)
C(3)-C(2)-C(1)	128.6(2)	C(9)-C(10)-C(11)	114.2(4)
C(3)-C(2)-S(3)	110.1(2)	C(9)-C(10)-H(10A)	104(2)
C(1)-C(2)-S(3)	121.3(2)	C(11)-C(10)-H(10A)	117(2)
C(2)-C(3)-C(4)	113.2(3)	C(9)-C(10)-H(10B)	108(2)
C(2)-C(3)-H(3)	122(2)	C(11)-C(10)-H(10B)	110(2)
C(4)-C(3)-H(3)	124(2)	H(10A)-C(10)-H(10B)	104(3)
C(5)-C(4)-C(3)	114.2(3)	C(10)-C(11)-H(11A)	116(3)
C(5)-C(4)-H(4)	124(2)	C(10)-C(11)-H(11B)	107(3)
C(3)-C(4)-H(4)	122(2)	H(11A)-C(11)-H(11B)	107(4)
C(4)-C(5)-C(6)	128.1(3)	C(10)-C(11)-H(11C)	113(2)
C(4)-C(5)-S(3)	110.2(2)	H(11A)-C(11)-H(11C)	101(4)
C(6)-C(5)-S(3)	121.8(2)	H(11B)-C(11)-H(11C)	113(4)
C(5)-C(6)-C(7)	115.9(2)	C(13)-C(12)-S(5)#1	120.6(2)
C(5)-C(6)-H(6A)	106.7(17)	C(13)-C(12)-S(4)	119.5(2)
C(7)-C(6)-H(6A)	109.2(18)	S(5)#1-C(12)-S(4)	119.84(15)
C(5)-C(6)-H(6B)	107(2)	C(14)-C(13)-C(12)	128.1(3)
C(7)-C(6)-H(6B)	110(2)	C(14)-C(13)-S(6)	110.4(2)
H(6A)-C(6)-H(6B)	108(3)	C(12)-C(13)-S(6)	121.3(2)
C(6)-C(7)-C(8)	112.6(3)	C(13)-C(14)-C(15)	112.6(3)
C(6)-C(7)-H(7A)	109.5(18)	C(13)-C(14)-H(14)	122.0(19)

C(15)-C(14)-H(14)	125.3(19)	C(20)-C(19)-H(19B)	112(2)
C(16)-C(15)-C(14)	114.3(3)	C(18)-C(19)-H(19B)	109(2)
C(16)-C(15)-H(15)	124.6(19)	H(19A)-C(19)-H(19B)	105(3)
C(14)-C(15)-H(15)	121.1(19)	C(19)-C(20)-C(21)	113.8(3)
C(15)-C(16)-C(17)	127.1(3)	C(19)-C(20)-H(20A)	107(2)
C(15)-C(16)-S(6)	110.5(2)	C(21)-C(20)-H(20A)	109(2)
C(17)-C(16)-S(6)	122.3(2)	C(19)-C(20)-H(20B)	111(2)
C(16)-C(17)-C(18)	116.7(3)	C(21)-C(20)-H(20B)	107(2)
C(16)-C(17)-H(17A)	102(2)	H(20A)-C(20)-H(20B)	109(3)
C(18)-C(17)-H(17A)	108(2)	C(22)-C(21)-C(20)	114.4(4)
C(16)-C(17)-H(17B)	103(2)	C(22)-C(21)-H(21A)	110(2)
C(18)-C(17)-H(17B)	112(2)	C(20)-C(21)-H(21A)	107(2)
H(17A)-C(17)-H(17B)	116(3)	C(22)-C(21)-H(21B)	112(3)
C(17)-C(18)-C(19)	112.3(3)	C(20)-C(21)-H(21B)	107(3)
C(17)-C(18)-H(18A)	105.2(16)	H(21A)-C(21)-H(21B)	106(4)
C(19)-C(18)-H(18A)	111.5(16)	C(21)-C(22)-H(22A)	105(3)
C(17)-C(18)-H(18B)	109.1(17)	C(21)-C(22)-H(22B)	111(3)
C(19)-C(18)-H(18B)	108.5(17)	H(22A)-C(22)-H(22B)	112(5)
H(18A)-C(18)-H(18B)	110(2)	C(21)-C(22)-H(22C)	110(3)
C(20)-C(19)-C(18)	113.9(3)	H(22A)-C(22)-H(22C)	107(4)
C(20)-C(19)-H(19A)	108.8(17)	H(22B)-C(22)-H(22C)	112(4)
C(18)-C(19)-H(19A)	108.2(18)		

Symmetry transformations used to generate equivalent atoms:

#1 -x,-y+1,-z

Table 4. Anisotropic displacement parameters (□^{2}x 10^3)for Zntiof. The anisotropic displacement factor exponent takes the form: -2p^2[h^{2}a*^{2}U^{11} + ... + 2 h k a* b* U^{12}]

	U^{11}	U^{22}	U^{33}	U^{23}	U^{13}	U^{12}
Zn(1)	45(1)	57(1)	28(1)	-4(1)	3(1)	6(1)
S(1)	48(1)	35(1)	34(1)	-1(1)	1(1)	-2(1)
S(2)	55(1)	38(1)	34(1)	-7(1)	-1(1)	-3(1)
S(3)	51(1)	33(1)	31(1)	-2(1)	-1(1)	-3(1)
S(4)	44(1)	40(1)	31(1)	-8(1)	6(1)	-3(1)
S(5)	55(1)	40(1)	32(1)	-2(1)	11(1)	9(1)
S(6)	54(1)	37(1)	29(1)	-2(1)	7(1)	1(1)
C(1)	35(1)	34(2)	32(1)	-4(1)	9(1)	0(1)
C(2)	34(1)	36(2)	29(1)	-3(1)	5(1)	0(1)
C(3)	43(2)	36(2)	37(2)	-5(1)	5(1)	-5(1)
C(4)	51(2)	34(2)	36(2)	4(1)	9(1)	0(1)
C(5)	41(1)	39(2)	27(1)	0(1)	5(1)	0(1)
C(6)	48(2)	45(2)	31(2)	-1(1)	2(1)	1(1)
C(7)	44(2)	47(2)	32(2)	-2(1)	6(1)	4(1)
C(8)	51(2)	49(2)	32(2)	-4(1)	6(1)	-1(2)
C(9)	55(2)	51(2)	38(2)	-5(2)	8(2)	0(2)
C(10)	74(2)	58(2)	43(2)	-13(2)	9(2)	1(2)
C(11)	99(4)	69(3)	68(3)	-30(2)	19(3)	-6(3)
C(12)	35(1)	39(2)	32(1)	-7(1)	10(1)	-5(1)
C(13)	38(1)	38(2)	30(1)	-4(1)	10(1)	-2(1)
C(14)	56(2)	40(2)	36(2)	-2(1)	14(1)	-6(1)
C(15)	65(2)	39(2)	38(2)	9(2)	16(2)	2(2)
C(16)	47(2)	45(2)	29(2)	1(1)	9(1)	2(1)
C(17)	66(2)	55(2)	33(2)	-2(2)	8(2)	2(2)
C(18)	45(2)	52(2)	33(2)	-2(1)	10(1)	2(1)
C(19)	57(2)	53(2)	32(2)	-3(2)	7(2)	-1(2)
C(20)	56(2)	54(2)	43(2)	-4(2)	12(2)	4(2)
C(21)	86(3)	60(2)	40(2)	-10(2)	13(2)	-10(2)
C(22)	100(4)	75(3)	73(3)	-31(3)	24(3)	-9(3)

Table 5. Hydrogen coordinates (x 10^4) and isotropic displacement parameters ($Å^2$x 10^3) for Zntiof.

	x	y	z	U(eq)
H(3)	1387(11)	-2320(50)	1775(12)	50(9)
H(4)	1922(11)	-2470(50)	2632(11)	53(9)
H(6A)	2699(11)	780(40)	3200(10)	52(9)
H(6B)	2299(12)	190(50)	3400(12)	67(11)
H(7A)	2032(11)	3700(40)	3307(10)	50(8)
H(7B)	2450(10)	4250(50)	3123(11)	55(9)
H(8A)	3068(12)	3180(50)	3936(11)	61(9)
H(8B)	2606(11)	2670(50)	4091(12)	55(10)
H(9A)	2376(12)	6360(50)	4022(12)	64(10)
H(9B)	2833(11)	6820(50)	3880(12)	52(9)
H(10A)	3377(14)	5540(60)	4651(13)	80(12)
H(10B)	2939(12)	5320(60)	4816(13)	74(12)
H(11A)	3295(16)	8650(70)	5122(18)	114(16)
H(11B)	2747(16)	8770(70)	4764(16)	105(16)
H(11C)	3209(14)	9320(60)	4611(14)	79(14)
H(14)	-90(11)	1450(50)	1187(12)	69(10)
H(15)	382(10)	1560(50)	2082(11)	45(8)
H(17A)	1078(14)	4730(60)	2680(13)	86(12)
H(17B)	584(13)	4360(60)	2827(14)	89(13)
H(18A)	429(10)	7880(40)	2708(10)	42(8)
H(18B)	910(10)	8230(40)	2571(11)	49(9)
H(19A)	1445(12)	7310(40)	3387(12)	56(9)
H(19B)	994(13)	7000(50)	3532(14)	75(12)
H(20A)	819(13)	10520(50)	3424(12)	65(10)
H(20B)	1277(12)	10930(60)	3279(13)	77(12)
H(21A)	1841(16)	9910(60)	4082(14)	104(14)
H(21B)	1355(17)	9560(70)	4217(17)	120(18)
H(22A)	1610(18)	13370(80)	3998(18)	120(20)
H(22B)	1160(20)	13150(80)	4160(20)	150(20)
H(22C)	1698(18)	12780(70)	4502(19)	111(18)

Table 6. Torsion angles [°] for Zntiof.

S(5)-Zn(1)-S(1)-C(1)	-108.43(10)	C(3)-C(4)-C(5)-S(3)	-0.3(3)
S(4)-Zn(1)-S(1)-C(1)	101.16(9)	C(2)-S(3)-C(5)-C(4)	0.4(2)
S(2)-Zn(1)-S(1)-C(1)	-2.98(9)	C(2)-S(3)-C(5)-C(6)	179.3(3)
S(4)#1-Zn(1)-S(1)-C(1)	-173.75(9)	C(4)-C(5)-C(6)-C(7)	-159.7(3)
S(5)-Zn(1)-S(2)-C(1)	135.31(9)	S(3)-C(5)-C(6)-C(7)	21.5(4)
S(1)-Zn(1)-S(2)-C(1)	3.01(9)	C(5)-C(6)-C(7)-C(8)	176.6(3)
S(4)-Zn(1)-S(2)-C(1)	-111.67(9)	C(6)-C(7)-C(8)-C(9)	178.0(3)
S(4)#1-Zn(1)-S(2)-C(1)	51.47(16)	C(7)-C(8)-C(9)-C(10)	178.5(3)
S(5)-Zn(1)-S(4)-C(12)	-141.90(10)	C(8)-C(9)-C(10)-C(11)	179.0(4)
S(1)-Zn(1)-S(4)-C(12)	16.91(10)	Zn(1)-S(4)-C(12)-C(13)	-68.6(2)
S(2)-Zn(1)-S(4)-C(12)	99.44(10)	Zn(1)-S(4)-C(12)-S(5)#1	110.40(14)
S(4)#1-Zn(1)-S(4)-C(12)	-76.99(10)	S(5)#1-C(12)-C(13)-C(14)	166.7(2)
S(1)-Zn(1)-S(5)-C(12)#1	-87.05(9)	S(4)-C(12)-C(13)-C(14)	-14.3(4)
S(4)-Zn(1)-S(5)-C(12)#1	66.35(9)	S(5)#1-C(12)-C(13)-S(6)	-17.6(3)
S(2)-Zn(1)-S(5)-C(12)#1	-176.57(9)	S(4)-C(12)-C(13)-S(6)	161.40(15)
S(4)#1-Zn(1)-S(5)-C(12)#1	-9.80(9)	C(16)-S(6)-C(13)-C(14)	0.4(2)
Zn(1)-S(2)-C(1)-C(2)	174.7(2)	C(16)-S(6)-C(13)-C(12)	-176.0(2)
Zn(1)-S(2)-C(1)-S(1)	-4.65(14)	C(12)-C(13)-C(14)-C(15)	175.9(3)
Zn(1)-S(1)-C(1)-C(2)	-174.5(2)	S(6)-C(13)-C(14)-C(15)	-0.1(3)
Zn(1)-S(1)-C(1)-S(2)	4.79(15)	C(13)-C(14)-C(15)-C(16)	-0.3(4)
S(2)-C(1)-C(2)-C(3)	2.9(4)	C(14)-C(15)-C(16)-C(17)	-176.9(3)
S(1)-C(1)-C(2)-C(3)	-177.8(2)	C(14)-C(15)-C(16)-S(6)	0.6(4)
S(2)-C(1)-C(2)-S(3)	-176.61(15)	C(13)-S(6)-C(16)-C(15)	-0.6(2)
S(1)-C(1)-C(2)-S(3)	2.7(3)	C(13)-S(6)-C(16)-C(17)	177.0(3)
C(5)-S(3)-C(2)-C(3)	-0.3(2)	C(15)-C(16)-C(17)-C(18)	-172.1(3)
C(5)-S(3)-C(2)-C(1)	179.2(2)	S(6)-C(16)-C(17)-C(18)	10.7(5)
C(1)-C(2)-C(3)-C(4)	-179.3(3)	C(16)-C(17)-C(18)-C(19)	-178.3(3)
S(3)-C(2)-C(3)-C(4)	0.2(3)	C(17)-C(18)-C(19)-C(20)	-179.3(3)
C(2)-C(3)-C(4)-C(5)	0.0(4)	C(18)-C(19)-C(20)-C(21)	179.7(3)
C(3)-C(4)-C(5)-C(6)	-179.2(3)	C(19)-C(20)-C(21)-C(22)	-177.1(4)

Symmetry transformations used to generate equivalent atoms:

#1 -x,-y+1,-z

Appendix 2

Crystal data and structure refinement for **12**

Table 1. Crystal data and structure refinement for MTSLReBT.

Identification code	mtslrebm	
Empirical formula	C13 H5 O4 Re S4	
Formula weight	539.61	
Temperature	293(2) K	
Wavelength	0.71073 Å	
Crystal system	monoclinic	
Space group	$P2_1/n$	
Unit cell dimensions	a = 5.9892(4) Å	α= 90°.
	b = 7.4933(5) Å	β= 93.8530(10)°.
	c = 35.247(3) Å	γ = 90°.
Volume	1578.27(19) $Å^3$	
Z	4	
Density (calculated)	2.271 Mg/m^3	
Absorption coefficient	8.240 mm^{-1}	
F(000)	1016	
Crystal size	0.34 x 0.10 x 0.06 mm^3	
Theta range for data collection	2.78 to 26.52°.	
Index ranges	-7<=h<=3, -8<=k<=7, -42<=l<=43	
Reflections collected	8226	
Independent reflections	2996 [R(int) = 0.0305]	
Completeness to theta = 25.00°	99.6 %	
Refinement method	Full-matrix least-squares on F^2	
Data / restraints / parameters	2996 / 0 / 199	
Goodness-of-fit on F^2	1.242	
Final R indices [I>2sigma(I)]	R1 = 0.0286, wR2 = 0.0726	
R indices (all data)	R1 = 0.0318, wR2 = 0.0745	
Largest diff. peak and hole	0.489 and -1.296 e.$Å^{-3}$	

Table 2. Atomic coordinates (x 10^4) and equivalent isotropic displacement parameters ($Å^2$x 10^3) for MTSLReBT. U(eq) is defined as one third of the trace of the orthogonalized U^{ij} tensor.

	x	y	z	U(eq)
Re(1)	7478(1)	2762(1)	647(1)	42(1)
S(1)	10667(2)	4037(2)	1061(1)	48(1)
S(2)	6573(2)	2737(2)	1329(1)	47(1)
S(3)	8383(2)	3220(2)	2197(1)	44(1)
S(4)	12189(2)	4199(2)	3276(1)	56(1)
C(1)	4805(9)	1596(9)	425(2)	57(1)
O(1)	3271(7)	882(7)	297(1)	80(1)
C(2)	8732(10)	2934(8)	154(2)	54(1)
O(2)	9482(9)	3069(7)	-129(1)	78(1)
C(3)	8889(9)	380(8)	740(2)	52(1)
O(3)	9672(8)	-977(7)	802(1)	75(1)
C(4)	6109(9)	5177(9)	570(2)	54(1)
O(4)	5397(8)	6543(7)	518(1)	80(1)
C(5)	9162(7)	3564(6)	1441(1)	37(1)
C(6)	9994(7)	3829(6)	1828(1)	37(1)
C(7)	12010(8)	4512(7)	1964(1)	43(1)
C(8)	12250(8)	4578(7)	2364(2)	46(1)
C(9)	10420(7)	3927(6)	2535(1)	39(1)
C(10)	10113(8)	3683(6)	2932(1)	40(1)
C(11)	8261(9)	2927(6)	3093(2)	44(1)
C(12)	8636(10)	2784(7)	3496(2)	51(1)
C(13)	10655(10)	3410(9)	3626(2)	57(1)

Table 3. Bond lengths [Å] and angles [°] for MTSLReBT.

Re(1)-C(1)	1.942(6)	C(3)-Re(1)-S(2)	87.29(15)
Re(1)-C(2)	1.943(6)	C(4)-Re(1)-S(2)	91.33(15)
Re(1)-C(3)	1.993(6)	C(1)-Re(1)-S(1)	168.26(18)
Re(1)-C(4)	1.998(6)	C(2)-Re(1)-S(1)	99.75(18)
Re(1)-S(2)	2.4974(14)	C(3)-Re(1)-S(1)	87.01(16)
Re(1)-S(1)	2.5124(12)	C(4)-Re(1)-S(1)	91.33(16)
S(1)-C(5)	1.701(4)	S(2)-Re(1)-S(1)	69.54(4)
S(2)-C(5)	1.692(5)	C(5)-S(1)-Re(1)	87.42(16)
S(3)-C(9)	1.729(5)	C(5)-S(2)-Re(1)	88.12(16)
S(3)-C(6)	1.733(4)	C(9)-S(3)-C(6)	91.9(2)
S(4)-C(13)	1.693(6)	C(13)-S(4)-C(10)	91.9(3)
S(4)-C(10)	1.721(5)	O(1)-C(1)-Re(1)	178.5(6)
C(1)-O(1)	1.131(7)	O(2)-C(2)-Re(1)	178.4(6)
C(2)-O(2)	1.128(7)	O(3)-C(3)-Re(1)	178.2(5)
C(3)-O(3)	1.134(7)	O(4)-C(4)-Re(1)	177.4(6)
C(4)-O(4)	1.120(7)	C(6)-C(5)-S(2)	121.8(3)
C(5)-C(6)	1.435(6)	C(6)-C(5)-S(1)	123.4(3)
C(6)-C(7)	1.368(6)	S(2)-C(5)-S(1)	114.7(3)
C(7)-C(8)	1.409(7)	C(7)-C(6)-C(5)	128.9(4)
C(8)-C(9)	1.374(6)	C(7)-C(6)-S(3)	110.9(3)
C(9)-C(10)	1.437(7)	C(5)-C(6)-S(3)	120.2(3)
C(10)-C(11)	1.398(7)	C(6)-C(7)-C(8)	113.1(4)
C(11)-C(12)	1.429(8)	C(9)-C(8)-C(7)	113.2(4)
C(12)-C(13)	1.348(8)	C(8)-C(9)-C(10)	129.0(4)
		C(8)-C(9)-S(3)	110.7(4)
C(1)-Re(1)-C(2)	91.5(2)	C(10)-C(9)-S(3)	120.1(4)
C(1)-Re(1)-C(3)	89.6(2)	C(11)-C(10)-C(9)	127.1(4)
C(2)-Re(1)-C(3)	91.2(2)	C(11)-C(10)-S(4)	111.2(4)
C(1)-Re(1)-C(4)	91.9(2)	C(9)-C(10)-S(4)	121.6(4)
C(2)-Re(1)-C(4)	89.9(2)	C(10)-C(11)-C(12)	110.9(5)
C(3)-Re(1)-C(4)	178.1(2)	C(13)-C(12)-C(11)	112.9(5)
C(1)-Re(1)-S(2)	99.09(17)	C(12)-C(13)-S(4)	113.1(4)
C(2)-Re(1)-S(2)	169.24(18)		

Symmetry transformations used to generate equivalent atoms:

Table 4. Anisotropic displacement parameters ($Å^2 x\ 10^3$)for MTSLReBT. The anisotropic displacement factor exponent takes the form: $-2\pi^2[\ h^2a^{*2}U^{11} + ... + 2\ h\ k\ a^*\ b^*\ U^{12}\ ]$

	U^{11}	U^{22}	U^{33}	U^{23}	U^{13}	U^{12}
Re(1)	37(1)	52(1)	37(1)	-3(1)	4(1)	-1(1)
S(1)	38(1)	68(1)	39(1)	0(1)	7(1)	-10(1)
S(2)	38(1)	61(1)	40(1)	-4(1)	7(1)	-9(1)
S(3)	37(1)	57(1)	39(1)	3(1)	4(1)	-6(1)
S(4)	53(1)	71(1)	45(1)	-3(1)	0(1)	-8(1)
C(1)	48(3)	68(4)	55(3)	-8(3)	11(3)	4(3)
O(1)	50(2)	103(4)	85(3)	-27(3)	-1(2)	-18(2)
C(2)	51(3)	58(4)	52(4)	-1(3)	9(3)	-5(2)
O(2)	93(4)	95(4)	47(3)	-7(2)	26(2)	-12(3)
C(3)	50(3)	64(4)	43(3)	-5(3)	14(2)	-6(3)
O(3)	86(3)	67(3)	73(3)	8(2)	19(2)	21(2)
C(4)	53(3)	72(4)	35(3)	-4(3)	-4(2)	2(3)
O(4)	95(3)	69(3)	73(3)	3(3)	-3(3)	26(3)
C(5)	38(2)	37(2)	38(2)	0(2)	9(2)	2(2)
C(6)	39(2)	39(3)	35(2)	1(2)	9(2)	3(2)
C(7)	41(2)	44(3)	45(3)	-3(2)	8(2)	-7(2)
C(8)	44(3)	46(3)	49(3)	-4(2)	3(2)	-8(2)
C(9)	41(2)	35(2)	40(3)	-2(2)	1(2)	2(2)
C(10)	43(2)	35(3)	42(3)	-3(2)	-1(2)	4(2)
C(11)	55(3)	40(3)	36(3)	-1(2)	7(2)	-3(2)
C(12)	57(3)	50(3)	49(3)	0(2)	16(3)	2(2)
C(13)	71(4)	64(4)	36(3)	0(3)	3(3)	0(3)

Table 5. Torsion angles [°] for MTSLReBT.

C(1)-Re(1)-S(1)-C(5)	-12.4(9)	S(1)-Re(1)-C(4)-O(4)	79(12)
C(2)-Re(1)-S(1)-C(5)	-176.3(2)	Re(1)-S(2)-C(5)-C(6)	-175.8(4)
C(3)-Re(1)-S(1)-C(5)	-85.6(2)	Re(1)-S(2)-C(5)-S(1)	4.0(3)
C(4)-Re(1)-S(1)-C(5)	93.6(2)	Re(1)-S(1)-C(5)-C(6)	175.8(4)
S(2)-Re(1)-S(1)-C(5)	2.63(16)	Re(1)-S(1)-C(5)-S(2)	-4.0(3)
C(1)-Re(1)-S(2)-C(5)	174.3(3)	S(2)-C(5)-C(6)-C(7)	-178.5(4)
C(2)-Re(1)-S(2)-C(5)	3.0(10)	S(1)-C(5)-C(6)-C(7)	1.7(8)
C(3)-Re(1)-S(2)-C(5)	85.2(2)	S(2)-C(5)-C(6)-S(3)	2.5(6)
C(4)-Re(1)-S(2)-C(5)	-93.6(2)	S(1)-C(5)-C(6)-S(3)	-177.3(3)
S(1)-Re(1)-S(2)-C(5)	-2.65(17)	C(9)-S(3)-C(6)-C(7)	1.0(4)
C(2)-Re(1)-C(1)-O(1)	87(21)	C(9)-S(3)-C(6)-C(5)	-179.9(4)
C(3)-Re(1)-C(1)-O(1)	-4(21)	C(5)-C(6)-C(7)-C(8)	179.9(5)
C(4)-Re(1)-C(1)-O(1)	177(100)	S(3)-C(6)-C(7)-C(8)	-1.1(6)
S(2)-Re(1)-C(1)-O(1)	-91(21)	C(6)-C(7)-C(8)-C(9)	0.6(7)
S(1)-Re(1)-C(1)-O(1)	-77(21)	C(7)-C(8)-C(9)-C(10)	175.9(5)
C(1)-Re(1)-C(2)-O(2)	147(22)	C(7)-C(8)-C(9)-S(3)	0.2(6)
C(3)-Re(1)-C(2)-O(2)	-124(22)	C(6)-S(3)-C(9)-C(8)	-0.7(4)
C(4)-Re(1)-C(2)-O(2)	55(22)	C(6)-S(3)-C(9)-C(10)	-176.8(4)
S(2)-Re(1)-C(2)-O(2)	-42(23)	C(8)-C(9)-C(10)-C(11)	-176.3(5)
S(1)-Re(1)-C(2)-O(2)	-36(22)	S(3)-C(9)-C(10)-C(11)	-1.0(7)
C(1)-Re(1)-C(3)-O(3)	-92(18)	C(8)-C(9)-C(10)-S(4)	-0.7(7)
C(2)-Re(1)-C(3)-O(3)	176(100)	S(3)-C(9)-C(10)-S(4)	174.6(3)
C(4)-Re(1)-C(3)-O(3)	49(21)	C(13)-S(4)-C(10)-C(11)	0.6(4)
S(2)-Re(1)-C(3)-O(3)	7(18)	C(13)-S(4)-C(10)-C(9)	-175.7(4)
S(1)-Re(1)-C(3)-O(3)	76(18)	C(9)-C(10)-C(11)-C(12)	175.4(5)
C(1)-Re(1)-C(4)-O(4)	-112(12)	S(4)-C(10)-C(11)-C(12)	-0.6(5)
C(2)-Re(1)-C(4)-O(4)	-20(12)	C(10)-C(11)-C(12)-C(13)	0.3(7)
C(3)-Re(1)-C(4)-O(4)	107(13)	C(11)-C(12)-C(13)-S(4)	0.2(7)
S(2)-Re(1)-C(4)-O(4)	149(12)	C(10)-S(4)-C(13)-C(12)	-0.5(5)

Symmetry transformations used to generate equivalent atoms:

Appendix 1

Crystal data and structure refinement for **8**

Table 1. Crystal data and structure refinement for Zntiof.

Identification code	zntiof_abs	
Empirical formula	$C_{44}\ H_{60}\ S_{12}\ Zn_2$	
Formula weight	1104.54	
Temperature	293(2) K	
Wavelength	0.71073 Å	
Crystal system	Monoclinic	
Space group	C 2/c	
Unit cell dimensions	a = 29.1118(19) Å	a= 90º
	b = 6.4571(4) Å	b= 112.5790(10)º.
	c = 28.8391(19) Å	g = 90º.
Volume	5005.6(6) $Å^3$	
Z	4	
Density (calculated)	1.465 Mg/m^3	
Absorption coefficient	1.490 mm^{-1}	
F(000)	2304	
Crystal size	0.34 x 0.14 x 0.05 mm^3	
Theta range for data collection	2.53 to 26.50º.	
Index ranges	-36<=h<=14, -7<=k<=7, -35<=l<=35	
Reflections collected	12744	
Independent reflections	4712 [R(int) = 0.0354]	
Completeness to theta = 25.00º	99.5 %	
Absorption correction	Semi-empirical from equivalents	
Max. and min. transmission	0.928 and 0.734	
Refinement method	Full-matrix least-squares on F^2	
Data / restraints / parameters	4712 / 0 / 382	
Goodness-of-fit on F^2	1.082	
Final R indices [I>2sigma(I)]	R1 = 0.0324, wR2 = 0.0718	
R indices (all data)	R1 = 0.0582, wR2 = 0.0838	
Extinction coefficient	0	
Largest diff. peak and hole	0.272 and -0.401 $e.Å^{-3}$	

Table 2. Atomic coordinates (x 10^4) and equivalent isotropic displacement parameters ($Å^2$x 10^3) for Zntiof. U(eq) is defined as one third of the trace of the orthogonalized U^{ij} tensor.

	x	y	z	U(eq)
Zn(1)	491(1)	2776(1)	329(1)	47(1)
S(1)	1116(1)	3935(1)	1089(1)	43(1)
S(2)	794(1)	-360(1)	836(1)	48(1)
S(3)	1786(1)	2517(1)	2214(1)	43(1)
S(4)	-359(1)	3361(1)	209(1)	41(1)
S(5)	446(1)	2323(1)	-498(1)	44(1)
S(6)	220(1)	6496(1)	1646(1)	43(1)
C(1)	1141(1)	1401(4)	1259(1)	35(1)
C(2)	1451(1)	749(4)	1761(1)	35(1)
C(3)	1528(1)	-1214(5)	1957(1)	42(1)
C(4)	1847(1)	-1275(5)	2459(1)	42(1)
C(5)	2022(1)	612(4)	2660(1)	38(1)
C(6)	2374(1)	1098(5)	3184(1)	45(1)
C(7)	2367(1)	3315(5)	3355(1)	43(1)
C(8)	2712(1)	3652(5)	3899(1)	47(1)
C(9)	2726(1)	5858(5)	4075(1)	51(1)
C(10)	3058(2)	6189(6)	4618(1)	62(1)
C(11)	3080(2)	8401(8)	4791(2)	83(1)
C(12)	-270(1)	5216(4)	665(1)	36(1)
C(13)	-37(1)	4650(4)	1185(1)	36(1)
C(14)	45(1)	2690(5)	1390(1)	45(1)
C(15)	310(1)	2714(5)	1907(1)	49(1)
C(16)	438(1)	4649(5)	2107(1)	42(1)
C(17)	743(2)	5185(5)	2642(1)	55(1)
C(18)	774(1)	7455(5)	2782(1)	45(1)
C(19)	1104(1)	7831(5)	3329(1)	50(1)
C(20)	1140(1)	10073(5)	3483(1)	53(1)
C(21)	1466(2)	10440(6)	4028(1)	66(1)
C(22)	1486(2)	12655(8)	4195(2)	86(1)

Table 3. Bond lengths [Å] and angles [º] for Zntiof.

Zn(1)-S(5)	2.3543(8)	C(10)-H(10B)	0.95(4)
Zn(1)-S(1)	2.3697(7)	C(11)-H(11A)	0.93(5)
Zn(1)-S(4)	2.3924(8)	C(11)-H(11B)	0.97(4)
Zn(1)-S(2)	2.4540(8)	C(11)-H(11C)	0.96(4)
Zn(1)-S(4)#1	2.8840(8)	C(12)-C(13)	1.435(4)
S(1)-C(1)	1.701(3)	C(12)-S(5)#1	1.683(3)
S(2)-C(1)	1.690(3)	C(13)-C(14)	1.379(4)
S(3)-C(5)	1.721(3)	C(14)-C(15)	1.391(4)
S(3)-C(2)	1.727(3)	C(14)-H(14)	0.98(3)
S(4)-C(12)	1.723(3)	C(15)-C(16)	1.366(4)
S(5)-C(12)#1	1.683(3)	C(15)-H(15)	0.88(3)
S(6)-C(16)	1.715(3)	C(16)-C(17)	1.497(4)
S(6)-C(13)	1.729(3)	C(17)-C(18)	1.513(4)
C(1)-C(2)	1.444(3)	C(17)-H(17A)	0.98(4)
C(2)-C(3)	1.371(4)	C(17)-H(17B)	0.98(4)
C(3)-C(4)	1.388(4)	C(18)-C(19)	1.519(4)
C(3)-H(3)	0.89(3)	C(18)-H(18A)	0.98(3)
C(4)-C(5)	1.362(4)	C(18)-H(18B)	0.98(3)
C(4)-H(4)	0.90(3)	C(19)-C(20)	1.507(5)
C(5)-C(6)	1.498(4)	C(19)-H(19A)	1.00(3)
C(6)-C(7)	1.517(4)	C(19)-H(19B)	0.94(4)
C(6)-H(6A)	0.95(3)	C(20)-C(21)	1.511(4)
C(6)-H(6B)	0.94(3)	C(20)-H(20A)	0.93(3)
C(7)-C(8)	1.519(4)	C(20)-H(20B)	0.99(4)
C(7)-H(7A)	0.96(3)	C(21)-C(22)	1.503(6)
C(7)-H(7B)	1.00(3)	C(21)-H(21A)	1.10(4)
C(8)-C(9)	1.507(4)	C(21)-H(21B)	0.92(5)
C(8)-H(8A)	1.05(3)	C(22)-H(22A)	0.91(5)
C(8)-H(8B)	0.97(3)	C(22)-H(22B)	0.98(5)
C(9)-C(10)	1.505(4)	C(22)-H(22C)	0.87(5)
C(9)-H(9A)	1.02(3)		
C(9)-H(9B)	0.97(3)	S(5)-Zn(1)-S(1)	134.47(3)
C(10)-C(11)	1.507(6)	S(5)-Zn(1)-S(4)	102.78(3)
C(10)-H(10A)	0.99(4)	S(1)-Zn(1)-S(4)	117.86(3)

S(5)-Zn(1)-S(2)	111.59(3)	C(8)-C(7)-H(7A)	110.1(17)
S(1)-Zn(1)-S(2)	74.74(3)	C(6)-C(7)-H(7B)	108.4(17)
S(4)-Zn(1)-S(2)	109.35(3)	C(8)-C(7)-H(7B)	111.9(17)
S(5)-Zn(1)-S(4)#1	67.62(2)	H(7A)-C(7)-H(7B)	104(2)
S(1)-Zn(1)-S(4)#1	96.96(3)	C(9)-C(8)-C(7)	113.9(3)
S(4)-Zn(1)-S(4)#1	82.43(3)	C(9)-C(8)-H(8A)	109.9(17)
S(2)-Zn(1)-S(4)#1	167.72(3)	C(7)-C(8)-H(8A)	107.5(17)
C(1)-S(1)-Zn(1)	83.99(9)	C(9)-C(8)-H(8B)	113.6(18)
C(1)-S(2)-Zn(1)	81.59(9)	C(7)-C(8)-H(8B)	105.6(19)
C(5)-S(3)-C(2)	92.31(13)	H(8A)-C(8)-H(8B)	106(2)
C(12)-S(4)-Zn(1)	98.94(9)	C(10)-C(9)-C(8)	114.1(3)
C(12)#1-S(5)-Zn(1)	93.72(9)	C(10)-C(9)-H(9A)	108.4(18)
C(16)-S(6)-C(13)	92.21(13)	C(8)-C(9)-H(9A)	110.5(18)
C(2)-C(1)-S(2)	119.9(2)	C(10)-C(9)-H(9B)	106.9(18)
C(2)-C(1)-S(1)	120.67(19)	C(8)-C(9)-H(9B)	112.8(18)
S(2)-C(1)-S(1)	119.44(15)	H(9A)-C(9)-H(9B)	104(2)
C(3)-C(2)-C(1)	128.6(2)	C(9)-C(10)-C(11)	114.2(4)
C(3)-C(2)-S(3)	110.1(2)	C(9)-C(10)-H(10A)	104(2)
C(1)-C(2)-S(3)	121.3(2)	C(11)-C(10)-H(10A)	117(2)
C(2)-C(3)-C(4)	113.2(3)	C(9)-C(10)-H(10B)	108(2)
C(2)-C(3)-H(3)	122(2)	C(11)-C(10)-H(10B)	110(2)
C(4)-C(3)-H(3)	124(2)	H(10A)-C(10)-H(10B)	104(3)
C(5)-C(4)-C(3)	114.2(3)	C(10)-C(11)-H(11A)	116(3)
C(5)-C(4)-H(4)	124(2)	C(10)-C(11)-H(11B)	107(3)
C(3)-C(4)-H(4)	122(2)	H(11A)-C(11)-H(11B)	107(4)
C(4)-C(5)-C(6)	128.1(3)	C(10)-C(11)-H(11C)	113(2)
C(4)-C(5)-S(3)	110.2(2)	H(11A)-C(11)-H(11C)	101(4)
C(6)-C(5)-S(3)	121.8(2)	H(11B)-C(11)-H(11C)	113(4)
C(5)-C(6)-C(7)	115.9(2)	C(13)-C(12)-S(5)#1	120.6(2)
C(5)-C(6)-H(6A)	106.7(17)	C(13)-C(12)-S(4)	119.5(2)
C(7)-C(6)-H(6A)	109.2(18)	S(5)#1-C(12)-S(4)	119.84(15)
C(5)-C(6)-H(6B)	107(2)	C(14)-C(13)-C(12)	128.1(3)
C(7)-C(6)-H(6B)	110(2)	C(14)-C(13)-S(6)	110.4(2)
H(6A)-C(6)-H(6B)	108(3)	C(12)-C(13)-S(6)	121.3(2)
C(6)-C(7)-C(8)	112.6(3)	C(13)-C(14)-C(15)	112.6(3)
C(6)-C(7)-H(7A)	109.5(18)	C(13)-C(14)-H(14)	122.0(19)

C(15)-C(14)-H(14)	125.3(19)	C(20)-C(19)-H(19B)	112(2)
C(16)-C(15)-C(14)	114.3(3)	C(18)-C(19)-H(19B)	109(2)
C(16)-C(15)-H(15)	124.6(19)	H(19A)-C(19)-H(19B)	105(3)
C(14)-C(15)-H(15)	121.1(19)	C(19)-C(20)-C(21)	113.8(3)
C(15)-C(16)-C(17)	127.1(3)	C(19)-C(20)-H(20A)	107(2)
C(15)-C(16)-S(6)	110.5(2)	C(21)-C(20)-H(20A)	109(2)
C(17)-C(16)-S(6)	122.3(2)	C(19)-C(20)-H(20B)	111(2)
C(16)-C(17)-C(18)	116.7(3)	C(21)-C(20)-H(20B)	107(2)
C(16)-C(17)-H(17A)	102(2)	H(20A)-C(20)-H(20B)	109(3)
C(18)-C(17)-H(17A)	108(2)	C(22)-C(21)-C(20)	114.4(4)
C(16)-C(17)-H(17B)	103(2)	C(22)-C(21)-H(21A)	110(2)
C(18)-C(17)-H(17B)	112(2)	C(20)-C(21)-H(21A)	107(2)
H(17A)-C(17)-H(17B)	116(3)	C(22)-C(21)-H(21B)	112(3)
C(17)-C(18)-C(19)	112.3(3)	C(20)-C(21)-H(21B)	107(3)
C(17)-C(18)-H(18A)	105.2(16)	H(21A)-C(21)-H(21B)	106(4)
C(19)-C(18)-H(18A)	111.5(16)	C(21)-C(22)-H(22A)	105(3)
C(17)-C(18)-H(18B)	109.1(17)	C(21)-C(22)-H(22B)	111(3)
C(19)-C(18)-H(18B)	108.5(17)	H(22A)-C(22)-H(22B)	112(5)
H(18A)-C(18)-H(18B)	110(2)	C(21)-C(22)-H(22C)	110(3)
C(20)-C(19)-C(18)	113.9(3)	H(22A)-C(22)-H(22C)	107(4)
C(20)-C(19)-H(19A)	108.8(17)	H(22B)-C(22)-H(22C)	112(4)
C(18)-C(19)-H(19A)	108.2(18)		

Symmetry transformations used to generate equivalent atoms:

#1 -x,-y+1,-z

Table 4. Anisotropic displacement parameters ($\square^2$x 10^3)for Zntiof. The anisotropic displacement factor exponent takes the form: $-2p^2[h^2a^{*2}U^{11} + ... + 2 h k a^* b^* U^{12}]$

	U^{11}	U^{22}	U^{33}	U^{23}	U^{13}	U^{12}
Zn(1)	45(1)	57(1)	28(1)	-4(1)	3(1)	6(1)
S(1)	48(1)	35(1)	34(1)	-1(1)	1(1)	-2(1)
S(2)	55(1)	38(1)	34(1)	-7(1)	-1(1)	-3(1)
S(3)	51(1)	33(1)	31(1)	-2(1)	-1(1)	-3(1)
S(4)	44(1)	40(1)	31(1)	-8(1)	6(1)	-3(1)
S(5)	55(1)	40(1)	32(1)	-2(1)	11(1)	9(1)
S(6)	54(1)	37(1)	29(1)	-2(1)	7(1)	1(1)
C(1)	35(1)	34(2)	32(1)	-4(1)	9(1)	0(1)
C(2)	34(1)	36(2)	29(1)	-3(1)	5(1)	0(1)
C(3)	43(2)	36(2)	37(2)	-5(1)	5(1)	-5(1)
C(4)	51(2)	34(2)	36(2)	4(1)	9(1)	0(1)
C(5)	41(1)	39(2)	27(1)	0(1)	5(1)	0(1)
C(6)	48(2)	45(2)	31(2)	-1(1)	2(1)	1(1)
C(7)	44(2)	47(2)	32(2)	-2(1)	6(1)	4(1)
C(8)	51(2)	49(2)	32(2)	-4(1)	6(1)	-1(2)
C(9)	55(2)	51(2)	38(2)	-5(2)	8(2)	0(2)
C(10)	74(2)	58(2)	43(2)	-13(2)	9(2)	1(2)
C(11)	99(4)	69(3)	68(3)	-30(2)	19(3)	-6(3)
C(12)	35(1)	39(2)	32(1)	-7(1)	10(1)	-5(1)
C(13)	38(1)	38(2)	30(1)	-4(1)	10(1)	-2(1)
C(14)	56(2)	40(2)	36(2)	-2(1)	14(1)	-6(1)
C(15)	65(2)	39(2)	38(2)	9(2)	16(2)	2(2)
C(16)	47(2)	45(2)	29(2)	1(1)	9(1)	2(1)
C(17)	66(2)	55(2)	33(2)	-2(2)	8(2)	2(2)
C(18)	45(2)	52(2)	33(2)	-2(1)	10(1)	2(1)
C(19)	57(2)	53(2)	32(2)	-3(2)	7(2)	-1(2)
C(20)	56(2)	54(2)	43(2)	-4(2)	12(2)	4(2)
C(21)	86(3)	60(2)	40(2)	-10(2)	13(2)	-10(2)
C(22)	100(4)	75(3)	73(3)	-31(3)	24(3)	-9(3)

Table 5. Hydrogen coordinates (x 10^4) and isotropic displacement parameters ($Å^2$x 10^3) for Zntiof.

	x	y	z	U(eq)
H(3)	1387(11)	-2320(50)	1775(12)	50(9)
H(4)	1922(11)	-2470(50)	2632(11)	53(9)
H(6A)	2699(11)	780(40)	3200(10)	52(9)
H(6B)	2299(12)	190(50)	3400(12)	67(11)
H(7A)	2032(11)	3700(40)	3307(10)	50(8)
H(7B)	2450(10)	4250(50)	3123(11)	55(9)
H(8A)	3068(12)	3180(50)	3936(11)	61(9)
H(8B)	2606(11)	2670(50)	4091(12)	55(10)
H(9A)	2376(12)	6360(50)	4022(12)	64(10)
H(9B)	2833(11)	6820(50)	3880(12)	52(9)
H(10A)	3377(14)	5540(60)	4651(13)	80(12)
H(10B)	2939(12)	5320(60)	4816(13)	74(12)
H(11A)	3295(16)	8650(70)	5122(18)	114(16)
H(11B)	2747(16)	8770(70)	4764(16)	105(16)
H(11C)	3209(14)	9320(60)	4611(14)	79(14)
H(14)	-90(11)	1450(50)	1187(12)	69(10)
H(15)	382(10)	1560(50)	2082(11)	45(8)
H(17A)	1078(14)	4730(60)	2680(13)	86(12)
H(17B)	584(13)	4360(60)	2827(14)	89(13)
H(18A)	429(10)	7880(40)	2708(10)	42(8)
H(18B)	910(10)	8230(40)	2571(11)	49(9)
H(19A)	1445(12)	7310(40)	3387(12)	56(9)
H(19B)	994(13)	7000(50)	3532(14)	75(12)
H(20A)	819(13)	10520(50)	3424(12)	65(10)
H(20B)	1277(12)	10930(60)	3279(13)	77(12)
H(21A)	1841(16)	9910(60)	4082(14)	104(14)
H(21B)	1355(17)	9560(70)	4217(17)	120(18)
H(22A)	1610(18)	13370(80)	3998(18)	120(20)
H(22B)	1160(20)	13150(80)	4160(20)	150(20)
H(22C)	1698(18)	12780(70)	4502(19)	111(18)

Table 6. Torsion angles [º] for Zntiof.

S(5)-Zn(1)-S(1)-C(1)	-108.43(10)	C(3)-C(4)-C(5)-S(3)	-0.3(3)
S(4)-Zn(1)-S(1)-C(1)	101.16(9)	C(2)-S(3)-C(5)-C(4)	0.4(2)
S(2)-Zn(1)-S(1)-C(1)	-2.98(9)	C(2)-S(3)-C(5)-C(6)	179.3(3)
S(4)#1-Zn(1)-S(1)-C(1)	-173.75(9)	C(4)-C(5)-C(6)-C(7)	-159.7(3)
S(5)-Zn(1)-S(2)-C(1)	135.31(9)	S(3)-C(5)-C(6)-C(7)	21.5(4)
S(1)-Zn(1)-S(2)-C(1)	3.01(9)	C(5)-C(6)-C(7)-C(8)	176.6(3)
S(4)-Zn(1)-S(2)-C(1)	-111.67(9)	C(6)-C(7)-C(8)-C(9)	178.0(3)
S(4)#1-Zn(1)-S(2)-C(1)	51.47(16)	C(7)-C(8)-C(9)-C(10)	178.5(3)
S(5)-Zn(1)-S(4)-C(12)	-141.90(10)	C(8)-C(9)-C(10)-C(11)	179.0(4)
S(1)-Zn(1)-S(4)-C(12)	16.91(10)	Zn(1)-S(4)-C(12)-C(13)	-68.6(2)
S(2)-Zn(1)-S(4)-C(12)	99.44(10)	Zn(1)-S(4)-C(12)-S(5)#1	110.40(14)
S(4)#1-Zn(1)-S(4)-C(12)	-76.99(10)	S(5)#1-C(12)-C(13)-C(14)	166.7(2)
S(1)-Zn(1)-S(5)-C(12)#1	-87.05(9)	S(4)-C(12)-C(13)-C(14)	-14.3(4)
S(4)-Zn(1)-S(5)-C(12)#1	66.35(9)	S(5)#1-C(12)-C(13)-S(6)	-17.6(3)
S(2)-Zn(1)-S(5)-C(12)#1	-176.57(9)	S(4)-C(12)-C(13)-S(6)	161.40(15)
S(4)#1-Zn(1)-S(5)-C(12)#1	-9.80(9)	C(16)-S(6)-C(13)-C(14)	0.4(2)
Zn(1)-S(2)-C(1)-C(2)	174.7(2)	C(16)-S(6)-C(13)-C(12)	-176.0(2)
Zn(1)-S(2)-C(1)-S(1)	-4.65(14)	C(12)-C(13)-C(14)-C(15)	175.9(3)
Zn(1)-S(1)-C(1)-C(2)	-174.5(2)	S(6)-C(13)-C(14)-C(15)	-0.1(3)
Zn(1)-S(1)-C(1)-S(2)	4.79(15)	C(13)-C(14)-C(15)-C(16)	-0.3(4)
S(2)-C(1)-C(2)-C(3)	2.9(4)	C(14)-C(15)-C(16)-C(17)	-176.9(3)
S(1)-C(1)-C(2)-C(3)	-177.8(2)	C(14)-C(15)-C(16)-S(6)	0.6(4)
S(2)-C(1)-C(2)-S(3)	-176.61(15)	C(13)-S(6)-C(16)-C(15)	-0.6(2)
S(1)-C(1)-C(2)-S(3)	2.7(3)	C(13)-S(6)-C(16)-C(17)	177.0(3)
C(5)-S(3)-C(2)-C(3)	-0.3(2)	C(15)-C(16)-C(17)-C(18)	-172.1(3)
C(5)-S(3)-C(2)-C(1)	179.2(2)	S(6)-C(16)-C(17)-C(18)	10.7(5)
C(1)-C(2)-C(3)-C(4)	-179.3(3)	C(16)-C(17)-C(18)-C(19)	-178.3(3)
S(3)-C(2)-C(3)-C(4)	0.2(3)	C(17)-C(18)-C(19)-C(20)	-179.3(3)
C(2)-C(3)-C(4)-C(5)	0.0(4)	C(18)-C(19)-C(20)-C(21)	179.7(3)
C(3)-C(4)-C(5)-C(6)	-179.2(3)	C(19)-C(20)-C(21)-C(22)	-177.1(4)

Symmetry transformations used to generate equivalent atoms:

#1 -x,-y+1,-z

Appendix 1

Crystal data and structure refinement for **8**

Table 1. Crystal data and structure refinement for Zntiof.

Identification code	zntiof_abs	
Empirical formula	$C_{44}\ H_{60}\ S_{12}\ Zn_2$	
Formula weight	1104.54	
Temperature	293(2) K	
Wavelength	0.71073 Å	
Crystal system	Monoclinic	
Space group	C 2/c	
Unit cell dimensions	a = 29.1118(19) Å	a= 90º
	b = 6.4571(4) Å	b= 112.5790(10)º.
	c = 28.8391(19) Å	g = 90º.
Volume	5005.6(6) $Å^3$	
Z	4	
Density (calculated)	1.465 Mg/m^3	
Absorption coefficient	1.490 mm^{-1}	
F(000)	2304	
Crystal size	0.34 x 0.14 x 0.05 mm^3	
Theta range for data collection	2.53 to 26.50º.	
Index ranges	-36<=h<=14, -7<=k<=7, -35<=l<=35	
Reflections collected	12744	
Independent reflections	4712 [R(int) = 0.0354]	
Completeness to theta = 25.00º	99.5 %	
Absorption correction	Semi-empirical from equivalents	
Max. and min. transmission	0.928 and 0.734	
Refinement method	Full-matrix least-squares on F^2	
Data / restraints / parameters	4712 / 0 / 382	
Goodness-of-fit on F^2	1.082	
Final R indices [I>2sigma(I)]	R1 = 0.0324, wR2 = 0.0718	
R indices (all data)	R1 = 0.0582, wR2 = 0.0838	
Extinction coefficient	0	
Largest diff. peak and hole	0.272 and -0.401 e.$Å^{-3}$	

Table 2. Atomic coordinates (x 10^4) and equivalent isotropic displacement parameters ($Å^2$x 10^3) for Zntiof. U(eq) is defined as one third of the trace of the orthogonalized U^{ij} tensor.

	x	y	z	U(eq)
Zn(1)	491(1)	2776(1)	329(1)	47(1)
S(1)	1116(1)	3935(1)	1089(1)	43(1)
S(2)	794(1)	-360(1)	836(1)	48(1)
S(3)	1786(1)	2517(1)	2214(1)	43(1)
S(4)	-359(1)	3361(1)	209(1)	41(1)
S(5)	446(1)	2323(1)	-498(1)	44(1)
S(6)	220(1)	6496(1)	1646(1)	43(1)
C(1)	1141(1)	1401(4)	1259(1)	35(1)
C(2)	1451(1)	749(4)	1761(1)	35(1)
C(3)	1528(1)	-1214(5)	1957(1)	42(1)
C(4)	1847(1)	-1275(5)	2459(1)	42(1)
C(5)	2022(1)	612(4)	2660(1)	38(1)
C(6)	2374(1)	1098(5)	3184(1)	45(1)
C(7)	2367(1)	3315(5)	3355(1)	43(1)
C(8)	2712(1)	3652(5)	3899(1)	47(1)
C(9)	2726(1)	5858(5)	4075(1)	51(1)
C(10)	3058(2)	6189(6)	4618(1)	62(1)
C(11)	3080(2)	8401(8)	4791(2)	83(1)
C(12)	-270(1)	5216(4)	665(1)	36(1)
C(13)	-37(1)	4650(4)	1185(1)	36(1)
C(14)	45(1)	2690(5)	1390(1)	45(1)
C(15)	310(1)	2714(5)	1907(1)	49(1)
C(16)	438(1)	4649(5)	2107(1)	42(1)
C(17)	743(2)	5185(5)	2642(1)	55(1)
C(18)	774(1)	7455(5)	2782(1)	45(1)
C(19)	1104(1)	7831(5)	3329(1)	50(1)
C(20)	1140(1)	10073(5)	3483(1)	53(1)
C(21)	1466(2)	10440(6)	4028(1)	66(1)
C(22)	1486(2)	12655(8)	4195(2)	86(1)

Table 3. Bond lengths [Å] and angles [°] for Zntiof.

Zn(1)-S(5)	2.3543(8)	C(10)-H(10B)	0.95(4)
Zn(1)-S(1)	2.3697(7)	C(11)-H(11A)	0.93(5)
Zn(1)-S(4)	2.3924(8)	C(11)-H(11B)	0.97(4)
Zn(1)-S(2)	2.4540(8)	C(11)-H(11C)	0.96(4)
Zn(1)-S(4)#1	2.8840(8)	C(12)-C(13)	1.435(4)
S(1)-C(1)	1.701(3)	C(12)-S(5)#1	1.683(3)
S(2)-C(1)	1.690(3)	C(13)-C(14)	1.379(4)
S(3)-C(5)	1.721(3)	C(14)-C(15)	1.391(4)
S(3)-C(2)	1.727(3)	C(14)-H(14)	0.98(3)
S(4)-C(12)	1.723(3)	C(15)-C(16)	1.366(4)
S(5)-C(12)#1	1.683(3)	C(15)-H(15)	0.88(3)
S(6)-C(16)	1.715(3)	C(16)-C(17)	1.497(4)
S(6)-C(13)	1.729(3)	C(17)-C(18)	1.513(4)
C(1)-C(2)	1.444(3)	C(17)-H(17A)	0.98(4)
C(2)-C(3)	1.371(4)	C(17)-H(17B)	0.98(4)
C(3)-C(4)	1.388(4)	C(18)-C(19)	1.519(4)
C(3)-H(3)	0.89(3)	C(18)-H(18A)	0.98(3)
C(4)-C(5)	1.362(4)	C(18)-H(18B)	0.98(3)
C(4)-H(4)	0.90(3)	C(19)-C(20)	1.507(5)
C(5)-C(6)	1.498(4)	C(19)-H(19A)	1.00(3)
C(6)-C(7)	1.517(4)	C(19)-H(19B)	0.94(4)
C(6)-H(6A)	0.95(3)	C(20)-C(21)	1.511(4)
C(6)-H(6B)	0.94(3)	C(20)-H(20A)	0.93(3)
C(7)-C(8)	1.519(4)	C(20)-H(20B)	0.99(4)
C(7)-H(7A)	0.96(3)	C(21)-C(22)	1.503(6)
C(7)-H(7B)	1.00(3)	C(21)-H(21A)	1.10(4)
C(8)-C(9)	1.507(4)	C(21)-H(21B)	0.92(5)
C(8)-H(8A)	1.05(3)	C(22)-H(22A)	0.91(5)
C(8)-H(8B)	0.97(3)	C(22)-H(22B)	0.98(5)
C(9)-C(10)	1.505(4)	C(22)-H(22C)	0.87(5)
C(9)-H(9A)	1.02(3)		
C(9)-H(9B)	0.97(3)	S(5)-Zn(1)-S(1)	134.47(3)
C(10)-C(11)	1.507(6)	S(5)-Zn(1)-S(4)	102.78(3)
C(10)-H(10A)	0.99(4)	S(1)-Zn(1)-S(4)	117.86(3)

S(5)-Zn(1)-S(2)	111.59(3)	C(8)-C(7)-H(7A)	110.1(17)
S(1)-Zn(1)-S(2)	74.74(3)	C(6)-C(7)-H(7B)	108.4(17)
S(4)-Zn(1)-S(2)	109.35(3)	C(8)-C(7)-H(7B)	111.9(17)
S(5)-Zn(1)-S(4)#1	67.62(2)	H(7A)-C(7)-H(7B)	104(2)
S(1)-Zn(1)-S(4)#1	96.96(3)	C(9)-C(8)-C(7)	113.9(3)
S(4)-Zn(1)-S(4)#1	82.43(3)	C(9)-C(8)-H(8A)	109.9(17)
S(2)-Zn(1)-S(4)#1	167.72(3)	C(7)-C(8)-H(8A)	107.5(17)
C(1)-S(1)-Zn(1)	83.99(9)	C(9)-C(8)-H(8B)	113.6(18)
C(1)-S(2)-Zn(1)	81.59(9)	C(7)-C(8)-H(8B)	105.6(19)
C(5)-S(3)-C(2)	92.31(13)	H(8A)-C(8)-H(8B)	106(2)
C(12)-S(4)-Zn(1)	98.94(9)	C(10)-C(9)-C(8)	114.1(3)
C(12)#1-S(5)-Zn(1)	93.72(9)	C(10)-C(9)-H(9A)	108.4(18)
C(16)-S(6)-C(13)	92.21(13)	C(8)-C(9)-H(9A)	110.5(18)
C(2)-C(1)-S(2)	119.9(2)	C(10)-C(9)-H(9B)	106.9(18)
C(2)-C(1)-S(1)	120.67(19)	C(8)-C(9)-H(9B)	112.8(18)
S(2)-C(1)-S(1)	119.44(15)	H(9A)-C(9)-H(9B)	104(2)
C(3)-C(2)-C(1)	128.6(2)	C(9)-C(10)-C(11)	114.2(4)
C(3)-C(2)-S(3)	110.1(2)	C(9)-C(10)-H(10A)	104(2)
C(1)-C(2)-S(3)	121.3(2)	C(11)-C(10)-H(10A)	117(2)
C(2)-C(3)-C(4)	113.2(3)	C(9)-C(10)-H(10B)	108(2)
C(2)-C(3)-H(3)	122(2)	C(11)-C(10)-H(10B)	110(2)
C(4)-C(3)-H(3)	124(2)	H(10A)-C(10)-H(10B)	104(3)
C(5)-C(4)-C(3)	114.2(3)	C(10)-C(11)-H(11A)	116(3)
C(5)-C(4)-H(4)	124(2)	C(10)-C(11)-H(11B)	107(3)
C(3)-C(4)-H(4)	122(2)	H(11A)-C(11)-H(11B)	107(4)
C(4)-C(5)-C(6)	128.1(3)	C(10)-C(11)-H(11C)	113(2)
C(4)-C(5)-S(3)	110.2(2)	H(11A)-C(11)-H(11C)	101(4)
C(6)-C(5)-S(3)	121.8(2)	H(11B)-C(11)-H(11C)	113(4)
C(5)-C(6)-C(7)	115.9(2)	C(13)-C(12)-S(5)#1	120.6(2)
C(5)-C(6)-H(6A)	106.7(17)	C(13)-C(12)-S(4)	119.5(2)
C(7)-C(6)-H(6A)	109.2(18)	S(5)#1-C(12)-S(4)	119.84(15)
C(5)-C(6)-H(6B)	107(2)	C(14)-C(13)-C(12)	128.1(3)
C(7)-C(6)-H(6B)	110(2)	C(14)-C(13)-S(6)	110.4(2)
H(6A)-C(6)-H(6B)	108(3)	C(12)-C(13)-S(6)	121.3(2)
C(6)-C(7)-C(8)	112.6(3)	C(13)-C(14)-C(15)	112.6(3)
C(6)-C(7)-H(7A)	109.5(18)	C(13)-C(14)-H(14)	122.0(19)

C(15)-C(14)-H(14)	125.3(19)	C(20)-C(19)-H(19B)	112(2)
C(16)-C(15)-C(14)	114.3(3)	C(18)-C(19)-H(19B)	109(2)
C(16)-C(15)-H(15)	124.6(19)	H(19A)-C(19)-H(19B)	105(3)
C(14)-C(15)-H(15)	121.1(19)	C(19)-C(20)-C(21)	113.8(3)
C(15)-C(16)-C(17)	127.1(3)	C(19)-C(20)-H(20A)	107(2)
C(15)-C(16)-S(6)	110.5(2)	C(21)-C(20)-H(20A)	109(2)
C(17)-C(16)-S(6)	122.3(2)	C(19)-C(20)-H(20B)	111(2)
C(16)-C(17)-C(18)	116.7(3)	C(21)-C(20)-H(20B)	107(2)
C(16)-C(17)-H(17A)	102(2)	H(20A)-C(20)-H(20B)	109(3)
C(18)-C(17)-H(17A)	108(2)	C(22)-C(21)-C(20)	114.4(4)
C(16)-C(17)-H(17B)	103(2)	C(22)-C(21)-H(21A)	110(2)
C(18)-C(17)-H(17B)	112(2)	C(20)-C(21)-H(21A)	107(2)
H(17A)-C(17)-H(17B)	116(3)	C(22)-C(21)-H(21B)	112(3)
C(17)-C(18)-C(19)	112.3(3)	C(20)-C(21)-H(21B)	107(3)
C(17)-C(18)-H(18A)	105.2(16)	H(21A)-C(21)-H(21B)	106(4)
C(19)-C(18)-H(18A)	111.5(16)	C(21)-C(22)-H(22A)	105(3)
C(17)-C(18)-H(18B)	109.1(17)	C(21)-C(22)-H(22B)	111(3)
C(19)-C(18)-H(18B)	108.5(17)	H(22A)-C(22)-H(22B)	112(5)
H(18A)-C(18)-H(18B)	110(2)	C(21)-C(22)-H(22C)	110(3)
C(20)-C(19)-C(18)	113.9(3)	H(22A)-C(22)-H(22C)	107(4)
C(20)-C(19)-H(19A)	108.8(17)	H(22B)-C(22)-H(22C)	112(4)
C(18)-C(19)-H(19A)	108.2(18)		

Symmetry transformations used to generate equivalent atoms:

#1 -x,-y+1,-z

Table 4. Anisotropic displacement parameters (□^{2}x 10^3)for Zntiof. The anisotropic displacement factor exponent takes the form: -2p^2[h^{2}a*^{2}U^{11} + ... + 2 h k a* b* U^{12}]

	U^{11}	U^{22}	U^{33}	U^{23}	U^{13}	U^{12}
Zn(1)	45(1)	57(1)	28(1)	-4(1)	3(1)	6(1)
S(1)	48(1)	35(1)	34(1)	-1(1)	1(1)	-2(1)
S(2)	55(1)	38(1)	34(1)	-7(1)	-1(1)	-3(1)
S(3)	51(1)	33(1)	31(1)	-2(1)	-1(1)	-3(1)
S(4)	44(1)	40(1)	31(1)	-8(1)	6(1)	-3(1)
S(5)	55(1)	40(1)	32(1)	-2(1)	11(1)	9(1)
S(6)	54(1)	37(1)	29(1)	-2(1)	7(1)	1(1)
C(1)	35(1)	34(2)	32(1)	-4(1)	9(1)	0(1)
C(2)	34(1)	36(2)	29(1)	-3(1)	5(1)	0(1)
C(3)	43(2)	36(2)	37(2)	-5(1)	5(1)	-5(1)
C(4)	51(2)	34(2)	36(2)	4(1)	9(1)	0(1)
C(5)	41(1)	39(2)	27(1)	0(1)	5(1)	0(1)
C(6)	48(2)	45(2)	31(2)	-1(1)	2(1)	1(1)
C(7)	44(2)	47(2)	32(2)	-2(1)	6(1)	4(1)
C(8)	51(2)	49(2)	32(2)	-4(1)	6(1)	-1(2)
C(9)	55(2)	51(2)	38(2)	-5(2)	8(2)	0(2)
C(10)	74(2)	58(2)	43(2)	-13(2)	9(2)	1(2)
C(11)	99(4)	69(3)	68(3)	-30(2)	19(3)	-6(3)
C(12)	35(1)	39(2)	32(1)	-7(1)	10(1)	-5(1)
C(13)	38(1)	38(2)	30(1)	-4(1)	10(1)	-2(1)
C(14)	56(2)	40(2)	36(2)	-2(1)	14(1)	-6(1)
C(15)	65(2)	39(2)	38(2)	9(2)	16(2)	2(2)
C(16)	47(2)	45(2)	29(2)	1(1)	9(1)	2(1)
C(17)	66(2)	55(2)	33(2)	-2(2)	8(2)	2(2)
C(18)	45(2)	52(2)	33(2)	-2(1)	10(1)	2(1)
C(19)	57(2)	53(2)	32(2)	-3(2)	7(2)	-1(2)
C(20)	56(2)	54(2)	43(2)	-4(2)	12(2)	4(2)
C(21)	86(3)	60(2)	40(2)	-10(2)	13(2)	-10(2)
C(22)	100(4)	75(3)	73(3)	-31(3)	24(3)	-9(3)

Table 5. Hydrogen coordinates (x 10^4) and isotropic displacement parameters ($Å^2$x 10^3) for Zntiof.

	x	y	z	U(eq)
H(3)	1387(11)	-2320(50)	1775(12)	50(9)
H(4)	1922(11)	-2470(50)	2632(11)	53(9)
H(6A)	2699(11)	780(40)	3200(10)	52(9)
H(6B)	2299(12)	190(50)	3400(12)	67(11)
H(7A)	2032(11)	3700(40)	3307(10)	50(8)
H(7B)	2450(10)	4250(50)	3123(11)	55(9)
H(8A)	3068(12)	3180(50)	3936(11)	61(9)
H(8B)	2606(11)	2670(50)	4091(12)	55(10)
H(9A)	2376(12)	6360(50)	4022(12)	64(10)
H(9B)	2833(11)	6820(50)	3880(12)	52(9)
H(10A)	3377(14)	5540(60)	4651(13)	80(12)
H(10B)	2939(12)	5320(60)	4816(13)	74(12)
H(11A)	3295(16)	8650(70)	5122(18)	114(16)
H(11B)	2747(16)	8770(70)	4764(16)	105(16)
H(11C)	3209(14)	9320(60)	4611(14)	79(14)
H(14)	-90(11)	1450(50)	1187(12)	69(10)
H(15)	382(10)	1560(50)	2082(11)	45(8)
H(17A)	1078(14)	4730(60)	2680(13)	86(12)
H(17B)	584(13)	4360(60)	2827(14)	89(13)
H(18A)	429(10)	7880(40)	2708(10)	42(8)
H(18B)	910(10)	8230(40)	2571(11)	49(9)
H(19A)	1445(12)	7310(40)	3387(12)	56(9)
H(19B)	994(13)	7000(50)	3532(14)	75(12)
H(20A)	819(13)	10520(50)	3424(12)	65(10)
H(20B)	1277(12)	10930(60)	3279(13)	77(12)
H(21A)	1841(16)	9910(60)	4082(14)	104(14)
H(21B)	1355(17)	9560(70)	4217(17)	120(18)
H(22A)	1610(18)	13370(80)	3998(18)	120(20)
H(22B)	1160(20)	13150(80)	4160(20)	150(20)
H(22C)	1698(18)	12780(70)	4502(19)	111(18)

Table 6. Torsion angles [°] for Zntiof.

S(5)-Zn(1)-S(1)-C(1)	-108.43(10)	C(3)-C(4)-C(5)-S(3)	-0.3(3)
S(4)-Zn(1)-S(1)-C(1)	101.16(9)	C(2)-S(3)-C(5)-C(4)	0.4(2)
S(2)-Zn(1)-S(1)-C(1)	-2.98(9)	C(2)-S(3)-C(5)-C(6)	179.3(3)
S(4)#1-Zn(1)-S(1)-C(1)	-173.75(9)	C(4)-C(5)-C(6)-C(7)	-159.7(3)
S(5)-Zn(1)-S(2)-C(1)	135.31(9)	S(3)-C(5)-C(6)-C(7)	21.5(4)
S(1)-Zn(1)-S(2)-C(1)	3.01(9)	C(5)-C(6)-C(7)-C(8)	176.6(3)
S(4)-Zn(1)-S(2)-C(1)	-111.67(9)	C(6)-C(7)-C(8)-C(9)	178.0(3)
S(4)#1-Zn(1)-S(2)-C(1)	51.47(16)	C(7)-C(8)-C(9)-C(10)	178.5(3)
S(5)-Zn(1)-S(4)-C(12)	-141.90(10)	C(8)-C(9)-C(10)-C(11)	179.0(4)
S(1)-Zn(1)-S(4)-C(12)	16.91(10)	Zn(1)-S(4)-C(12)-C(13)	-68.6(2)
S(2)-Zn(1)-S(4)-C(12)	99.44(10)	Zn(1)-S(4)-C(12)-S(5)#1	110.40(14)
S(4)#1-Zn(1)-S(4)-C(12)	-76.99(10)	S(5)#1-C(12)-C(13)-C(14)	166.7(2)
S(1)-Zn(1)-S(5)-C(12)#1	-87.05(9)	S(4)-C(12)-C(13)-C(14)	-14.3(4)
S(4)-Zn(1)-S(5)-C(12)#1	66.35(9)	S(5)#1-C(12)-C(13)-S(6)	-17.6(3)
S(2)-Zn(1)-S(5)-C(12)#1	-176.57(9)	S(4)-C(12)-C(13)-S(6)	161.40(15)
S(4)#1-Zn(1)-S(5)-C(12)#1	-9.80(9)	C(16)-S(6)-C(13)-C(14)	0.4(2)
Zn(1)-S(2)-C(1)-C(2)	174.7(2)	C(16)-S(6)-C(13)-C(12)	-176.0(2)
Zn(1)-S(2)-C(1)-S(1)	-4.65(14)	C(12)-C(13)-C(14)-C(15)	175.9(3)
Zn(1)-S(1)-C(1)-C(2)	-174.5(2)	S(6)-C(13)-C(14)-C(15)	-0.1(3)
Zn(1)-S(1)-C(1)-S(2)	4.79(15)	C(13)-C(14)-C(15)-C(16)	-0.3(4)
S(2)-C(1)-C(2)-C(3)	2.9(4)	C(14)-C(15)-C(16)-C(17)	-176.9(3)
S(1)-C(1)-C(2)-C(3)	-177.8(2)	C(14)-C(15)-C(16)-S(6)	0.6(4)
S(2)-C(1)-C(2)-S(3)	-176.61(15)	C(13)-S(6)-C(16)-C(15)	-0.6(2)
S(1)-C(1)-C(2)-S(3)	2.7(3)	C(13)-S(6)-C(16)-C(17)	177.0(3)
C(5)-S(3)-C(2)-C(3)	-0.3(2)	C(15)-C(16)-C(17)-C(18)	-172.1(3)
C(5)-S(3)-C(2)-C(1)	179.2(2)	S(6)-C(16)-C(17)-C(18)	10.7(5)
C(1)-C(2)-C(3)-C(4)	-179.3(3)	C(16)-C(17)-C(18)-C(19)	-178.3(3)
S(3)-C(2)-C(3)-C(4)	0.2(3)	C(17)-C(18)-C(19)-C(20)	-179.3(3)
C(2)-C(3)-C(4)-C(5)	0.0(4)	C(18)-C(19)-C(20)-C(21)	179.7(3)
C(3)-C(4)-C(5)-C(6)	-179.2(3)	C(19)-C(20)-C(21)-C(22)	-177.1(4)

Symmetry transformations used to generate equivalent atoms:

#1 -x,-y+1,-z

Appendix 2

Crystal data and structure refinement for **12**

Table 1. Crystal data and structure refinement for MTSLReBT.

Identification code	mtslrebm	
Empirical formula	C13 H5 O4 Re S4	
Formula weight	539.61	
Temperature	293(2) K	
Wavelength	0.71073 Å	
Crystal system	monoclinic	
Space group	$P2_1/n$	
Unit cell dimensions	a = 5.9892(4) Å	α= 90°.
	b = 7.4933(5) Å	β= 93.8530(10)°.
	c = 35.247(3) Å	γ = 90°.
Volume	1578.27(19) $Å^3$	
Z	4	
Density (calculated)	2.271 Mg/m^3	
Absorption coefficient	8.240 mm^{-1}	
F(000)	1016	
Crystal size	0.34 x 0.10 x 0.06 mm^3	
Theta range for data collection	2.78 to 26.52°.	
Index ranges	-7<=h<=3, -8<=k<=7, -42<=l<=43	
Reflections collected	8226	
Independent reflections	2996 [R(int) = 0.0305]	
Completeness to theta = 25.00°	99.6 %	
Refinement method	Full-matrix least-squares on F^2	
Data / restraints / parameters	2996 / 0 / 199	
Goodness-of-fit on F^2	1.242	
Final R indices [I>2sigma(I)]	R1 = 0.0286, wR2 = 0.0726	
R indices (all data)	R1 = 0.0318, wR2 = 0.0745	
Largest diff. peak and hole	0.489 and -1.296 e.$Å^{-3}$	

Table 2. Atomic coordinates (x 10^4) and equivalent isotropic displacement parameters ($Å^2$x 10^3) for MTSLReBT. U(eq) is defined as one third of the trace of the orthogonalized U^{ij} tensor.

	x	y	z	U(eq)
Re(1)	7478(1)	2762(1)	647(1)	42(1)
S(1)	10667(2)	4037(2)	1061(1)	48(1)
S(2)	6573(2)	2737(2)	1329(1)	47(1)
S(3)	8383(2)	3220(2)	2197(1)	44(1)
S(4)	12189(2)	4199(2)	3276(1)	56(1)
C(1)	4805(9)	1596(9)	425(2)	57(1)
O(1)	3271(7)	882(7)	297(1)	80(1)
C(2)	8732(10)	2934(8)	154(2)	54(1)
O(2)	9482(9)	3069(7)	-129(1)	78(1)
C(3)	8889(9)	380(8)	740(2)	52(1)
O(3)	9672(8)	-977(7)	802(1)	75(1)
C(4)	6109(9)	5177(9)	570(2)	54(1)
O(4)	5397(8)	6543(7)	518(1)	80(1)
C(5)	9162(7)	3564(6)	1441(1)	37(1)
C(6)	9994(7)	3829(6)	1828(1)	37(1)
C(7)	12010(8)	4512(7)	1964(1)	43(1)
C(8)	12250(8)	4578(7)	2364(2)	46(1)
C(9)	10420(7)	3927(6)	2535(1)	39(1)
C(10)	10113(8)	3683(6)	2932(1)	40(1)
C(11)	8261(9)	2927(6)	3093(2)	44(1)
C(12)	8636(10)	2784(7)	3496(2)	51(1)
C(13)	10655(10)	3410(9)	3626(2)	57(1)

Table 3. Bond lengths [Å] and angles [°] for MTSLReBT.

Re(1)-C(1)	1.942(6)	C(3)-Re(1)-S(2)	87.29(15)
Re(1)-C(2)	1.943(6)	C(4)-Re(1)-S(2)	91.33(15)
Re(1)-C(3)	1.993(6)	C(1)-Re(1)-S(1)	168.26(18)
Re(1)-C(4)	1.998(6)	C(2)-Re(1)-S(1)	99.75(18)
Re(1)-S(2)	2.4974(14)	C(3)-Re(1)-S(1)	87.01(16)
Re(1)-S(1)	2.5124(12)	C(4)-Re(1)-S(1)	91.33(16)
S(1)-C(5)	1.701(4)	S(2)-Re(1)-S(1)	69.54(4)
S(2)-C(5)	1.692(5)	C(5)-S(1)-Re(1)	87.42(16)
S(3)-C(9)	1.729(5)	C(5)-S(2)-Re(1)	88.12(16)
S(3)-C(6)	1.733(4)	C(9)-S(3)-C(6)	91.9(2)
S(4)-C(13)	1.693(6)	C(13)-S(4)-C(10)	91.9(3)
S(4)-C(10)	1.721(5)	O(1)-C(1)-Re(1)	178.5(6)
C(1)-O(1)	1.131(7)	O(2)-C(2)-Re(1)	178.4(6)
C(2)-O(2)	1.128(7)	O(3)-C(3)-Re(1)	178.2(5)
C(3)-O(3)	1.134(7)	O(4)-C(4)-Re(1)	177.4(6)
C(4)-O(4)	1.120(7)	C(6)-C(5)-S(2)	121.8(3)
C(5)-C(6)	1.435(6)	C(6)-C(5)-S(1)	123.4(3)
C(6)-C(7)	1.368(6)	S(2)-C(5)-S(1)	114.7(3)
C(7)-C(8)	1.409(7)	C(7)-C(6)-C(5)	128.9(4)
C(8)-C(9)	1.374(6)	C(7)-C(6)-S(3)	110.9(3)
C(9)-C(10)	1.437(7)	C(5)-C(6)-S(3)	120.2(3)
C(10)-C(11)	1.398(7)	C(6)-C(7)-C(8)	113.1(4)
C(11)-C(12)	1.429(8)	C(9)-C(8)-C(7)	113.2(4)
C(12)-C(13)	1.348(8)	C(8)-C(9)-C(10)	129.0(4)
		C(8)-C(9)-S(3)	110.7(4)
C(1)-Re(1)-C(2)	91.5(2)	C(10)-C(9)-S(3)	120.1(4)
C(1)-Re(1)-C(3)	89.6(2)	C(11)-C(10)-C(9)	127.1(4)
C(2)-Re(1)-C(3)	91.2(2)	C(11)-C(10)-S(4)	111.2(4)
C(1)-Re(1)-C(4)	91.9(2)	C(9)-C(10)-S(4)	121.6(4)
C(2)-Re(1)-C(4)	89.9(2)	C(10)-C(11)-C(12)	110.9(5)
C(3)-Re(1)-C(4)	178.1(2)	C(13)-C(12)-C(11)	112.9(5)
C(1)-Re(1)-S(2)	99.09(17)	C(12)-C(13)-S(4)	113.1(4)
C(2)-Re(1)-S(2)	169.24(18)		

Symmetry transformations used to generate equivalent atoms:

Table 4. Anisotropic displacement parameters ($Å^2 x\ 10^3$)for MTSLReBT. The anisotropic displacement factor exponent takes the form: $-2\pi^2[\ h^2a^{*2}U^{11} + ... + 2\ h\ k\ a^*\ b^*\ U^{12}\ ]$

	U^{11}	U^{22}	U^{33}	U^{23}	U^{13}	U^{12}
Re(1)	37(1)	52(1)	37(1)	-3(1)	4(1)	-1(1)
S(1)	38(1)	68(1)	39(1)	0(1)	7(1)	-10(1)
S(2)	38(1)	61(1)	40(1)	-4(1)	7(1)	-9(1)
S(3)	37(1)	57(1)	39(1)	3(1)	4(1)	-6(1)
S(4)	53(1)	71(1)	45(1)	-3(1)	0(1)	-8(1)
C(1)	48(3)	68(4)	55(3)	-8(3)	11(3)	4(3)
O(1)	50(2)	103(4)	85(3)	-27(3)	-1(2)	-18(2)
C(2)	51(3)	58(4)	52(4)	-1(3)	9(3)	-5(2)
O(2)	93(4)	95(4)	47(3)	-7(2)	26(2)	-12(3)
C(3)	50(3)	64(4)	43(3)	-5(3)	14(2)	-6(3)
O(3)	86(3)	67(3)	73(3)	8(2)	19(2)	21(2)
C(4)	53(3)	72(4)	35(3)	-4(3)	-4(2)	2(3)
O(4)	95(3)	69(3)	73(3)	3(3)	-3(3)	26(3)
C(5)	38(2)	37(2)	38(2)	0(2)	9(2)	2(2)
C(6)	39(2)	39(3)	35(2)	1(2)	9(2)	3(2)
C(7)	41(2)	44(3)	45(3)	-3(2)	8(2)	-7(2)
C(8)	44(3)	46(3)	49(3)	-4(2)	3(2)	-8(2)
C(9)	41(2)	35(2)	40(3)	-2(2)	1(2)	2(2)
C(10)	43(2)	35(3)	42(3)	-3(2)	-1(2)	4(2)
C(11)	55(3)	40(3)	36(3)	-1(2)	7(2)	-3(2)
C(12)	57(3)	50(3)	49(3)	0(2)	16(3)	2(2)
C(13)	71(4)	64(4)	36(3)	0(3)	3(3)	0(3)

Table 5. Torsion angles [°] for MTSLReBT.

C(1)-Re(1)-S(1)-C(5)	-12.4(9)	S(1)-Re(1)-C(4)-O(4)	79(12)
C(2)-Re(1)-S(1)-C(5)	-176.3(2)	Re(1)-S(2)-C(5)-C(6)	-175.8(4)
C(3)-Re(1)-S(1)-C(5)	-85.6(2)	Re(1)-S(2)-C(5)-S(1)	4.0(3)
C(4)-Re(1)-S(1)-C(5)	93.6(2)	Re(1)-S(1)-C(5)-C(6)	175.8(4)
S(2)-Re(1)-S(1)-C(5)	2.63(16)	Re(1)-S(1)-C(5)-S(2)	-4.0(3)
C(1)-Re(1)-S(2)-C(5)	174.3(3)	S(2)-C(5)-C(6)-C(7)	-178.5(4)
C(2)-Re(1)-S(2)-C(5)	3.0(10)	S(1)-C(5)-C(6)-C(7)	1.7(8)
C(3)-Re(1)-S(2)-C(5)	85.2(2)	S(2)-C(5)-C(6)-S(3)	2.5(6)
C(4)-Re(1)-S(2)-C(5)	-93.6(2)	S(1)-C(5)-C(6)-S(3)	-177.3(3)
S(1)-Re(1)-S(2)-C(5)	-2.65(17)	C(9)-S(3)-C(6)-C(7)	1.0(4)
C(2)-Re(1)-C(1)-O(1)	87(21)	C(9)-S(3)-C(6)-C(5)	-179.9(4)
C(3)-Re(1)-C(1)-O(1)	-4(21)	C(5)-C(6)-C(7)-C(8)	179.9(5)
C(4)-Re(1)-C(1)-O(1)	177(100)	S(3)-C(6)-C(7)-C(8)	-1.1(6)
S(2)-Re(1)-C(1)-O(1)	-91(21)	C(6)-C(7)-C(8)-C(9)	0.6(7)
S(1)-Re(1)-C(1)-O(1)	-77(21)	C(7)-C(8)-C(9)-C(10)	175.9(5)
C(1)-Re(1)-C(2)-O(2)	147(22)	C(7)-C(8)-C(9)-S(3)	0.2(6)
C(3)-Re(1)-C(2)-O(2)	-124(22)	C(6)-S(3)-C(9)-C(8)	-0.7(4)
C(4)-Re(1)-C(2)-O(2)	55(22)	C(6)-S(3)-C(9)-C(10)	-176.8(4)
S(2)-Re(1)-C(2)-O(2)	-42(23)	C(8)-C(9)-C(10)-C(11)	-176.3(5)
S(1)-Re(1)-C(2)-O(2)	-36(22)	S(3)-C(9)-C(10)-C(11)	-1.0(7)
C(1)-Re(1)-C(3)-O(3)	-92(18)	C(8)-C(9)-C(10)-S(4)	-0.7(7)
C(2)-Re(1)-C(3)-O(3)	176(100)	S(3)-C(9)-C(10)-S(4)	174.6(3)
C(4)-Re(1)-C(3)-O(3)	49(21)	C(13)-S(4)-C(10)-C(11)	0.6(4)
S(2)-Re(1)-C(3)-O(3)	7(18)	C(13)-S(4)-C(10)-C(9)	-175.7(4)
S(1)-Re(1)-C(3)-O(3)	76(18)	C(9)-C(10)-C(11)-C(12)	175.4(5)
C(1)-Re(1)-C(4)-O(4)	-112(12)	S(4)-C(10)-C(11)-C(12)	-0.6(5)
C(2)-Re(1)-C(4)-O(4)	-20(12)	C(10)-C(11)-C(12)-C(13)	0.3(7)
C(3)-Re(1)-C(4)-O(4)	107(13)	C(11)-C(12)-C(13)-S(4)	0.2(7)
S(2)-Re(1)-C(4)-O(4)	149(12)	C(10)-S(4)-C(13)-C(12)	-0.5(5)

Symmetry transformations used to generate equivalent atoms: